

IAEA-TECDOC-1275

# ***Specialized software utilities for gamma ray spectrometry***

*Final report of a co-ordinated research project  
1996–2000*



INTERNATIONAL ATOMIC ENERGY AGENCY

IAEA

March 2002

The originating Section of this publication in the IAEA was:

Physics Section  
International Atomic Energy Agency  
Wagramer Strasse 5  
P.O. Box 100  
A-1400 Vienna, Austria

SPECIALIZED SOFTWARE UTILITIES FOR GAMMA RAY SPECTROMETRY  
IAEA, VIENNA, 2002  
IAEA-TECDOC-1275  
ISSN 1011-4289

© IAEA, 2002

Printed by the IAEA in Austria  
March 2002

## FOREWORD

A Co-ordinated Research Project (CRP) on Software Utilities for Gamma Ray Spectrometry was initiated by the International Atomic Energy Agency in 1996 for a three year period. In the CRP, several basic applications of nuclear data handling were assayed which also dealt with the development of PC computer codes for various spectrometric purposes.

The CRP produced several software packages for the analysis of low level NaI spectra; user controlled analysis of gamma ray spectra from HPGe detectors; a set of routines for the definition of the detector resolution function and for the unfolding of experimental annihilation spectra; a program for the generation of gamma ray libraries (using new, evaluated data) for specific applications; a program to calculate true coincidence corrections; a program to calculate the full-energy peak efficiency calibration curve for homogeneous cylindrical sample geometries including self-attenuation correction; and a program for the library driven analysis of gamma ray spectra and for the quantification of radionuclide contents in samples. In addition, the CRP addressed problems of the analysis of naturally occurring radioactive soil material gamma ray spectra, questions of quality assurance and quality control in gamma ray spectrometry, and verification of the expert system SHAMAN for the analysis of air filter spectra obtained within the framework of the Comprehensive Nuclear Test Ban Treaty.

This TECDOC presents the final results of the CRP and an attached CD-ROM contains all software packages produced under the CRP. The TECDOC and the software included in the CD-ROM will be useful to those involved in gamma ray spectrum analysis, particularly to inexperienced groups starting activities in this field.

The IAEA is grateful to the participants of the CRP who contributed to this TECDOC. S. Fazinic of the Division of Physical and Chemical Sciences was the IAEA officer responsible for this publication.

## *EDITORIAL NOTE*

*This publication has been prepared from the original material as submitted by the authors. The views expressed do not necessarily reflect those of the IAEA, the governments of the nominating Member States or the nominating organizations.*

*The use of particular designations of countries or territories does not imply any judgement by the publisher, the IAEA, as to the legal status of such countries or territories, of their authorities and institutions or of the delimitation of their boundaries.*

*The mention of names of specific companies or products (whether or not indicated as registered) does not imply any intention to infringe proprietary rights, nor should it be construed as an endorsement or recommendation on the part of the IAEA.*

*The authors are responsible for having obtained the necessary permission for the IAEA to reproduce, translate or use material from sources already protected by copyrights.*

## CONTENTS

Summary.....	1
Analysis of low-intensity scintillation spectra .....	7
<i>V. Muravsky, S.A. Tolstov</i>	
User controlled analysis of gamma ray spectra.....	17
<i>P. Mishev</i>	
Nuclear data libraries for gamma analysis programs, including special purpose libraries.....	23
<i>W. Westmeier, U. Reus, K. Siemon, H. Westmeier</i>	
“TrueCoinc”, a software utility for calculation of the true coincidence correction.....	37
<i>S. Sudár</i>	
Calculation of the counting efficiency for extended sources.....	49
<i>M. Korun, T. Vidmar</i>	
Librarian driven analysis of gamma ray spectra .....	55
<i>V. Kondrashov, I. Petersone</i>	
Analysis of fine structure in Doppler broadened annihilation peaks.....	61
<i>L. Calderin, R. Capote</i>	
Quality assurance and quality control in gamma ray spectrometry .....	69
<i>K. Heydorn</i>	
Compton suppression gamma ray spectrometry .....	81
<i>S. Landsberger, F.Y. Iskander, M. Niset, K. Heydorn</i>	
Expert system SHAMAN and verification of the Comprehensive Nuclear Test Ban Treaty.....	93
<i>P.A. Aarnio, J.J. Ala-Heikkilä, T.T. Hakulinen, M.T. Nikkinen</i>	
Contributors to drafting and review .....	101



## SUMMARY

### Introduction

This CRP was recommended by the meeting on Software for Nuclear Spectrometry, held in Vienna in 1994 [1]. The meeting first initiated activities aiming at the improvement of the available tools for nuclear spectrometry. These activities dealt with a thorough intercomparison in which the most frequently used spectrometry software packages were tested for their capabilities and reliability of the results for peak area calculation [2]. Other activities of this CRP, in which were the assay of several basic applications of nuclear data handling that also dealt with the development of new PC programs for various spectrometric purposes.

### Brief description of programs developed under the CRP

#### *Analysis of low-intensity scintillation spectra*

The maximum likelihood algorithms for nuclides activities estimation from low intensities scintillation  $\gamma$  ray spectra have been created. The algorithms treat full energy peaks and Compton parts of spectra, and they are more effective than least squares estimators [3]. The factors that could lead to the bias of activity estimates are taken into account.

Theoretical analysis of the problem of choosing the optimal set of initial spectra for the spectrum model to minimize errors of the activities estimation has been carried out for the general case of the  $N$ -components with Gaussian or Poisson statistics [4]. The obtained criterion allows to exclude superfluous initial spectra of nuclides from the model.

A special calibration procedure for scintillation  $\gamma$ -spectrometers has been developed. This procedure is required for application of the maximum likelihood activity estimators processing all the channels of the scintillation  $\gamma$ -spectrum, including the Compton part. It allows one to take into account the influence of the sample mass density variation.

The algorithm for testing the spectrum model adequacy to the processed scintillation spectrum has been developed. The algorithms are realized in Borland Pascal 7 as a library of procedures and functions. The developed library is compatible with Delphi 1.0 and higher versions. It can be used as the algorithmic basis for analysis of highly sensitive scintillation  $\gamma$ - and  $\beta$ -spectrometric devices.

#### *User controlled analysis of gamma ray spectra*

The program "ANGES" was designed as a general purpose high-resolution  $\gamma$  ray spectrometry program. It offers all main features as commercial software packages except control of acquisition process. The program is able to perform automatic analysis of spectra but it is announced as "user controlled" because it supplies all intermediate results and gives the opportunity these results to be analyzed and corrected by the user. ANGES offers:

- Multi document Windows interface.
- Detailed visualization of spectra.
- Nuclide library based on another contribution to CRP (see the next contribution).
- Energy and FWHM calibrations calculated by means of orthonormal polynomial fitting.
- Peak processing engine, based on a non-linear LSQ method for fitting peaks. The procedure can be applied to the whole spectrum or to a single Region-of-Interest (ROI). The assumed peak shape is pure Gaussian. All peaks in single ROI are assumed to have the same FWHM. The maximum number of peaks in a single ROI is restricted to 25, the maximum ROI length is 512 channels, and the baseline is described with a polynomial of a degree up to 4.

- Peak location engine, based on first derivative method is provided to ease the preparation of a spectrum for processing.
- Two methods for efficiency calibration: an efficiency calibration curve and reference table.
- Peak identification and activity calculation procedure.
- A number of corrections: True coincidence summing, background correction, pile up rejection and so on.
- An option for processing series of similar spectra.

As a result of the identification procedure a report file is issued containing spectrum processing results, list of identified and not identified peaks, list of identified nuclides and background nuclides.

### ***Generation of specific nuclear data libraries***

Updating a previous catalog [5] nuclear data for radionuclides are compiled from electronic sources and from publications (published before January 1998) in all major scientific journals. All compiled data are critically reviewed, evaluated and consistency checked. A maximum of 350 energies is compiled for one nuclide. Relative photon intensities are converted to number of photons per 100 decays, provided that the decay schemes are sufficiently well determined.

Due to very diverging needs of data in libraries for different users and applications it was decided to provide a master library that contains only the basic data needed for quantitative nuclide assignment, i.e. the nuclide name, the half-life and up to 32  $\gamma$  lines with their abundances.

A 32-bit WINDOWS program (NUC\_MAN) was developed that allows for easy editing of the library data and generation of user libraries. The transfer of data from the NUC\_MAN program to other spectrometry programs is most easily achieved through a file with the unique name NUC\_MAN.OUT in which the data from each library opened with the NUC\_MAN program are listed in ASCII representation.

Libraries supplied with the NUC\_MAN program are:

- MASTER.LIB (containing 1627 nuclides with 32456  $\gamma$  lines, i.e. all nuclides with a half-life  $\geq 10$  seconds);
- INAA.LIB (with data for 221 nuclides that are generated in thermal neutron activation analysis);
- KKW.LIB (data for 134 nuclides that are relevant for measurements in nuclear power plants);
- STANDARD.LIB (data for 105 nuclides that are frequently used for calibration purposes);
- IMIS.LIB (data for 76 nuclides used for environmental supervision in Germany);
- SIPPING.LIB (data for 34 nuclides used for sipping analyses in nuclear power plants);
- NUCMED.LIB (data for 17 nuclides frequently used in nuclear medicine applications);
- NATURE.LIB (containing data for 10 nuclides found in the environment).

### ***True coincidence corrections***

The true coincidence correction plays an important role in the overall accuracy of the  $\gamma$  ray spectrometry especially in the case of present-day high volume detectors. The calculation of true coincidence corrections needs detailed nuclear structure information. Recently these data are available in computerized form from the Nuclear Data Centers through the Internet or on a CD-ROM of the Table of Isotopes. The aim has been to develop software for this calculation, using available databases for the levels data. The user has to supply only the parameters of the detector to be used.

The new computer program runs under the Windows 95/98 operating system. In the framework of the project a new formula was prepared for calculating the summing out correction and calculation of the intensity of alias lines (sum peaks). The file converter for reading the ENDSF-2 type files was completed. Reading and converting the original ENDSF was added to the program. A computer accessible database of the X rays energies and intensities was created. The X ray emissions were taken in account in the “summing out” calculation. Calculation of the true coincidence “summing in” correction was done. The output was arranged to show independently two types of corrections and to calculate the final correction as multiplication of the two. A minimal intensity threshold can be set to show the final list only for the strongest lines. The calculation takes into account all the transitions, independently of the threshold. The program calculates the intensity of X rays (K, L lines). The true coincidence corrections for X rays were calculated. The intensities of the alias  $\gamma$  lines were calculated.

### ***Efficiency calculation software for extended (large) sources***

A computer program for the calculation of efficiency calibration curves for extended samples counted on  $\gamma$ - and X ray spectrometers was developed. The program calculates the efficiency calibration curves for homogeneous cylindrical samples placed coaxially with the symmetry axis of the detector. The calculation method is based on integration over the sample volume of the efficiencies for point sources measured in free space on a square grid. Attenuation of photons within the sample is taken into account using the self-attenuation function calculated with a two-dimensional detector model. The detector model simulates the processes of photon detection at low energies well, since that is where the interaction between the photons and the detector crystal takes place at the crystal surface. The model therefore yields good results at low energies. Since the self-attenuation function is defined as the ratio of efficiencies for a point source embedded in the sample matrix and the point source positioned at the same point in free space, and the attenuation coefficients decrease with energy, the model yields good results at higher energies as well.

The program uses the sample data file, detector characterization file and attenuation data for all materials present in the sample and in the detector as input. The sample data file contains the data on the dimensions of the sample, its distance from the detector, density and composition. The detector characterization file comprises the data on the detector crystal dimensions and position, and data on the spatial dependence of the efficiencies for the point source at all characterization energies. The program calculates the efficiency calibration curve for all detector characterization energies and at all energies where the attenuation coefficients are given. The program, several input data files and the documentation are available on the web site: <http://rubin.ijs.si/vlg>.

### ***Librarian driven analysis of gamma ray spectra***

A software package DIMEN, which performs radionuclides quantification and partial identification by using the librarian approach for analysis of  $\gamma$  ray spectra, has been upgraded to the Windows environment.

For a set of a priori given nuclides taken from a library, DIMEN uses median estimates of the peak areas and estimates of their errors to produce a list of possible nuclides matching a  $\gamma$  ray line and some measure of the reliability of this assignment. Identification of a given radionuclide is obtained by searching for a match with the energy information from a database. This procedure is performed in an interactive graphical mode by markers that superimpose on the experimental spectra data, with the energy information given by a previously elaborated data library. This library includes 16712  $\gamma$  ray energy lines related to 756 known  $\gamma$  emitter radioisotopes.

The WINDIMEN program is a Windows application and together with the  $\gamma$  ray analysis software package ANGES would be valuable for tasks of radiological protection, radiochemistry and environmental control. The original DOS version (i.e. DIMEN) has been transferred to a Windows application using the object-oriented software platform DELPHI.

## ***Analysis of doppler-broadened annihilation peaks***

A doppler annihilation spectra general unfolding algorithm was developed. This general algorithm has two programs: (i) RESFIT for fitting of the detector system resolution function; and (ii) DPPUNFOL for unfolding the experimental annihilation spectra.

It should be mentioned that the asymmetric characteristic of this kind of spectra was considered as a part of the resolution function, instead of including it into the background. Both programs were tested using modeled data with statistical noise from 1- to 3-sigma levels added. A good agreement between the “true” parameters and the unfolded ones was achieved for all studied cases.

## **Additional activities under the CRP**

### ***Research in quality assurance and quality control***

In accordance with the goals outlined at the first Research Co-ordination Meeting in Vienna in May 1997, efforts to improve methods for predicting the uncertainty of analytical results obtained in radioanalytical chemistry or more specifically in neutron activation analysis have been continued. We have now completed validation of our computer programs for calculating peak areas and their corresponding uncertainty in  $\gamma$  spectrometry; completely reliable standard uncertainties for use in conventional NAA are now provided under all practical conditions of analysis [6] — provided the Poisson statistic is correctly applied.

In specialized  $\gamma$  spectrometry it was found that the introduction of loss-free counting (LFC) systems resulted in significant deviations from the undisturbed Poisson statistic, which led to a loss of statistical control of the analytical results. This was the subject of a special study that subsequently gave rise to the thorough investigations of LFC spectra carried out at the Belgian Nuclear Research Centre in Mol.

Deviations from Poisson statistics could also be expected in other types of corrected spectra, such as those produced under Compton suppression. This was studied in co-operation with the University of Illinois and based on their Compton-suppression system and reported here later.

Finally we have aimed at implementing statistical control also in radiochemical neutron activation analysis (RNAA), where the propagation of uncertainty has caused problems, particularly in cases with significant corrections for chemical yield and nuclear interference. A spread-sheet program has been set up that will calculate all corrections and their uncertainties, when a reliable input of peak areas and their uncertainties is available. This program was verified by an actual set of experimental results for Pt in biological materials, where substantial corrections need to be made for the nuclear interference from gold.

### ***Compton suppression gamma ray spectrometry***

In the past decade there have been many studies using Compton suppression methods in routine neutron activation analysis as well as in the traditional role for low level  $\gamma$  ray counting of environmental samples. There have been many new PC based software packages that have been developed to enhance photopeak fitting. Although the newer PC based algorithms have had significant improvements, they still are not effectively used in analyzing weak  $\gamma$  ray lines in natural samples or in neutron activated samples that have very high Compton backgrounds. We have completed a series of experiments to show the usefulness of Compton suppression. We have shown the pitfalls when using Compton suppression methods for high counting dead-times as in the case of neutron activated samples. We have investigated whether counting statistics are the same for both suppressed and normal modes. Results are presented in four separate experiments. These experiments include influence of dead-time in Compton suppression, influence of Compton suppression on counting statistics, and the use of Compton suppression in determining Cs-137 in soil samples. We have also

prepared four sets of spectra of natural soil samples using normal and Compton with high and low values of Cs-137. These spectra are to be distributed to the other participants in testing their  $\gamma$  ray software for photopeaks arising from naturally occurring radioactive material.

The results of the experiments have shown the following: (i) standards and samples should have very similar dead-times when using the Compton mode for counting; (ii) samples should not be counted with high dead-times (<10%) in the Compton mode; (iii) counting statistics are preserved when comparing samples counted in the normal and counting mode; (iv) Compton suppression is ideal to count low concentrations of Cs-137 in soil samples.

### ***Verification of the expert system SHAMAN for the analysis of air filter spectra***

SHAMAN [7] is an expert system developed at Helsinki University of Technology for carrying out the nuclide identification and peak interpretation in gamma spectrum analysis. SHAMAN utilizes a comprehensive reference library with 2600 radionuclides and 80,000 gamma lines, as well as a rule base of sixty inference rules. The code has to be interfaced with advanced peak analysis software like UniSAMPO [8], for example. SHAMAN takes the spectrum, calibration information, and peak analysis results and applies the rules and the library to produce comprehensive quantitative information of the radionuclides present and full interpretation of the peaks.

SHAMAN has been tested and compared with other programs using the air filter spectra obtained within the framework of the Comprehensive Nuclear-Test-Ban Treaty. The results of the comparison show that SHAMAN outperforms the programs having highly optimized nuclide libraries. Because its comprehensive general purpose library it is to be expected that SHAMAN will perform even better when more complicated test cases are used.

### **Conclusion**

Several basic applications of nuclear data handling were assayed under the CRP, which also dealt with the development of programs for various spectrometric purposes. In addition, the CRP addressed several research topics. The achievements of the CRP have been briefly presented in the previous sections. In the following sections, every project under the CRP will be elaborated with more details.

The first versions of software produced under the CRP are available on requests as a CD-ROM containing programs, manuals and other useful documentation important to run the programs. The CRP participants expect and emphasize their interest in receiving considerable feedback from the users and want to stipulate user's feedback, criticism and suggestions for improvements.

### **REFERENCES**

- [1] INTERNATIONAL ATOMIC ENERGY AGENCY, Software for Nuclear Spectrometry, IAEA-TECDOC-1049, Vienna, 1998.
- [2] INTERNATIONAL ATOMIC ENERGY AGENCY, Intercomparison of Gamma Ray Analysis Software Packages, IAEA-TECDOC-1011, Vienna, 1998.
- [3] MURAVSKY, V.A., TOLSTOV, S.A., KHOLMETSII, A.L., Nucl. Instr. Meth. **B145** (1998) 573–577.
- [4] MURAVSKY, V.A., TOLSTOV, S.A., Program of 5<sup>th</sup> International Conference on Application of semiconductor detectors in nuclear physics, Riga, May 18-22 1998, P. 103.
- [5] REUS, U., WESTMEIER, W., Atomic Data and Nuclear Data Tables, **Vol. 29**, Nos. 1&2 (1983).
- [6] HEYDORN, K., Validation of Neutron Activation Analysis Techniques, in Quality Assurance for Environmental Analysis (Quevauviller, Ph., et al., Eds), Elsevier (1995) 89–110.

- [7] AARNIO, P.A., ALA-HEIKKILÄ, J.J., HAKULINEN, T.T., NIKKINEN, M.T., The Nuclide Identification System SHAMAN in the Verification of the CTBT, MARC V Conference, Kailua-Kona, Hawaii, April 9–14 2000.
- [8] AARNIO, P.A., NIKKINEN, M.T., ROUTTI, J.T., UniSAMPO, Comprehensive Software for Gamma Spectrum Processing, MARC V Conference, Kailua-Kona, Hawaii, April 9–14 2000.

# ANALYSIS OF LOW-INTENSITY SCINTILLATION SPECTRA

V. Muravsky, S.A. Tolstov

International Sakharov Institute of Radioecology,  
Minsk, Belarus

**Abstract.** The maximum likelihood algorithms for nuclides activities estimation from low intensity scintillation  $\gamma$ -ray spectra have been created. The algorithms treat full energy peaks and Compton parts of spectra, and they are more effective than least squares estimators. The factors that could lead to the bias of activity estimates are taken into account. Theoretical analysis of the problem of choosing the optimal set of initial spectra for the spectrum model to minimize errors of the activities estimation has been carried out for the general case of the  $N$ -components with Gaussian or Poisson statistics. The obtained criterion allows to exclude superfluous initial spectra of nuclides from the model. A special calibration procedure for scintillation  $\gamma$ -spectrometers has been developed. This procedure is required for application of the maximum likelihood activity estimators processing all the channels of the scintillation  $\gamma$ -spectrum, including the Compton part. It allows one to take into account the influence of the sample mass density variation. The algorithm for testing the spectrum model adequacy to the processed scintillation spectrum has been developed. The algorithms are realized in Borland Pascal 7 as a library of procedures and functions. The developed library is compatible with Delphi 1.0 and higher versions. It can be used as the algorithmic basis for analysis of highly sensitive scintillation  $\gamma$ - and  $\beta$ -spectrometric devices.

## Estimators for nuclide activities in low-intensity scintillation spectrometry

### *Calculation of the nuclides activities estimates by the maximum likelihood method*

Ionizing radiation has a random character, therefore the number of counts  $S(i)$  in the  $i$ -th channel of the spectrum  $S$  with a finite accumulation time  $T$  is a random variable with the mean value  $y(i)$ . A distribution of counts in each of the spectrum channels is a Poisson or polynomial distribution. A polynomial distribution takes place if spectrum is accumulated so long as the spectrum integral less than a definite value.

In a case of the low-intensity radiation one may write the mean value  $y(i)$  of the number of counts in the  $i$ -th spectrum channel as

$$y(i) = T \sum_{k=1}^{M+1} A_k f_k(i), \quad (1)$$

where  $T$  is the number of nuclides;  $M$  is the number of nuclides;  $f_k(i)$  ( $k \leq M$ ) is the spectrum of the  $k$ -th nuclide, normalized to unit activity and unit time (the "initial spectrum" of the  $k$ -th nuclide);  $A_k$  ( $k \leq M$ ) is the activity of the  $k$ -th nuclide;  $f_{M+1}(i)$  is the "initial spectrum" of a background;  $A_{M+1}$  is the relative intensity of a background.

The problem of nuclide activity estimation should be solved by the statistical methods. A general approach to the problem of the correct estimation of random distribution parameters was investigated in a number of classical works. It was shown in ref. [1,2] that the best parameter estimates are obtained by the maximum likelihood (ML) method. In case of a Gaussian distribution the ML method is reduced to the well developed least squares method. However, for a Poisson distribution (or other distributions) the maximum likelihood method is optimal [1,2].

Let us suppose that  $x$  is a discrete random value (one-dimensional or multidimensional) with a probability function  $P(x, Q_1, \dots, Q_M)$ , where  $Q_k$  ( $k = 1, 2, \dots, M$ ) are the unknown parameters of the distribution. The ML estimates of the parameters  $Q_k$  for observed  $N$  values  $\{x_1, \dots, x_N\}$  are obtained by maximizing the likelihood function  $L$

$$L(x_1, \dots, x_N, Q_1, \dots, Q_M) = \prod_{i=1}^N P(x_i, Q_1, \dots, Q_M) \quad (2)$$

or its logarithm.

Usually, one uses the inverse matrix to the Fisher's information matrix [1,2] as an estimate of the covariance matrix of ML estimates. Elements  $I_{kl}$  of the Fisher's information matrix are equal to

$$I_{kl} = -E \left[ \frac{\partial^2 \ln L}{\partial Q_k \partial Q_l} \right], \quad (3)$$

where  $E$  means averaging.

The logarithm of the likelihood function for a Poisson distribution in spectrum channels is equal to

$$\ln L = \sum_{i=1}^N \left( -T \sum_{k=1}^{M+1} A_k f_k(i) + S(i) \ln \left( T \sum_{k=1}^{M+1} A_k f_k(i) \right) - \ln(S(i)!) \right). \quad (4)$$

The logarithm of the likelihood function for a polynomial distribution in spectrum channels is equal to

$$\ln L = \ln(I!) + \sum_{i=1}^N \left( S(i) \ln \left( T \sum_{k=1}^{M+1} A_k f_k(i) \right) - S(i) \ln I - \ln(S(i)!) \right), \quad (5)$$

$$\text{where } I = \sum_{i=1}^N S(i) = T \sum_{i=1}^N \sum_{k=1}^{M+1} A_k f_k(i). \quad (6)$$

It could be shown, that the activity estimates for both Poisson and polynomial statistics can be found from the set of the  $M+1$  equations

$$\sum_{i=1}^N \left( \frac{S(i) f_j(i)}{\sum_{k=1}^{M+1} A_k f_k(i)} - T f_j(i) \right) = 0 \quad (7)$$

where  $j = 1, 2, \dots, M+1$ .

In general, the set of equations (7) is non-linear, so it should be solved by numerical methods. We proposed in [3] an effective iteration scheme for solution of (7). In every  $q$ -th iteration ( $q = 1, 2, \dots$ ), one solves the set of linear equations:

$$\sum_{k=1}^{M+1} A_k T \sum_{i=1}^N \frac{f_k(i) f_j(i)}{D_q(i)} = \sum_{i=1}^N \frac{S(i) f_j(i)}{D_q(i)}, \quad (8)$$

where

$$D_q(i) = \begin{cases} \sum_{k=1}^{M+1} A_k^{(q-1)} f_k(i), & \text{if } q > 1, \\ [S(i) + 1]/T, & \text{if } q = 1 \end{cases}$$

$A_k^{(q-1)}$  are the estimates of the activities, obtained in  $q-1$  iteration.

The elements of the Fisher's information matrix are equal to

$$I = T \sum_{i=1}^N \frac{f_k(i) f_j(i)}{D_q(i)}. \quad (9)$$

So, the covariance matrix of ML estimates of the activities can be found by inversion of the matrix (9).

As a rule, in a case of the low-intensity scintillation  $\gamma$ -spectrometry the initial spectra  $f_k(i)$  are obtained experimentally during spectrometer calibration with a set of standard samples (sources) of nuclides activities.

However, the initial spectra, obtained in such way, inescapably contain the statistical noise. The presence of the noise leads to a bias of the estimates, obtained from the iteration scheme (8), because the diagonal elements of the matrix of the set of linear equations, solved in each iteration, are biased. To compensate that bias it is necessary to modify the iteration scheme (8) in the following way [4]:

$$\sum_{k=1}^{M+1} A_k T \sum_{i=1}^N \left[ \frac{f_k(i, \rho) f_j(i, \rho) - \delta_{kj} d_k(i, \rho)}{D_q(i)} \right] = \sum_{i=1}^N \frac{S(i, \rho) f_j(i, \rho)}{D_q(i)}, \quad (10)$$

where  $\rho$  is a mass density of an investigated sample;  $\delta_{kj} = \begin{cases} 1, & \text{if } k = j \\ 0, & \text{if } k \neq j \end{cases}$ ,

$d_j(i)$  is the statistical noise variation in  $j$ -th initial spectrum ("variation" of the  $j$ -th initial spectrum),

$$D_q(i) = \begin{cases} 0.5 \cdot [P_q(i-1) + P_q(i+1)], & \text{if } 1 < i < N, \\ P_q(i), & \text{if } i = 1 \text{ or } i = N \end{cases}$$

$$P_q(i) = \begin{cases} \sum_{k=1}^{M+2} A_k^{(q-1)} [f_k(i) + T \cdot A_k^{(q-1)} d_k(i)], & \text{if } q > 1. \\ [S(i) + 1]/T, & \text{if } q = 1 \end{cases}$$

The way of calculation of  $D_q(i)$  allows to eliminate the correlation between the numerator and the denominator in the terms

$$\frac{f_k(i, \rho) f_j(i, \rho) - \delta_{kj} d_j(i, \rho)}{D_q(i)} \text{ and } \frac{S(i, \rho) f_j(i, \rho)}{D_q(i)}.$$

That correlation being not eliminated gives additional bias of the activities estimates.

The iteration process (10) is exited, if the following condition is true:

$$\left| A_k^{(q)} - A_k^{(q-1)} \right| < \varepsilon \left| A_k^{(q)} \right| + \tau, \text{ for } k = 1, 2, \dots, M+2, \quad (11)$$

where  $\varepsilon$  is desirable accuracy of the approximation,  $\tau$  is the small constant added for the compensation of the influence of the floating-point operations precision on the exit from the iteration scheme. Our experience shows that the recommended values of these constants are  $\varepsilon = 10^{-6 \dots -8}$ ,  $\tau = 10^{-8 \dots -10}$  (when using the Borland Pascal real types single (4 bytes) or double (8 bytes)).

The covariance matrix of the activities estimates is calculated by the inversion of the Fisher's information matrix  $I$ :

$$I_{vj} = T \sum_{i=1}^N \frac{f_v(i, \rho) f_j(i, \rho) - \delta_{vj} d_j(i, \rho)}{D_q(i)}. \quad (12)$$

As far as the information matrix (12) is the matrix of the set of linear equations of the iteration scheme (10), it is convenient to use in (10) the Gauss-Jordan algorithm [6] for solution of the set of linear equations. The Gauss-Jordan algorithm produces a vector of the solutions of a set of linear equations and the inverse matrix to the matrix of a set of equations. Therefore, the estimates of activities and the covariance matrix of these estimates will be calculated simultaneously.

It is necessary to emphasize that the absence of the correlation between neighboring channels of initial spectra is the necessary condition for application of the iteration scheme (10).

### ***Calibration of scintillation spectrometer***

The necessary for activity estimation set of the initial spectra  $f_k(i, \rho)$  and their variations  $d_k(i, \rho)$  are created from the library of the experimentally obtained during spectrometer calibration initial spectra  $f_k(i, \rho_m)$  and their variations  $d_k(i, \rho_m)$ , here  $\rho$  is the density of the investigated sample. The  $f_k(i, \rho)$  are calculated as:

$$f_k(i, \rho) = \frac{\rho_{m+1} - \rho}{\rho_{m+1} - \rho_m} f_k(i, \rho_m) + \frac{\rho - \rho_m}{\rho_{m+1} - \rho_m} f_k(i, \rho_{m+1}), \quad (13)$$

and accordingly,

$$d_k(i, \rho) = \left( \frac{\rho_{m+1} - \rho}{\rho_{m+1} - \rho_m} \right)^2 d_k(i, \rho_m) + \left( \frac{\rho - \rho_m}{\rho_{m+1} - \rho_m} \right)^2 d_k(i, \rho_{m+1}), \quad (14)$$

where  $m$  has to satisfy to the condition  $\rho_m \leq \rho < \rho_{m+1}$ .

Initial spectra  $f_k(i, \rho_m)$  and their variations  $d_k(i, \rho_m)$  are calculated during calibration of scintillation spectrometer in the next way:

$$f_k(i, \rho_m) = \frac{1}{A_{km}} \left[ \frac{S_k(i, \rho_m)}{T_k} - \frac{S_{Ph}(i, \rho_m)}{T_{Ph}} \right], \quad (15)$$

$$d_k(i, \rho_m) = \frac{1}{A_{km}^2} \left[ \frac{S_k(i, \rho_m)}{T_k^2} + \frac{S_{Ph}(i, \rho_m)}{T_{Ph}^2} \right], \quad (16)$$

where  $S_k(i, \rho_m)$  is the spectrum of a sample with the mass density  $\rho_m$  containing the  $k$ -th nuclide;  $T_k$  is the accumulation time of  $S_k(i, \rho_m)$ ;  $A_{km}$  is known activity of the  $k$ -th nuclide in a sample with the mass density  $\rho_m$ ;  $S_{Ph}(i, \rho_m)$  is the spectrum of a background measured from a sample without nuclides and with the density  $\rho_m$ ;  $T_{Ph}$  is the accumulation time of  $S_{Ph}(i, \rho_m)$ .

Spectra  $S_k(i, \rho_m)$  and  $S_{Ph}(i, \rho_m)$  are accumulated from standard samples during calibration of scintillation spectrometer.

Those standard samples have to answer the following requirements:

- 1) The set of the standard samples should have such values of the density to represent all operating range of the mass density of the investigated samples.
- 2) The standard samples have to be measured in fixed geometry. The geometry is to be identical to the geometry of measurements of the investigated samples. That is, the same beakers have to be used to fill samples in, samples should fill the beakers at the same level, the samples should be homogeneous in volume and they should have homogeneous distribution of nuclides in volume, etc.
- 3) Deviations of the spectrometric scale should be compensated in each spectrum of the standard samples. Our Software includes procedures, which perform compensation of the deviations of spectrometric scale by means of stretching or compression of the processed spectrum. Such stretching or compression of the processed spectrum is done according to position of a well-resolved full-energy peak in a preliminarily accumulated special reference source (for example  $^{137}\text{Cs}$ ) of  $\gamma$ -radiation.

### ***Choosing of the spectrum model***

Under processing the multi-component spectra it is important to choose an adequate spectrum model. If the number of initial spectra in the chosen spectrum model is less than in reality, then the nuclides activity estimates obtained will be biased. Hence, at the first sight, it seems that the chosen model should include as many initial spectra of the nuclides as it is possible. However, the nuclide activity estimation accuracy depends on the number of initial spectra of the nuclides in the spectrum model. And what is more, the accuracy decreases with increasing of the nuclide number included in a model (till the model is true). Thus, one need a criterion for choosing such a model that allows to minimize the errors of the nuclides activities estimates.

If we know *apriory*, that activity of some nuclide does not exceed  $A_{max}$  in the investigated samples with given confidence probability  $P$ , then it could be shown theoretically, that the criterion of the exclusion of such nuclide (we shall call it "e-nuclide") from the spectrum model looks like:

$$A_{max} < t_P \sqrt{D(\hat{A})}. \quad (17)$$

Here  $t_p$  is the quantile of the normal distribution, corresponding to the given confidence probability  $P$ ;  $D(\hat{A})$  is variance of the maximum likelihood estimate  $\hat{A}$  of the activity of the "e-nuclide", obtained from the spectrum model including that "e-nuclide".

The criterion (17) has been obtained from comparison for any nuclide, which is not "e-nuclide", of full errors of maximum likelihood nuclide activity estimate in the spectrum model including "e-nuclide" and in the spectrum model not including "e-nuclide".

This criterion says, that if we know, that activity of some nuclide does not exceed some know threshold, then that nuclide should be included in the spectrum model only if this threshold does not satisfy condition (17). Thus minimal error of activities estimates of other nuclides is provided.

As far as one does not know  $A_{max}$  in practice, it should be reasonable to use estimate of activity of corresponding nuclide instead. Corresponding criterion looks like [5]:

$$\hat{A} < t_p \sqrt{D(\hat{A})}. \quad (18)$$

It could be seen, that obtained criterion very similar to test of statistical hypothesis of equality to zero of nuclide activity.

### ***Test of goodness of fit***

After calculating of nuclide activities it should be reasonable to test the goodness of fit of the experimental spectrum with the spectrum model (1). This test could be done by means of  $\chi^2$  test with modified  $\chi^2$  functional. That modified functional looks like:

$$\chi^2 = \sum_{i=1}^N \frac{\left[ S(i) - T \sum_{k=1}^{M+1} A_k f_k(i) \right]^2}{T \sum_{k=1}^{M+1} A_k \left[ f_k(i) + A_k T d_k(i) + A_k T g_k^2(i) D \right]}, \quad (19)$$

where  $g_k(i)$  is a function, by means of which we may describe approximately the modification of the shape of  $k$ -th initial spectrum influenced by the variation of the spectrometric scale;  $D$  is a variance of the scale variation factor  $\delta$ , which is equal to the relative deviation of the width of the channels of the spectrometer from a give value. The scale variation factor  $\delta$  is proportional to the gain of the photomultiplier tube (PMT) and the spectrometric amplifier in the scintillation spectrometry.

The meaning of  $\delta$  and  $g_k(i)$  could be seen from the next Taylor's series expansion of the initial spectrum of  $k$ -th nuclide:

$$f_k(i) = f_k^{(0)}(i \cdot [1 + \delta_k]) = f_k^{(0)}(i) + \frac{df_k^{(0)}(i)}{di} \cdot i \cdot \delta_k + \dots \approx f_k^{(0)}(i) + \delta_k \cdot g_k(i), \quad (20)$$

Here  $f_k^{(0)}(i)$  is initial spectra of  $k$ -th nuclide with  $\delta_k = 0$ ;  $\delta_k$  is the scale variation factor in that initial spectrum.

The scale variation factor  $\delta$  is variate, which depends on the external factors, which change the gain of the PMT and of the spectrometric amplifier. The mean value of  $\delta$  is equal to zero, and its variance  $D$  could be defined from the technical characteristics of the concrete scintillation spectrometer.

Let us give an example of the calculation of  $D$ . Suppose it is indicated in the technical documentation of the scintillation spectrometer, that the maximum of the full energy peak of  $^{137}\text{Cs}$  is located in the 220-th channel, and the absolute error of this location is 2 channels for the 95% of the confidence probability. Therefore, the absolute error of the  $\delta$  for the given confidence probability is equal to  $2/220 \approx 0,009$ . Let's divide this number by 1,96 (the quantile of the normal distribution, corresponding to the confidence probability being equal to 0,95). As a result, we get the value of the standard deviation of the  $\delta$ , what is equal to 0,0046. After that, we square this value and get  $D$ , which is equal to the  $2,1 \cdot 10^{-5}$  in the considered case.

As far as  $A_k$  in (19) are the nuclides activities estimates, calculated from  $S(i)$  by the maximum likelihood method, we can suppose, that the distribution of functional (19) is tended to the  $\chi^2$ -distribution with  $N-M-1$  degrees of freedom, if the theoretical model (1) of spectrum is adequate to the processed experimental scintillation spectrum.

To provide closeness of the distribution of functional (19) to the  $\chi^2$ -distribution it is necessary to join some channels of the processed spectrum. In practice, it is sufficient to make

$$T \sum_{k=1}^{M+1} A_k f_k(i) > 30 \quad (21)$$

for that [1].

Thus, the testing of the goodness of fit of the processed experimental scintillation spectrum with the spectrum model (1) should be executed after nuclides activities estimation by the maximum likelihood method in the next way.

The value of  $\chi^2$  is calculated according to (19). The value  $\chi^2_{P(N-M-1)}$  is determined from the tables of  $\chi^2$ -distribution or is calculated in some way, here  $P$  is a given confidence probability and  $N-M-1$  is a number of the degrees of freedom.

And if the inequality

$$T < T_P(N-M-1) \quad (22)$$

is satisfied, then the hypothesis about adequacy of the spectrum model to the experimental spectrum is adopted. Otherwise, this hypothesis is turned down and obtained estimates of the nuclides activities are believed wrong. It is necessary to eliminate the reason of the inadequacy of the theoretical model and to repeat accumulation of the spectrum with consequent estimation of the nuclides activities and testing of the adequacy of the spectrum model. The reason of the inadequacy could be, for example, radioactive contamination of the spectrometer's components, or spectrometer's malfunction, or misfit of the shape of the background spectrum, used in theoretical model, or something else.

Function  $g_k(i)$  in (19) may be obtained from  $f_k(i)$ . Indeed, it follows from (20), that

$$g_k(i) = \frac{df_k^{(0)}(i)}{di} \cdot i \approx i [f_k(i+1) - f_k(i)]. \quad (23)$$

## How to use developed software for maximum likelihood estimation of nuclides activities

### *Library of the algorithms*

Developed algorithms for maximum likelihood estimation of nuclides activities are realized in Borland Pascal 7.0 computing language. The library of the procedures and functions, realizing developed algorithms, is organized as the set of the following program modules:

- GLOBUNT.PAS is the library of the auxiliary procedures and functions.
- MATHUNIT.PAS is the library of the auxiliary mathematical function and procedures.
- POLINUNIT.PAS is the library of the functions for processing of polynomials. Where are functions for polynomial spectrum approximation by the least squares method here.
- SPECUNIT.PAS is the library of the functions and procedures for working with the spectra. The structure *TSpectrum* with spectrum data, functions of spectrum saving to disk and spectrum loading from disk are defined here.
- FORMSUNT.PAS is the library of the functions and procedures for working with initial spectra of the nuclides and variations of the initial spectra. There are the function of the spectrometer calibration *MakeNuclideBase* and the function of the spectrometric data preparation *PrepareSpectrometricData* in this module.
- MLMUNIT.PAS is the library of the functions of the nuclides activities estimation by the maximum likelihood method. The functions *MAXLIKMETHOD\_WITH\_SELECTION*, *MAXLIKMETHOD* and *ChiSqr* are here.

Developed library has been tested for compatibility with Delphi 3.0 and Borland Pascal 7.0. To use developed library in Borland Pascal 7.0 programs you must set DOS in conditional defines.

### *Testing of the developed program modules*

We have developed the programs MLMTEST.EXE, MKSPEC.EXE and VIEWSPEC.EXE for testing of the developed program modules. It is also an example of the usage of the developed program modules. Executable file of the programs and source-code are in the main directory of the Software.

The program MLMTEST.EXE has been optimized for using in the Software of the scintillation  $\gamma$ -spectrometers as a module for the nuclides activities estimation by the ML method. The program is used for the calculation of the spectrometric scale parameters, for the spectrometer calibration and for the estimation of the nuclides activities from the spectra of investigated samples by the ML method.

The program MKSPEC.EXE has been developed for simulation of the  $\gamma$ -spectra of the mixture of nuclides  $^{137}\text{Cs}$ ,  $^{40}\text{K}$ ,  $^{228}\text{Ra}$  and  $^{226}\text{Th}$ . The input data of the program are the spectrum accumulation time and the activities of the nuclides  $^{137}\text{Cs}$ ,  $^{40}\text{K}$ ,  $^{228}\text{Ra}$  and  $^{226}\text{Th}$ . The initial spectra of the nuclides  $^{137}\text{Cs}$ ,  $^{40}\text{K}$ ,  $^{228}\text{Ra}$ ,  $^{226}\text{Th}$  and background, used for the spectrum simulation, was obtained from the samples with the density  $1.0\text{ g/cm}^3$  in Marinelli's beaker of 0.5 liter on the  $\gamma$ -spectrometer with NaI(Tl) scintillator (diameter 40 mm and height 40 mm) and 1024-channel analyzer. The files with the initial spectra, used for the spectrum simulation, are found in the directory MKSPEC in files CS137, K40, RA228, TH226 and PHON. The size of the each file is  $1024 \times 4$  bytes (1024 channels and four bytes (single) for each channel).

The program VIEWSPEC.EXE has been developed to view the spectra, stored in files in the format used by the developed programs and program modules.

### *Current application of the developed software*

Developed program modules are used in production-run equipment: scintillation  $\beta$ - $\gamma$ -spectrometer EL 1315 with CsI(Na)  $\gamma$ -scintillator (diameter 63 mm and height 63 mm) and  $\beta$ - $\gamma$ -

radiometer EL 1311 with CsI(Na)  $\gamma$ -scintillator (diameter 150 mm and height 40 mm) and 1024-channel analyzers and radiometer RUG91M with NaI(Tl) scintillator (diameter 40 mm and height 40 mm) and 256-channel analyzer.

### ***Some remarks on application of the developed algorithms***

Using the developed algorithms one should take into account the following:

1. The algorithm of the activities estimation were developed on the assumption of the Poisson statistics of counts in spectrum channels. Application of spectra with other statistics, for example, the smoothed spectra, will always lead to the activities estimates with lower accuracy.
2. Another assumption is an absence of the correlation between the statistical noise components of the initial spectra of the nuclides, a background and investigated sample spectrum, used in activity estimation. Therefore, activity estimates, obtained from the spectrum used in spectrometer calibration or from the spectrum being equal to the background spectrum used in the activity estimation, are not correct.

Therefore, while checking the work of the algorithm for activity estimation from a background spectrum, one should have two spectra of a background independently accumulated. One spectrum should be used as the spectrum of a background, the other spectrum should be used as a spectrum of an investigated sample with unknown nuclides activities.

If it is necessary to check the work of the algorithm in activity estimation from the standard sample, used for the spectrometer calibration, one should use separately accumulated spectrum of that standard sample and separately accumulated spectrum of a background.

3. The developed algorithm of the spectrum model choosing based on the elaborated statistical criteria could be applied in expert systems for nuclides identification. This is because the result of this algorithm execution is a list of the identified nuclides with estimated activities and their errors and the result of the test of goodness of fit.

### **REFERENCES**

- [1] JANOSSY, L., Theory and practice of the evaluation of measurements (Oxford University Press, 1965).
- [2] EADIE, W.T. , DRYARD, D., JAMES, F.E., ROOS, M., SADOULET, B., Statistical methods in experimental physics (North-Holland Publishing Company Amsterdam London, 1971).
- [3] MURAVSKY, V.A., TOLSTOV, S.A., KHOLMETSII, A.L., Comparison of the least squares and the maximum likelihood estimators for gamma-spectrometry, Nucl. Instr. and Meth. in Phys. Res., **B145** (1998) 573-577.
- [4] MURAVSKY, V.A., TOLSTOV, S.A., Algorithms of nuclides activities estimation by the maximum likelihood method, Application of semiconductor detectors in nuclear physics: Abstracts of 5<sup>th</sup> International Conference (Riga, Latvia, May 18-22) 1998, p. 102.
- [5] MURAVSKY, V.A., TOLSTOV, S.A., Statistical criterion for choosing of optimal model of ionizing radiation spectra, Application of semiconductor detectors in nuclear physics: Abstracts of 5<sup>th</sup> International Conference (Riga, Latvia, May 18-22) 1998, p. 103.
- [6] PRESS, W.H., FLANNERY, B.P., VETTERLING, W.T., Numerical recipes: the art of scientific computing (Cambridge University Press, 1986), 206-208.



# USER CONTROLLED ANALYSIS OF GAMMA RAY SPECTRA

**P. Mishev**

Institute of Nuclear Research and Nuclear Energy,  
Bulgarian Academy of Sciences,  
Sofia, Bulgaria

**Abstract.** The program “ANGES” was designed as a general purpose high-resolution  $\gamma$  ray spectrometry program. It offers all main features as commercial software packages except control of acquisition process. The program is able to perform automatic analysis of spectra but it is announced as “user controlled” because it supplies all intermediate results and gives the opportunity these results to be analyzed and corrected by the user. ANGES offers: multi document Windows interface; detailed visualization of spectra; nuclide library based on another contribution to CRP; energy and FWHM calibrations calculated by means of orthonormal polynomial fitting; peak processing engine based on a non-linear LSQ method for fitting peaks; peak location engine, based on first derivative method is provided to ease the preparation of a spectrum for processing; two methods for efficiency calibration (an efficiency calibration curve and reference table); peak identification and activity calculation procedure; a number of corrections (true coincidence summing, background correction, pile up rejection and so on); an option for processing series of similar spectra. The fitting procedure can be applied to the whole spectrum or to a single Region-of-Interest (ROI). The assumed peak shape is pure Gaussian. All peaks in single ROI are assumed to have the same FWHM. The maximum number of peaks in a single ROI is restricted to 25, the maximum ROI length is 512 channels, and the baseline is described with a polynomial of a degree up to 4. As a result of the identification procedure a report file is issued containing spectrum processing results, list of identified and not identified peaks, list of identified nuclides and background nuclides.

ANGES is a general purpose program for high-resolution gamma ray spectrometry. It contains all the components of qualitative and quantitative spectrum processing. The name **ANGES** stands for the **A**nalysis of **GE** detector **S**pectra.

Two main principles was kept into account while designing the program:

- The program is intended for experienced users,
- The program is to help not to guide/restrict the user.

It seems that above principles makes the program just the opposite of so called “automatic” spectrum processing programs. They are very important for routine analysis, but before a program become “automatic” a significant effort is necessary to prepare it for the particular task. At this stage experts on applied gamma ray spectrometry are involved. ANGES is intended not for routine analyses, it is designed to perform the “dirty work” for an expert, but not to stay on her/his way when some corrections are necessary. It offers maximum flexibility and traceability: all intermediate results are available and can be reviewed and controlled. From the other hand once adjusted it can be used easily for routine analyses. It offers all options as commercial software for processing a spectrum with several mouse clicks. The main difference between ANGES and most commercial software packages is that ANGES is not able to control the acquisition process. It is not related to any hardware. This makes it a good solution for free upgrade of analysis software for a well-known and good serving hardware. We offer free support if a kind of discrepancy between file formats of acquisition software and ANGES spectrum file formats appears.

The accepted spectrum file formats are: IAEA ASCII (.spe), ORTEC (.chn), SILENA (.dat) and its internal binary format (.spc).

Spectrum visualisation is based on the multidocument approach. The number of open spectra depends on the computer resources only. All basic visualisation functions are provided in a flexible Windows interface. The program itself uses about 7 MB RAM. Each opened spectrum requires approximately 150KB in addition.

The nuclide library contains complete set of nuclear data for all gamma ray emitters included and additional information as well. The nuclear data includes nuclide name, half-life, energies and yields for all gamma ray lines. Gamma ray lines are subdivided into analytical and additional ones. The analytical lines of a gamma ray emitter are those whose presence or absence determines presence or absence of the emitter itself. The user is free to select the most suitable set of analytical lines for each nuclide depending on the particular task. The rest of gamma ray lines are assigned as additional. The supplementary information includes the user estimation of analytical lines as well as TCS (True Coincidence Summing) factors for 10 different source-detector geometries. The nuclide library is based on data from "Gamma rays from Radioactive Decay" by U. Reus and W. Westmeier (to be published). The original library contains data on 1553 nuclides with over 31000 gamma rays. The abundance cut-off is set at 0.005% and a maximum of 32 lines are listed for a nuclide. In cases of short-lived daughter the intensities are pre-calculated for parent-daughter equilibrium. The nuclide library provided contains a subset of natural nuclides, fission and corrosion products and some long lived activation products. New nuclides can be added manually.

A nuclide table consists of analytical lines of a subset of nuclides. The nuclide tables serve different tasks in energy and efficiency calibration, background correction etc. Both the table and the library are involved in the procedure of nuclide identification. A user-friendly interface is developed to facilitate table creation/edition with only a few mouse clicks.

Energy and FWHM calibrations are calculated simultaneously by means of orthonormal polynomial fitting. The maximal polynomial degree is three and it can be fourthly restricted by the user. The maximum number of peaks involved in the procedure is 25. The calibration data and corresponding fit can be stored in a calibration file and assigned to any other spectrum of the same size. The assignment of a previously stored energy/FWHM calibration to a spectrum can be satisfactory for the FWHM calibration, but not for energy calibration. A procedure is provided to calculate the energy calibration only, while keeping the FWHM calibration unchanged, which allows the user to achieve precise calibration of nearly all sample spectra.

Peak processing engine is based on a nonlinear LSQ method for fitting peaks. All peaks in the spectrum (singlets and multiplets) are fitted. The procedure can be applied on the whole spectrum or inside a single ROI. The assumed peak shape is pure Gaussian. All peaks in a single ROI are assumed to have the same FWHM. The underlying background is approximated with a polynomial function. The algorithm allows guessed peaks in a ROI to be rejected but not added in order to achieve the best approximation.

The maximum number of peaks in a single ROI is restricted to 20. The maximum ROI length is 512 channels. The baseline is described with a polynomial of degree up to four.

Results of spectrum processing are stored automatically to an ASCII file for reviewing and for further usage. Results for single ROI processing are presented graphically and an option is provided to save the numerical results in an ASCII file.

A peak location engine is provided to facilitate preparation of a spectrum for processing. The method used is the analysis of the first derivative of the spectral data. Located peaks are marked and ROIs are created around them using FWHM calibration in such a way that closely situated peaks are marked together in a single ROI. The results of peak search procedure are presented graphically on the spectrum as marked ROIs and located peak positions inside them. After the procedure is completed, the user is free to intervene and to correct the results: to add ROIs and peaks and/or to remove spurious peaks. This way the most powerful peak search instrument - the eye of experienced user can be applied.

Two methods for efficiency calibration are provided: efficiency calibration curve and comparative activity estimation. The efficiency curve method may be used to estimate a large number of nuclides and their activity within a wide energy range, which is often the case in an emergency situation. The disadvantage of the method is that for precise analysis it is necessary to apply TCS (True Coincidence Summing) correction. Obtaining the correction factors is not a trivial task, especially for large volume samples in close-to-detector geometries. The program provides the

possibility for a number of TCS correction factors (for different source-detector assembly) to be stored in the nuclide library and to be available during the efficiency calibration and/or activity calculation procedures. It is the user responsibility to obtain the proper TCS correction factors. The comparative method offers a direct comparison between analytical lines of nuclides presented in both the sample and the standard. The comparative method is free of TCS influence and is suitable for precise measurements. The main disadvantage of this method is based on the restricted number of nuclides presented in the standard that can only be identified and analysed in the samples. Providing the both possibilities the program combines the advantages of both methods.

The efficiency curve is built by orthonormal polynomial approximation of the experimental data collected from the standard reference material. The maximal polynomial degree depends on the number of reference peaks involved. When the number of reference peaks is less than four, line fitting is only available. When four and more peaks are involved in the calibration procedure, the maximal polynomial degree is restricted to  $n-2$ , where  $n$  is the number of peaks.

The peak identification engine is based on an original method. The procedure depends on the method used for efficiency calibration. In both cases only nuclides included in a single nuclide table (reference table, when the direct comparison method is involved) could be identified. It is the user's responsibility to create an appropriate nuclide table. When applying the efficiency curve method the ideal case will be to use a nuclide table containing all nuclides presented in the spectrum and only them. If some nuclides have been omitted, their peaks will be reported as unidentified. Adding too many lines to the table can impede the peak recognition. When the comparative method is used, the number of the nuclides underlying the identification is restricted to the number of nuclides present in the standard (reference table). If there are nuclides in the spectrum covered by two or more reference tables, a separate procedure has to be performed with each table. Only the analytical lines are used for nuclide identification and activity calculation.

The identification procedure uses two criteria to recognise nuclides:

1. Comparison of the peak position energy with that of gamma-lines from the nuclide table. The comparison is successful when a match is found within a user-defined energy interval.
2. Comparison of the results for nuclide activity obtained using different analytical lines. The comparison is considered successful when the activities coincide in a range defined by the user.

The criterion 2 is applied only when the criterion 1 has been satisfied. Once a nuclide is identified, each peak in the spectrum is tested whether it matches any of the additional lines of that same nuclide and if so, found peaks are removed from the list of peaks awaiting identification. After the identification procedure is over (the last peak from the list is processed) a procedure for calculation of MDA/MDC for all nuclides not identified in the spectrum, but included in the nuclide table is applied.

The last procedure to follow is that of escape peaks identification.

A number of corrections can be applied on user's request:

- Detector background correction,
- Dry mass correction,
- Reference date and time correction,
- Decay during the counting correction,
- Live Time/Pile Up Rejection correction,
- True Coincidence Summing correction.

A report file is created as a result of identification procedure. It contains: spectrum processing results, list of identified peaks, list of not identified peaks, list of background peaks, list of escape peaks, list of identified nuclides, list of background nuclides (if background correction was involved), and a list of controlled nuclides. Those are all nuclides from the nuclide table except the identified and background ones. LLD and MDA are calculated and reported for all of them.

After a successful identification an option is provided to pack in a file the whole information involved in obtaining the final result. The pack file includes:

- Spectrum,
- Energy and FWHM calibrations,
- ROIs,
- Peak search settings,
- Nuclide table,
- Efficiency calibration file,
- User settings,
- Corrections applied,
- Identification report.

A comprehensive on-line help and manual are provided. All algorithms used are described in the manual. The on-line help is oriented to describe definitions of terms and procedures included.

Bellow a summary of the characteristics of the program is given according to the requirements and recommendations of K. Debertin [1]. The topics concerned are: peak search, peak fitting, deconvolution of multiple peaks, choice of analysis range, background subtraction, energy and efficiency calibration, uncertainties, detection limits, dead-time and pile-up losses, coincidence summing effects, self-attenuation corrections, data libraries, activity determination, quality assurance and program documentation. The left column of the table contains requirements and recommendations and the right column indicates the ANGES features. The requirements are emphasized by bold face.

#### **Peak search**

---

The sensitivity to be variable	Yes
The manual must describe the mathematical base of the program, the meaning of the sensitivity parameters and their effect of the number of peaks identified	Yes
A test spectrum with small and large peaks to be supplied	Yes
The routine should be able to identify multiple peaks	Yes
The multiple peaks should be tagged in the edited list	No
The peaks found should be markable on the display	Yes
The user must be able to erase and add marks on the display	Yes

#### **Peak analysis**

---

The user must be able to choice the peak regions used for the analysis manually and automatically	Yes
If neighbouring regions overlap, the program should warn the user, who may decide to analyse them individually or as a group	No, overlapping peaks always are marked to be analysed together
The simplest way to calculate peak area should be available	Yes
A peak-fitting algorithm must be available.	Yes
Fixing of all fitting parameters should be available	No
For fitting the background a choice between first- and second-order polynomial should be possible	Yes
Step function should be covered by an additional term	No
In the program description it must be clearly stated which terms of the fitting function are used	Yes
In the analysis of multiple peaks the FWHM and shape components may be the same for all components	Yes
In the analysis of multiple peaks the background may be represented by one function	Yes
Final results should be stored in a file	Yes
The entry for one peak must comprise all fitted and fixed parameters	Yes

If the parameters were fitted, uncertainties must be given	Yes
The reduced chi-square value must be given	Yes
In multiple peak analyses the results must be clearly arranged in a group	<b>Yes</b> , when a single ROI is analysed <b>No</b> , if the whole spectrum is processed

### **Calibration features**

---

The program must provide routines for energy, shape and full-peak efficiency calibration	Yes
The relevant data must be stored in a file	Yes
The program must provide first- and second-order polynomial to fit the calibration data	Yes
The parameters of the fit and residuals should be given in a table .....	Yes
The energy calibration parameters must be stored for use in the actual measurements	Yes
For FWHM calibration a function of the type $\sqrt{(a_1 + a_2 E)}$ should be available	Yes
A plot of the parameters versus energy should be possible	Yes
For the efficiency calibration, the calibration sources and the relevant data should be listed in a extra file	Yes
Tables and plots of the efficiency data and the residuals should be provided	Yes
The efficiency calibration parameters must be stored for use in the actual measurements	No
There should be an option for calculating and storing the radionuclide-specific efficiencies	Yes
Any peaks in the background must be subtracted from actual peaks at the same energy	Yes
A background file must be available, where energies, count rates and uncertainties are stored	Yes
This file should allow several entries at different time, which can be averaged	No, each calibration provides a separate file.

### **Evaluation of a sample spectrum**

---

The user must have the opportunity to look at the peaks found by the search routine	Yes
Peaks may then be erased or added	Yes
It must be decided which peak parameters will be kept fixed in the fitting procedure	No
The program must allocate to each energy the possible radionuclides and calculate the activity	Yes
If a radionuclide emits gamma rays with more than one energy, the activity is to be calculated for all energies	Yes
The final file with the identified nuclides must contain all energies, the corresponding activities, the relative standard uncertainties and a tag indicating whether the peak is a component of a multiple peak	Yes, without indication for multiple peaks.
For each radionuclide the weighted mean of the activity values should be calculated	Yes
Determination of specific activities should be possible	Yes
An export of the data in all files mentioned up to now must be foreseen	Yes

### **Data library**

---

A data library with entries for natural and artificial radionuclides must be available	Yes
The data should be grouped according to fields of application	Yes
If a nuclide has a short-lived daughter, separate data sets for the daughter, the parent and parent/daughter equilibrium should be given.	No, only data for parent/daughter equilibrium.
The data format must allow the entry of additional data (correction factors)	Yes
It must be possible to enter additional data for different source-to-detector geometries	Yes
Minimum ten additional entries per gamma ray should be possible	Yes

### **Corrections**

---

Dead-time and pile-up corrections	Yes
Coincidence summing corrections	Yes
Corrections for differences in the attenuation properties	No
Corrections for differences in the measuring geometries	No
Correction for decay during the measurement	Yes
Correction for parent/daughter relationship	No

### **Uncertainties and detection limits**

---

All uncertainties should be quoted in terms of standard deviations	Yes
The full covariance matrix resulting from the peaks should be available	No
The uncertainties must be given for all fitted parameters in the peak analysis, the data library, efficiency values and activities	Yes (not for data library)
A special option must be available to calculate detection limits for different gamma rays	Yes
The algorithm for this calculation must be quoted	Yes

### **Quality assurance**

---

Mathematical formulas, functions and algorithms used must be clearly and explicitly given	Yes
The source of the data in the library must be quoted	Yes
The user should be guided to initiate special runs for quality assurance purposes	No

## **REFERENCE**

- [1] K. DEBERTIN, K., *Requirements on Gamma-Ray Spectrum Analysis Programs*, Software for Nuclear Spectrometry, IAEA-TECDOC-1049, 1998, p.11.

# NUCLEAR DATA LIBRARIES FOR GAMMA ANALYSIS PROGRAMS, INCLUDING SPECIAL PURPOSE LIBRARIES

W. Westmeier, U. Reus, K. Siemon, H. Westmeier

Gesellschaft fuer Kernspektrometrie mbH,  
Ebsdorfergrund-Moelln, Germany

**Abstract.** A complete set of gamma ray and other data relating to the decay of all known nuclides has been compiled from the literature and electronic sources. The data were critically reviewed, evaluated and the consistency was checked. The total catalogue is comprised of data-sets for 3841 nuclides and isomers with 106,355 gamma ray and 19,347 X ray entries. A subset of 1,627 nuclides with 32,456 gamma ray entries is extracted into a database, which provides the basis for the generation of nuclide libraries for the application in spectrometry programmes. The WINDOWS based program NUC\_MAN was developed which serves for the updating and editing of the database as well as the generation of task-specific user libraries for special purposes. The literature cut-off date for this catalogue is January 1, 1998.

## Introduction

A compilation of gamma rays originating from radioactive decay is primarily designed for the use of workers engaged in quantitative assay of radionuclides such as activation analysis, contamination control, environmental supervision and cross-section measurements. It should also be a helpful tool in nuclear spectrometry where, for example, it can be used to identify gamma rays emitted from daughter nuclei or source impurities.

As an update of an earlier catalog of gamma rays from radioactive decay [1] we have compiled and evaluated the data published since then and generated a database of gamma ray and other data for all known nuclides. The data are comprised of nuclide name and half-life, spin and parity, decay modes and branching intensities, Q-values,  $(n,\gamma)$  cross sections, gamma- and X ray energies with their intensities and associated information, precursor information, literature references as well as comment and text lines. Uncertainties are given for most numerical values.

A short explanation of the compilation and evaluation policies and of the library data is given in the following.

## Literature coverage

The data are obtained from literature referenced in Nuclear Data Sheets [2] and publications, which we received before January 1, 1998. At present, the catalogue contains data on 3841 nuclides and isomers with more than 120,000 photon energies.

## Data selected

Preference is given to data which have been consistently determined in several different studies. In cases of conflicting results, data which are confirmed by the majority of researchers are chosen. Reference to the data omitted is then explicitly given in a comment.

## Gamma ray energies

Up to 350 gamma ray energies are included for each nuclide or isomer. Usually, gamma rays with very low abundance are not included, except for a few nuclides where only weak gamma lines are present. Annihilation radiation from positron emitters is listed only in cases where no gamma or X rays of the respective nuclide are readily discernible. Gamma ray energies above 10 MeV are not listed. Notice should be taken that the applied intensity cutoff is on the absolute intensity and that in the case of relative intensities a different cutoff may have been used.

## Gamma ray abundances

Gamma ray abundances are listed as number of photons per 100 disintegrations. Relative abundance values are marked with an asterisk (\*). In the latter cases the strongest line is normalized to 100%.

## Normalization

Relative photon intensities are converted to number of photons per 100 decays, provided that decay schemes are sufficiently well determined. For the calculations, the internal conversion coefficients are interpolated from the tables of Hager and Seltzer [3]. If no experimental information about the intensity of the beta decay or electron capture branch to the ground state of the daughter nucleus is available, log-ft values from comparison with similar decay schemes are assumed, and intensity estimates are obtained using the log-f tables of Gove and Martin [4]. With these estimates one calculates at least the order of magnitude of the normalization factor, which then is given in a comment.

## X rays

X ray information, which allows the identification of the emitting element, is supplied. X rays listed here are labelled by atomic species only. X ray energies are taken from the tables of Bearden [5].

Data on K x rays accompanying the decay of individual nuclides are given whenever possible. Components listed are:  $K_{\alpha 1}$ ,  $K_{\alpha 2}$ ,  $K'_{\beta 1}$  ( $=K_{\beta 1} + K_{\beta 3}$ ), and  $K'_{\beta 2}$  ( $=K_{\beta 2} + K_{\beta 4}$ ). For elements with atomic number  $Z < 50$ , the separation is made into  $K_{\alpha}$  and  $K_{\beta}$  X rays only.

Quoted abundances of K X rays are based on measurements, where possible. However, since the number of measurements reported in the literature is small, many abundances had to be calculated. These calculations yield reliable results provided that the decay scheme of the nuclide is well established. Quantities used for the calculation are: internal conversion coefficients from the tables of Hager and Seltzer [3], ratios of electron capture to positron decay ( $\epsilon/\beta^+$ ) and the fractions of K capture ( $\epsilon_K/\epsilon$ ) from the tables of Gove and Martin [4], fluorescence yields from an empirical fit by Bambynek et al. [6], and relative X ray intensities from tables of Salem et al. [7]. L X rays are listed if measured abundances are known. They are calculated only for a few nuclides emitting no K X rays and no strong gamma rays. The same references as stated above have been used. It should be noted, however, that for L X rays the calculations are afflicted with large systematic uncertainties and that calculated L X ray abundances should be considered as tentative. Calculated L X ray abundances are accompanied by a comment. Omitting X rays in connection with a specific nuclide does not imply that no x rays are emitted in the decay. There are two reasons for the omission of X rays:

- X ray abundances are negligible, which is true for many nuclides decaying by negatron emission;
- the existing decay scheme data are insufficient for the calculation of X ray abundances. These cases are not separately indicated.

## Stable nuclei

Isotopic abundances of naturally occurring isotopes are taken from the tabulation of Holden [8]. Thermal neutron cross sections are adopted from Mughabghab et al. [9]. Spins and other details are from Nuclear Data Sheets [2] if no other reference is given. These three references are implied in the literature abbreviation KNK [10], which is used in the catalog. The authors of KNK refer to essentially the same three references as quoted above.

## References (literature sources)

The literature sources from which data were taken are indicated with the data sets. There may be different references for e.g. the gamma ray data, spin and parity, Q-values or half-life. Large differences encountered in various publications are noted in a comment.

The table below lists the most frequently used journals and sources of information for this Gamma-Ray Catalogue.

TABLE 1. LITERATURE SOURCES FROM WHICH THE MAJORITY OF THE GAMMA RAY DATA LISTED ARE TAKEN.

APPOB	Acta Physica Polonica B
CERN	CERN report (see below)
CJPH	Canadian Journal of Physics
CZJPB	Czechoslovak Journal of Physics B
IANFA	Izvestija Akademii Nauk SSSR, Serija Fizika
IJARA	International Journal of Applied Radiation and Isotopes
JINC	Journal of Inorganic and Nuclear Chemistry
JPHG	Journal of Physics (London) G
JPHP	Journal of Physique (Paris)
JPSJ	Journal of the Physical Society of Japan
KNK	Karlsruher Nuklidkarte, 6. Auflage 1995
NDS	Nuclear Data Sheets
NIM	Nuclear Instruments and Methods in Physics Research
NPA	Nuclear Physics A
PHSC	Physica Scripta
PRC	Physical Review C
PRLT	Physical Review Letters
PYLB	Physics Letters B
RAAC	Radiochimica Acta
RAAL	Radiochemical and Radioanalytical Letters
ZPA	Zeitschrift für Physik A - Atoms and Nuclei

Literature in the form of laboratory reports is not included in the compilation except for: CERN Reports 76-13 and 81-09, Proceedings of the International Conference on Nuclei For from Stability. The number of literature sources actually scanned for the compilation of this catalogue was greater than that represented by the list of abbreviations given above.

## Daughter nuclides

In the decay of a parent nucleus, a daughter whose half-life is short compared to that of the parent may be formed. Provided that the difference in half-lives is large, transient equilibrium will be reached after some time. For practical purposes we define the parent's half-life to be at least twice as long as that of the daughter in order to consider the decay as being in transient equilibrium. If this condition is fulfilled, gamma rays from the decay of the daughter are also listed with the parent. Abundances of these daughter gammas are calculated for the case of transient equilibrium, that is:

$$I_E = I_D \frac{\lambda_D}{\lambda_D - \lambda_P} BR \quad (1)$$

where  $I_E$  is the abundance observed in the case of transient equilibrium;  $I_D$  is the abundance of the same transition in the decay of the daughter alone;  $\lambda_P$  and  $\lambda_D$  are the decay constants of parent and

daughter, respectively; and BR is the branching ratio for the decay from parent to daughter. The quoted abundance of daughter lines thus corresponds to the abundance actually measured. It can be used directly in calculations (for example, to determine the yield of the parent in nuclear reactions) without further corrections, provided that transient equilibrium has been reached in the experiment. The same algorithm applies to gamma rays labelled G which partially arise from the decay of an isomeric state of the daughter. In cases where the parent's half-life is less than twice that of the daughter, the comment "DAUGHTER GAMMAS FROM..." is given in the catalog and the daughter gammas are not listed with the parent.

The catalog contains extensive data for each nuclide together with the relevant references, supplementary information and comments. In some cases, where data from different literature sources are in disagreement, we have made every effort to choose the results which seem most reasonable. If we could not find any reason for discrepancies, we have included a comment about those publications which have been omitted from the data compilation. We believe that these comments are of great importance, because they point out uncertainties and inconsistencies in the data and may help to solve some of the user's problems.

### **Gamma spectrometry libraries**

The initial goal of this research agreement was the creation of a database and a managing computer program that could fit the needs of all workers in gamma ray spectrometry and all its applications. The program should be able to create libraries to be used in all spectrometry programs on the market. However, it was found that such universal library creation under the conditions of this CRP research agreement is an unmanageable task and that very stringent restrictions are needed. There is a common set of data needed by researchers in for example: reaction cross sections or in prompt gamma assay or in environmental surveys or in nuclear level systematics. For each of these tasks there is another set of very specific data that is also needed but which is of no relevance to the others. Furthermore, in each spectrometry programme there is a different structure and completeness of the nuclide library, sometimes the internal data are pre-processed for specific applications and often the library structure is proprietary and not accessible. Therefore it was decided that the library facility provided by this work should supply the basic information for each nuclide and that each user according to need must add application-specific information.

A master library (MASTER.LIB) was generated which holds data for all gamma-emitting radionuclides with a half-life in excess of 10 seconds. For each nuclide the name is listed in the usual representation: IUPAC symbol for the element, followed by a hyphen, followed by the mass number of the nuclide, and where applicable followed by the letter m (metastable state). The letter m may be followed by a running number 1,2,... if several long-lived metastable states exist. Examples of nuclide names in the library are Be-7, Na-22, V-50, Co-54m or Pm-152m1. The half-life of each nuclide is stored with up to five significant digits in scientific (exponential) notation and the units are Second, Minute, Hour, Day or Year. For each nuclide a maximum of 32 gamma ray energies and the concurrent absolute intensities are provided. There are several nuclides that have very many intense and important lines. For these nuclides Eu-152, Eu-154, Bi-214, Ac-227, Ac-228, Ra-226, Th-228, and Th-232 a second data set with up to 32 lines is created where the nuclide name is extended by -x; example : Th-232-x. The intensity cut-off for all nuclides is set at an absolute intensity of 0.005%. X ray energies are omitted from the master library.

For practical purposes the lines in the library are sorted in the order of falling "detectability", i.e. the typical efficiency function of a p-type germanium detector and the typical relative height of the baseline distribution are considered. Thus, a line should only be assigned to a nuclide if the other lines prior in the list are also detected in the spectrum.

The MASTER.LIB at present holds data for 1627 nuclides with a total of 32456 gamma ray entries. All energies in the master library were compared to the recommended "best" data given in a recent publication by Helmer et al. [11]. There are small differences encountered between the data in the MASTER.LIB and the data from Helmer; however, as the differences are within uncertainties we have not modified our data sets.

A 32-bit WINDOWS programme named NUC\_MAN was developed which allows the very easy handling of the library data. The programme is written so that it is operative under all current versions of WINDOWS 95, 98 and NT. Standard options and structures from WINDOWS are used wherever possible. Thus NUC\_MAN is a programme that is very easy to use for all who are already familiar with WINDOWS programmes. There are two folders in the display page of NUC\_MAN; one folder serves for the creation of a new (target) library or the extension of an existing (target) library through excerpting of data from another (source) library. The other folder provides the tools to edit the data in a library and to delete, create or re-order nuclides. The open access to nuclide library data is a frequent request from users that has also been provided. It is particularly useful when the user wants to generate his own setup-specific library, for example, with data that quantitatively consider summing effects or absorption losses through apparent line intensities. We of course are not responsible for the correctness of data that were edited or otherwise modified.

In order to simplify work for many users we have created several special purpose libraries containing only data for those nuclides that are relevant in a field. Libraries supplied with the NUC\_MAN programme are:

MASTER.LIB	Containing data for 1627 nuclides with 32456 gamma ray entries, i.e. all nuclides with a half-life $\geq 10$ seconds. This library must always be present in the same directory where NUC_MAN is started and it is automatically opened at program start.
INAA.LIB	Containing data for 221 nuclides with 3260 gamma ray entries. This library holds data for all nuclides that can be produced by activation with thermal and epithermal neutrons.
KKW.LIB	Containing data for 134 nuclides with 3162 gamma ray entries. This library holds data for all negatron emitting nuclides with a half-life $\geq 10$ minutes whose isobaric yield in the fission of $^{235}\text{U}$ induced with thermal neutrons exceeds 0.01%. A few nuclides frequently found as activation products are also included. The library is mainly provided for nuclear power plant applications.
STANDARD.LIB	Containing data for 105 nuclides with 1596 gamma ray entries. This library holds data for nuclides that are frequently used for calibration purposes, that are commercially available, or that are listed in publications which recommend standards [11,12].
IMIS.LIB	Containing data for 76 nuclides with 1570 gamma ray entries. This library holds data for nuclides used for the environmental supervision in Germany.
SIPPING.LIB	Containing data for 34 nuclides with 642 gamma ray entries. This library holds data for nuclides assayed in sipping analyses in nuclear power plants.
NUCMED.LIB	Containing data for 17 nuclides with 120 gamma ray entries. This library holds data for nuclides frequently used in nuclear medicine applications.
NATURE.LIB	Containing data for 10 nuclides with 280 gamma ray entries. This library holds data for nuclides found in the environment and in external background spectra.

When the NUC\_MAN program is delivered with the above libraries all files are "zipped" into the self-extracting file NUCL\_ZIP.EXE. This file of ca. 620k bytes length is to be copied into the target directory (e.g. C:\NUCLIB) and started there. The program NUCL\_ZIP will automatically come up in the DOS shell of your WINDOWS system and extract all files. The user can then start the NUC\_MAN program from the WINDOWS environment. When the NUC\_MAN program is linked to the desktop it will automatically provide its own icon.

In the following the handling of libraries and data with the NUC\_MAN program is briefly explained. For simplification, the operator will be guided in the "you" form which allows for easier and more understandable explanations:

When the programme is started you will see the Company Identification page and you must click OK to enter the programme. There are two dialog pages (folders) indicated by the indexing labels "Make Library" and "Edit Library". On entering the programme the "Make Library" page is active with the MASTER.LIB loaded as shown in Figure 1.

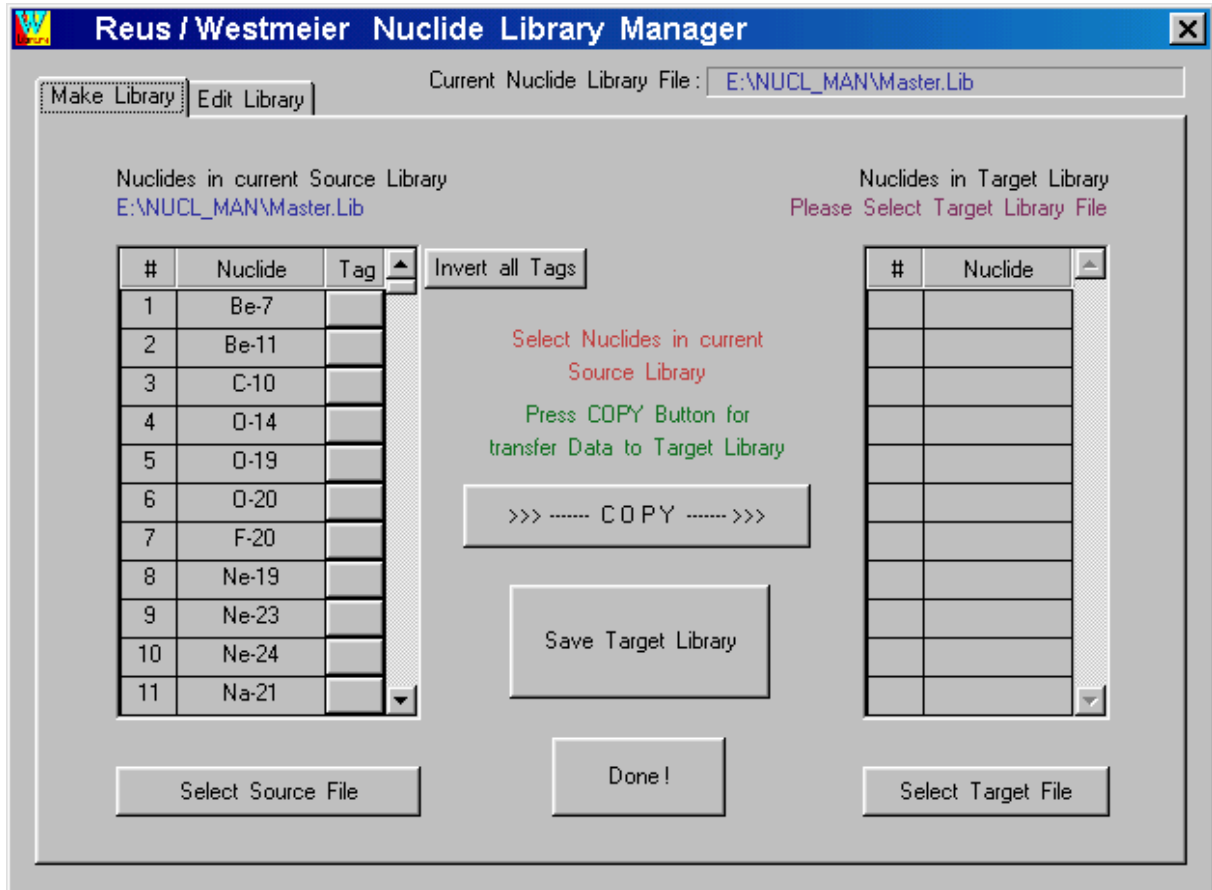


Fig.1. Opening window of the NUCL\_MAN programme used for creating new libraries.

Basically the page consists of two scroll boxes, one for a source library on the left and the other for a target library on the right, plus several buttons to operate the libraries.

You may select another source library with the "Select Source File" button on the left side under the box listing the nuclides. The standard WINDOWS file-handling window will then open and you can select the source library from any desired unit and path. The name of the current (source) library file is listed in the top right corner of the window under the Programme Identification bar. The names of nuclides in that library are listed in the scroll box on the left and you can browse through the sequentially numbered list by pulling the scroll button or clicking the up/down arrows.

## Creation of new libraries

You may create a new user (target) library from data in any other (source) library. On the right end of each nuclide name in the source library is a toggle button called "Tag" which is activated when clicked, i.e. the button is white, and deactivated with the second click. In a first step you may activate all nuclides that you want to transfer into the new user library. Then you click the "COPY" button and data for all activated nuclides are copied into the target library. You will see the names of the copied nuclides in the right (target) scroll box. If you want to add nuclides from another source library you may Select Source Library, Tag the required nuclides and COPY to the target library. All nuclides that exist in a target library will be automatically tagged in the source library as well. When the target library is complete it may be saved with the "Save Target Library" button which will again open the WINDOWS file handling window. You may also select any existing library file as the target library with the "Select Target Library" button and extend this library from other source libraries.

When you exit the NUC\_MAN programme with the "Done" button the program will for safety reasons always ask if you want to save the target library.

## Viewing and editing of data

The "Edit Library" page serves for the viewing and editing of data in a library. In this folder you see the data for one nuclide at a time where the gamma ray energy and intensity data are listed in a scroll box as shown in Figure 2. Over the box you will see the index number of this nuclide in the library, the Nuclide name and the halflife. The name of the active library is listed on the top in the right half of the page. The active library in the "Edit" page is the same as the source library in the "Make" page. Below the name are buttons for saving the current library file or opening a new library for editing.

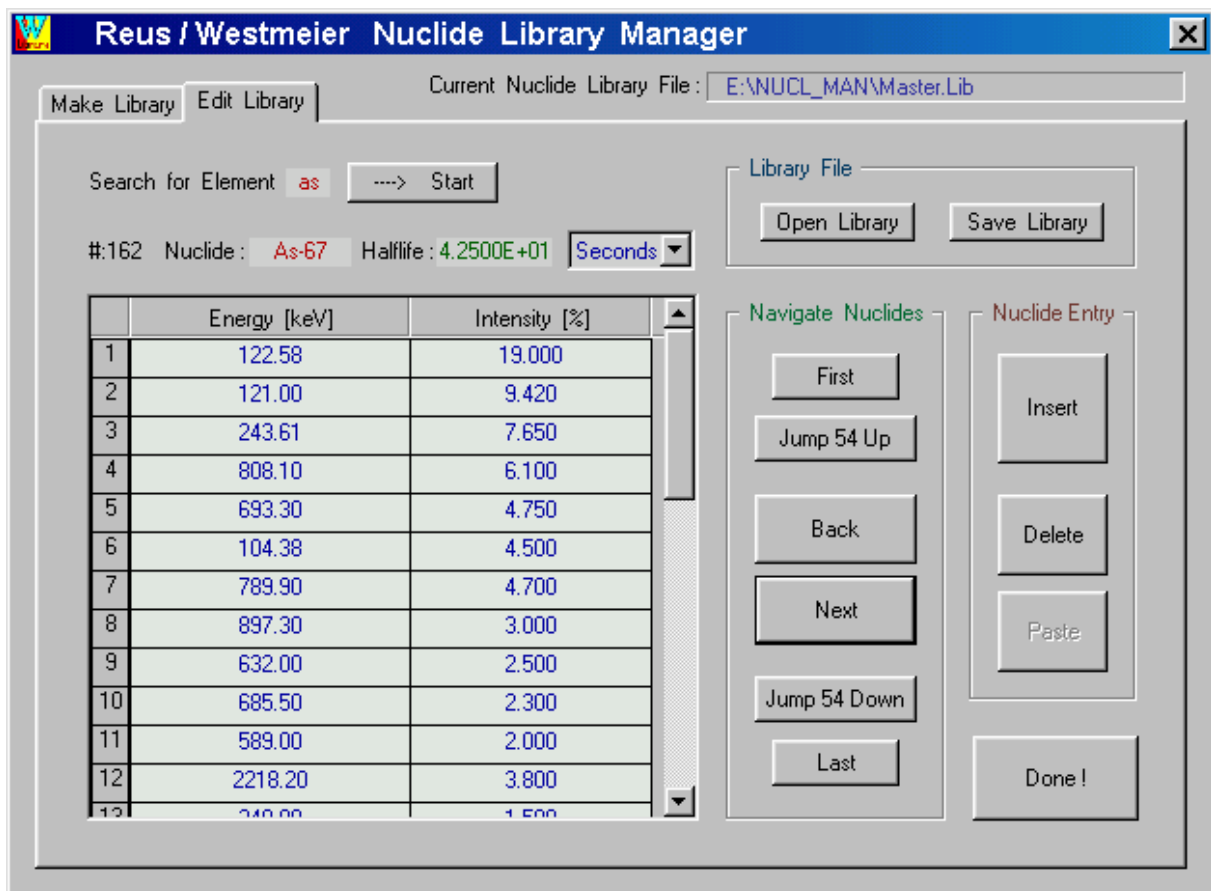


Fig. 2. "Edit Library" screen of the NUC\_MAN programme.

The buttons in the "Navigate Nuclides" section are used to:

- select the first or last nuclide in the list (top and bottom button)
- select the following (Next) or preceding( Back) nuclide or
- jump through the library in bigger steps (Jump Up or Jump Down).

For the jump function the library is divided into 30 steps of equal length, thus a library containing 121 nuclides will allow Jump steps over 4 nuclides. Another useful feature for scanning larger libraries is the "search for element". You may enter the symbol for an element in the box over the nuclide name (**not** case sensitive) and search for the next following nuclide of this element in the library with the "start" button. When the end of the library is reached during the search, the programme will continue searching from the beginning of the library.

The buttons in the "nuclide entry" section serve for the re-ordering of nuclides or for deleting complete data sets.

- ❑ **To edit data** of a nuclide you just click into the respective data field and erase or modify the data as desired. There is no check as to whether the new data are meaningful or not. The unit for the half-life is selected from the drop-down box.
- ❑ **To delete a line** from the list just delete the energy value, i.e. blank the energy field; the line will be deleted when the next nuclide is selected or when the library is saved.
- ❑ **To delete a nuclide** from the library use the "delete" button. The data set is then taken out of the library and stored in an internal one-nuclide buffer for retrieval. When you delete a second nuclide the data from the first deleted nuclide are overwritten in this buffer.
- ❑ **To move a nuclide** entry to another place within the library you must first delete this nuclide. You may note that the "paste" button is activated when a nuclide was deleted. Then select the nuclide **after** which you want to place the nuclide and push the "paste" button. The retrievable nuclide is now listed in the selected place.
- ❑ **To create a new nuclide** entry in the library select that nuclide after which the new entry shall be found and press the "insert" button. The program will create empty space for one nuclide which can be filled with data as described above under "To edit data".
- ❑ **To save the library** use the "save library" button and define the filename and destination for the file in the WINDOWS file managing window.

When you exit from the NUC\_MAN program with the "done" button the program will for reasons of safety always ask if you want to save the current library.

- ❑ **To export data for other programmes** the NUC\_MAN programme has a built-in ASCII-file feature. Whenever a library is read into the programme it will automatically write an ASCII file with the dedicated filename NUC\_MAN.OUT in which all data from the currently open library are listed in a fixed, pre-defined format (see listing of the NATURE.LIB below). The last NUC\_MAN.OUT file is always overwritten when the programme is restarted. If you want to keep the ASCII data from the last session you must rename the file. You may use these ASCII data to create libraries according to the specifications of your spectrum analysis programme.

Listing of the library NATURE.LIB as found in the ASCII transfer file NUC\_MAN.OUT is given below as example of user created library.

Reading Library : E:\NUCL\_MAN\Nature.lib  
Number of Nuclides in Library : 13

Be-7 5.3150E+01 D  
1 477.603 10.520

K-40 1.2770E+09 Y  
1 1460.830 10.670

Cs-134 2.0648E+00 Y  
1 604.722 97.620  
2 795.865 85.530  
3 569.331 15.380  
4 563.245 8.350  
5 801.951 8.690  
6 1365.193 3.014  
7 475.364 1.486  
8 1167.964 1.789  
9 1038.607 0.988  
10 242.743 0.027  
11 326.589 0.016  
12 847.040 3.00E-04

Cs-137 3.0070E+01 Y  
1 661.660 85.100  
2 283.410 5.80E-04

Bi-214 1.9900E+01 M  
1 609.315 45.300  
2 1120.292 14.950  
3 1764.490 15.480  
4 1238.111 5.830  
5 768.357 4.890  
6 1377.670 3.960  
7 934.056 3.120  
8 2204.120 4.980  
9 1729.604 2.970  
10 1407.980 2.370  
11 1509.230 2.130  
12 665.440 1.470  
13 1155.183 1.633  
14 1847.422 2.070  
15 1280.970 1.420  
16 806.171 1.210  
17 1401.490 1.290  
18 1661.270 1.120  
19 2447.680 1.543  
20 2118.541 1.169  
21 1385.310 0.761  
22 1583.240 0.688  
23 703.060 0.468  
24 388.940 0.386  
25 1207.690 0.446  
26 719.870 0.380  
27 964.090 0.364  
28 454.850 0.302  
29 386.823 0.290  
30 1538.460 0.383  
31 786.420 0.310  
32 1051.960 0.309

Bi-214-x 1.9900E+01 M  
1 1599.350 0.321  
2 1070.020 0.268  
3 1543.369 0.300  
4 1838.380 0.349  
5 1133.660 0.249

6 1594.810 0.271  
7 405.730 0.166  
8 2293.330 0.307  
9 273.790 0.130  
10 1684.020 0.215  
11 821.180 0.156  
12 469.756 0.126  
13 1873.130 0.210  
14 752.850 0.128  
15 349.010 0.100  
16 474.520 0.106  
17 826.450 0.098  
18 1895.880 0.146  
19 1303.730 0.107  
20 1103.610 0.095  
21 351.936 0.070  
22 572.670 0.077  
23 683.200 0.080  
24 333.350 0.067  
25 280.890 0.065  
26 542.850 0.071  
27 710.730 0.074  
28 904.320 0.075  
29 536.780 0.066  
30 1104.780 0.078  
31 1316.920 0.077  
32 649.180 0.059

Ra-226 1.6000E+03 Y

1 609.315 45.300  
2 351.932 36.270  
3 295.220 18.600  
4 1120.292 14.950  
5 1764.490 15.480  
6 241.997 7.360  
7 1238.111 5.830  
8 768.357 4.890  
9 186.211 3.530  
10 1377.670 3.960  
11 934.056 3.120  
12 2204.120 4.980  
13 1729.604 2.970  
14 1407.980 2.370  
15 1509.230 2.130  
16 665.440 1.470  
17 1155.183 1.633  
18 1847.422 2.070  
19 1280.970 1.420  
20 806.171 1.210  
21 1401.490 1.290  
22 785.770 1.080  
23 1661.270 1.120  
24 2447.680 1.543  
25 2118.541 1.169  
26 1385.310 0.761  
27 258.870 0.511  
28 839.000 0.571  
29 1583.240 0.688  
30 274.800 0.440  
31 703.060 0.468  
32 487.070 0.419

Ra-226-x 1.6000E+03 Y

1 388.940 0.386  
2 1207.690 0.446  
3 46.539 4.310  
4 719.870 0.380

5 580.130 0.350  
6 480.440 0.322  
7 9.470 5.00E-04  
8 964.090 0.364  
9 454.850 0.302  
10 386.823 0.290  
11 1538.460 0.383  
12 786.420 0.310  
13 1051.960 0.309  
14 1599.350 0.321  
15 461.970 0.224  
16 1070.020 0.268  
17 1543.369 0.300  
18 1838.380 0.349  
19 53.227 1.050  
20 1133.660 0.249  
21 1594.810 0.271  
22 533.670 0.180  
23 405.730 0.166  
24 2293.330 0.307  
25 273.790 0.130  
26 1684.020 0.215  
27 821.180 0.156  
28 469.756 0.126  
29 1873.130 0.210  
30 752.850 0.128  
31 349.010 0.100  
32 474.520 0.106

Th-232 1.4050E+10 Y

1 13.520 1.600  
2 12.880 0.300  
3 238.632 43.300  
4 583.192 30.511  
5 911.207 25.800  
6 2614.533 35.870  
7 968.966 15.800  
8 338.319 11.270  
9 510.650 8.090  
10 727.329 6.580  
11 240.982 4.100  
12 209.255 3.890  
13 463.010 4.400  
14 964.766 4.990  
15 860.560 4.460  
16 270.244 3.460  
17 794.947 4.250  
18 300.089 3.280  
19 328.000 3.070  
20 129.064 2.420  
21 277.370 2.320  
22 1588.189 3.220  
23 409.452 1.920  
24 835.702 1.610  
25 772.296 1.490  
26 99.495 1.260  
27 1630.629 1.510  
28 1620.731 1.490  
29 84.373 1.220  
30 785.370 1.100  
31 755.314 1.000  
32 562.505 0.870

Th-232-x 1.4050E+10 Y

1 153.983 0.722  
2 840.370 0.910  
3 904.192 0.770

4 1495.980 0.860  
5 1459.126 0.830  
6 115.183 0.592  
7 763.280 0.647  
8 726.872 0.620  
9 830.485 0.540  
10 1078.630 0.564  
11 508.946 0.450  
12 782.144 0.485  
13 1580.519 0.600  
14 332.369 0.400  
15 1247.043 0.500  
16 340.962 0.369  
17 452.820 0.378  
18 288.080 0.337  
19 199.407 0.315  
20 1501.566 0.460  
21 893.406 0.378  
22 1638.278 0.470  
23 215.985 0.254  
24 252.630 0.259  
25 1110.612 0.305  
26 321.644 0.226  
27 958.640 0.280  
28 1512.690 0.290  
29 278.910 0.191  
30 478.394 0.209  
31 546.469 0.201  
32 145.848 0.158

U-234 2.4550E+05 Y

1 120.900 0.034  
2 53.220 0.123  
3 454.910 2.50E-05  
4 508.130 1.50E-05  
5 581.680 1.20E-05  
6 677.510 9.00E-07  
7 503.390 8.00E-07  
8 624.290 8.00E-07

U-235 7.0380E+08 Y

1 185.714 57.200  
2 6.380 0.090  
3 269.480 13.800  
4 235.970 12.400  
5 351.060 12.990  
6 143.762 10.960  
7 271.230 10.900  
8 14.380 0.016  
9 9.920 0.014  
10 256.245 6.800  
11 401.810 6.400  
12 154.180 5.640  
13 163.357 5.080  
14 205.309 5.010  
15 84.216 6.600  
16 300.032 4.580  
17 329.919 4.080  
18 323.890 3.950  
19 404.854 4.040  
20 144.260 3.240  
21 831.951 3.770  
22 302.670 2.800  
23 338.270 2.810  
24 286.103 1.720  
25 427.099 1.840  
26 283.690 1.660

27 109.180 1.540  
28 79.722 1.990  
29 210.600 1.180  
30 445.030 1.280  
31 93.930 1.460  
32 122.310 1.200

U-238 4.4680E+09 Y  
1 609.315 45.300  
2 351.932 36.200  
3 295.220 18.600  
4 1120.292 14.950  
5 1764.490 15.480  
6 241.997 7.360  
7 1238.111 5.830  
8 768.357 4.890  
9 186.211 3.539  
10 1377.670 3.960  
11 934.055 3.110  
12 92.370 2.800  
13 2204.120 4.980  
14 92.800 2.770  
15 63.300 4.800  
16 1729.604 2.970  
17 1407.980 2.370  
18 1509.230 2.130  
19 665.440 1.470  
20 1155.183 1.633  
21 1847.422 2.070  
22 1280.970 1.420  
23 806.171 1.210  
24 1401.490 1.290  
25 785.770 1.080  
26 1661.270 1.120  
27 1001.030 0.839  
28 2447.680 1.543  
29 2118.541 1.169  
30 1385.310 0.761  
31 258.870 0.511  
32 839.000 0.571

## Conclusion

A compilation of up-to-date gamma ray and other data relating to the decay of radionuclides has been completed. Data that were taken from recent publications in the scientific literature and other sources were critically reviewed, evaluated and the consistency was checked. A sub-set of data was defined for inclusion in a smaller database for the generation of specific user-libraries. With the aid of a newly developed programme NUC\_MAN the user can create his own task-specific libraries or edit and update the data in the database. The programme is developed to run in the 32-bit WINDOWS environment, i.e. all versions of WINDOWS 95, 98 and NT. The programme employs standard features of WINDOWS programmes wherever possible, thus enabling all users to operate it without major instruction. A brief documentation of the policies of data collection and evaluation as well as the handling of the NUC\_MAN programme has been provided.

## REFERENCES

- [1] REUS, U., WESTMEIER, W., Catalog of Gamma-Rays from Radioactive Decay, Part I and Part II, Atomic Data and Nuclear Data Tables, **Vol. 29**, Nos. 1&2 (1983).
- [2] Nuclear Data Sheets, edited by The National Nuclear Data Center for The International Network for Nuclear Structure Data Evaluation (Academic Press, New York).

- [3] HAGER, R.S., SELTZER, E.C., Nuclear Data Tables **A4** (1968) 1.
- [4] GOVE, N.B., MARTIN, M.J., Nuclear Data Tables **A10** (1971) 205.
- [5] BEARDEN, J.A., Rev. Mod. Phys. **39** (1967) 78.
- [6] BAMBYNEK, W., CRASEMANN, B., FINK, R. W., FREUND, H.-U., MARK, H., SWIFT, C.D., PRICE, R.E., VENUGOPALA RAO, P., Rev. Mod. Phys. **44** (1972) 716.
- [7] SALEM, S.I., PANOSSIAN, S. L., KRAUSE, R.A Atomic Data and Nuclear Data Tables **14** (1974) 91.
- [8] HOLDEN, N.E., IUPAC, Commission on Atomic Weights and Isotopic Abundances, Pure Appl. Chem. **52** (1980) 2349.
- [9] MUGHABGHAB, S.F., GARBER, D.I., National Neutron Cross Section Centre, BNL-325, 3<sup>rd</sup> ed., **Vol. 1** (1973); for  $Z \leq 60$ : MUGHABGHAB, S.F., DIVADEENAM, M., HOLDEN, N.E., Neutron Cross Sections (Academic Press, New York), 1981, **Vol.1**.
- [10] PFENNIG, G., KLEWE-NEBENIUS, H., SEELMANN-EGGEBERT, W.†, Nuklidkarte, 6. Auflage, Kernforschungszentrum Karlsruhe GmbH, Karlsruhe, Germany (1995).
- [11] HELMER, R.G., VAN DER LEUN, C. †, Recommended Standards for  $\gamma$ -Ray Energy Calibration, Nucl. Instr. And Meth. , to be published
- [12] HERMAN, M., NICHOLS, A., Update of X-Ray and  $\gamma$ -Ray Decay Data Standards for Detector Calibration and Other Applications, IAEA RCM Summary Report, INDC(NDS)-403, July 1999.

# “TRUECOINC”, A SOFTWARE UTILITY FOR CALCULATION OF THE TRUE COINCIDENCE CORRECTION

S. Sudár

Institute of Experimental Physics,  
University of Debrecen, Hungary

**Abstract.** The true coincidence correction plays an important role in the overall accuracy of the  $\gamma$  ray spectrometry especially in the case of present-day high volume detectors. The calculation of true coincidence corrections needs detailed nuclear structure information. Recently these data are available in computerized form from the Nuclear Data Centers through the Internet or on a CD-ROM of the Table of Isotopes. The aim has been to develop software for this calculation, using available databases for the levels data. The user has to supply only the parameters of the detector to be used. The new computer program runs under the Windows 95/98 operating system. In the framework of the project a new formula was prepared for calculating the summing out correction and calculation of the intensity of alias lines (sum peaks). The file converter for reading the ENDSF-2 type files was completed. Reading and converting the original ENDSF was added to the program. A computer accessible database of the X rays energies and intensities was created. The X ray emissions were taken in account in the “summing out” calculation. Calculation of the true coincidence “summing in” correction was done. The output was arranged to show independently two types of corrections and to calculate the final correction as multiplication of the two. A minimal intensity threshold can be set to show the final list only for the strongest lines. The calculation takes into account all the transitions, independently of the threshold. The program calculates the intensity of X rays (K, L lines). The true coincidence corrections for X rays were calculated. The intensities of the alias  $\gamma$  lines were calculated.

## Introduction

Whenever radioactive nucleus decays through beta-, positron-, alpha decay or electron captures process, the daughter nucleus remains in a short live excited state. The states may decay by emission of a gamma ray or a cascade of gamma rays as shown on Fig. 1. Most of these photon emission processes proceed on a time scale, which are too short for the semiconductor detector and its electronic device to distinguish the individual processes. The detector measure the full deposited energy produced by several gamma lines. This is called “true coincidence” and it complicates the quantitative evaluation of the spectra. The effects of the “true coincidence” depend on the characteristic of the detector, the geometry of the measurement and the decay scheme of the radioactive isotope. The complications are more pronounced in close geometry and high efficiency detectors. Using low-energy detectors, additional coincidence summing effect due to the X rays produced through the electron shells of the daughter nucleus.

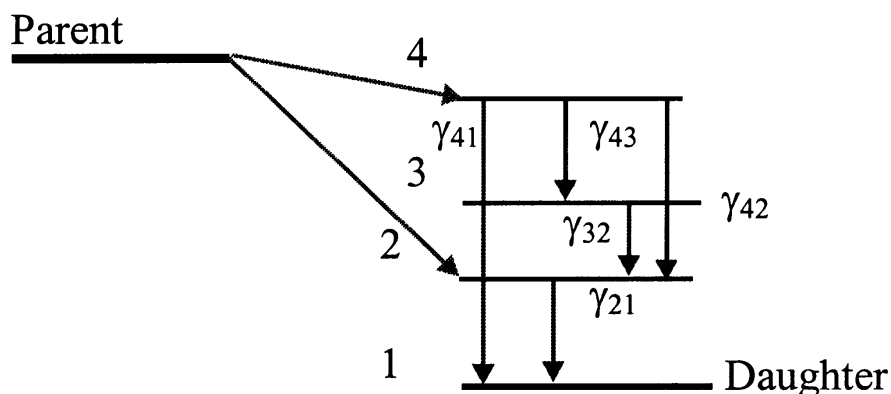


Fig.1. Decay scheme a radioactive nucleus.

Three type of effect result from “true coincidence”, usually referred as summing out (peak intensity loss), summing in (peak intensity increase), and coincidence or alias lines (new lines in the spectrum). The detection process of a gamma photon can be multi step process including photo effect, Compton scattering, pair production, etc. When the full energy of the photon deposited in the sensitive volume of the detector the electronic produces pules to the full energy peak, which is usually used in the evaluation of the spectra. The detection probability of the photon in the full energy peak is called the full energy peak-efficiency of the detector. If the photon deposits energy by any process to the detector then it contributes to the spectrum (not necessary the full energy of the gamma ray deposited). The detection probability of the photon in any way is called the total efficiency of the detector. The total efficiency of the detector ( $\epsilon^T$ ) is always higher than the full energy peak of efficiency ( $\epsilon^p$ ) of it at a given photon energy. The  $\epsilon^T / \epsilon^p$  ratio depends on the energy and it can be a large value at higher energy (i.e. it can be about 5-6 at 600 keV).

## Summing out

The summing out is the most important from the three type of coincidence summing effect. If more photons are emitted during the time resolution of the detector and electronics then all photon could deposit energy in the detector and the final signal will be the sum of the individual contribution. When one of the photon deposited its full energy into the detector, a pulse into the full energy peak will be produced only the other photons have not detected by the detector. If any other photon has also detected, then the pulse would have been counted, but because of the existence of the other photons, the pulse moved out from the full energy peak.

While in this case the detection of the other photons is depend on their total efficiencies, which can be manifold of its full energy efficiency, the effect can be even large. The Fig. 2 shows the full energy peak efficiency curve of a low energy detector at large distance when the summing effect is negligible. The gamma and X ray lines from the different calibration source are fitted well on a calibration curve. Using the same detector, but measuring in a close geometry, the measured efficiency data are depicted on Fig. 3. It can be seen that the measured raw efficiency data show a large spread, indicating the necessity of the true coincidence corrections. The deviations exceed the error limits of the measurements. The summing out effect could be take into account for all gamma lines of the nuclide depicted on Fig. 1, except  $\gamma_{41}$ .

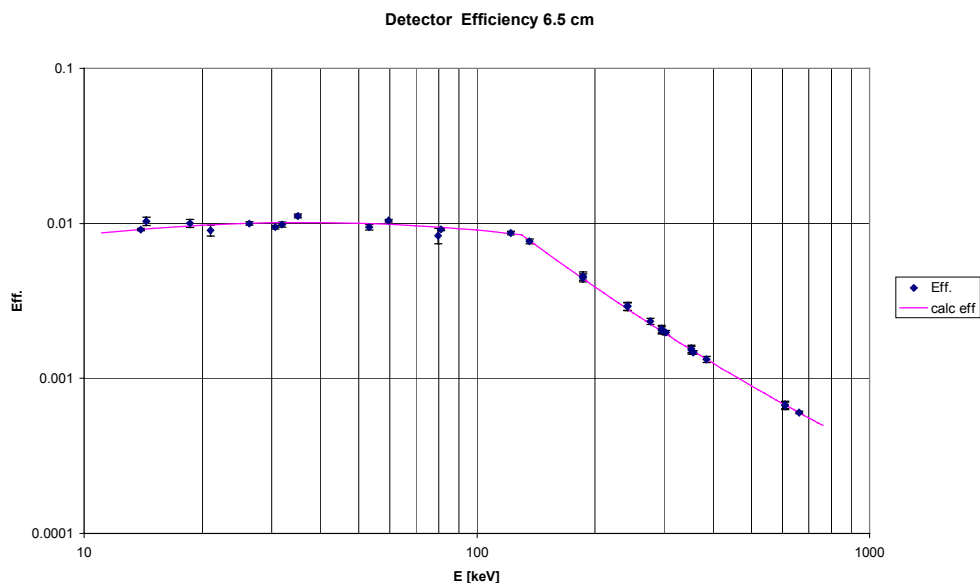


Fig. 2. Full energy peak efficiency data with negligible coincidence summing effect.

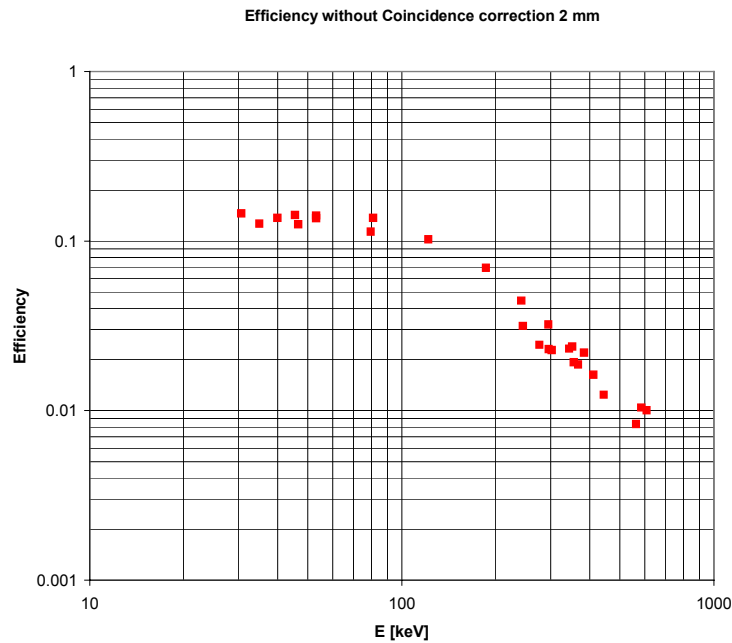


Fig. 3. Full energy peak efficiency data with coincidence summing effect.

## Summing in

When the coincident count is also a full energy event, the signal will be counted as a sum peak event. If the energy of this sum peak equal to energy of other gamma line from the cascade, its intensity will be increased. E.g.  $\gamma_{43}$  and  $\gamma_{32}$  summing could increase the intensity of the  $\gamma_{42}$  in the case of the nuclide on Fig. 1. This effect proportional with the full energy peak-efficiencies therefore it is smaller than the summing out effect. It could be important (in the case of the example) if the branching ratio from level 4 to level 2 is much smaller than it is through the level 4-3-2 cascade.

## Alias lines

The summing in effect could not only be increasing the intensity of the gamma line but it can produce new peaks in the spectrum. E.g. There is a cascade, containing  $\gamma_{43}$  and  $\gamma_{21}$  lines therefore they can produce a sum peak at the energy  $E=E(\gamma_{43})+E(\gamma_{21})$  but there is not level energy difference, which would be equal with it. Similarly, the gamma lines with coincidence with X rays will also produce new peaks in the spectrum. An example is shown in Fig. 4 where the marked peaks are new lines produced by the coincidence summing. Some other effect also produce new line in the spectrum, such type of peaks are the escape peaks connected to the low energy X rays and the escape peaks connected to pair production and the  $\beta^+$  annihilation peak at 511 keV. These alias lines could disturb the evaluation of the data mainly when the measured sample contains many radioactive isotopes with complicated spectrum. Such cases alias lines could unexpectedly overlapped the analyzed peak and falsify the results.

## Methods of calculation of true coincidence correction

The calculation of the effect of the true coincidence on the measured intensity is relatively simple in the case of the few cascading gamma lines [1,2]. Debertin and Schötzig [1] have investigated the problem of the large volume samples too. Their detailed calculation was based on the calculation model of McCallum and Coote [2] and Andreev et al. [3,4]. (The total efficiency plays an important role in the calculations. The method of the determination of it is also presented in [1].)

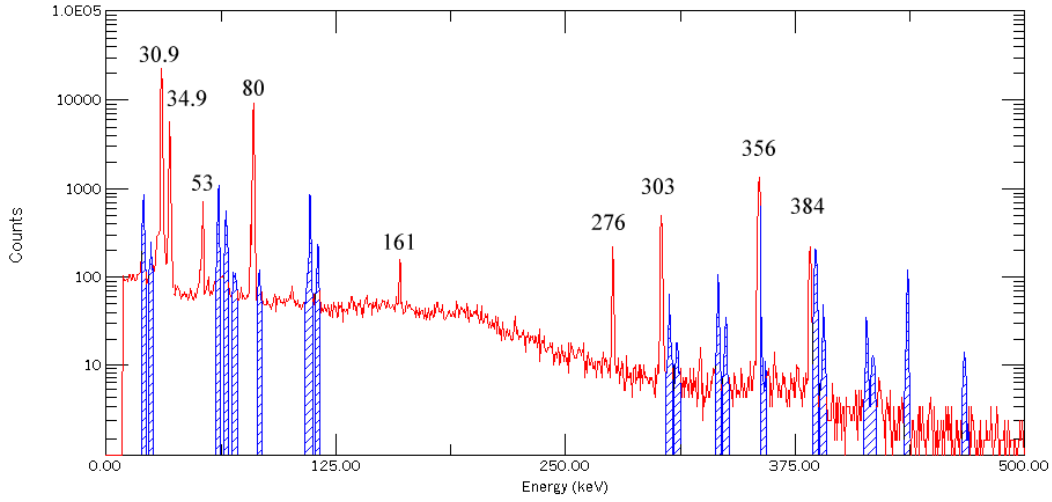


Fig.4. Alias gamma lines are marked in a  $^{133}\text{Ba}$  spectrum.

### Recursive method

An algorithm for the calculation of the true coincidence effect was developed by Andreev et al. for alpha, negatron (but not for positron) decay. McCallum and Coote extended the calculation model for positron emitters too. The calculations usually do not take into account the angular correlation between gamma rays, except in Ref. 2 for a special case of three levels decay schema. The observed full energy peak intensity ( $S_{ik}$ ) for the gamma line emitted from the level  $i$  to level  $j$  is:

$$S_{ik} = N_i A_{ik} M_k, \quad (1)$$

where

$$N_i = N_i^* + \sum_{n=i+1}^m N_n b_{ni} \quad (2)$$

$$A_{ik} = a_{ik} + \sum_{j=k+1}^{i-1} a_{ij} A_{jk} \quad (3)$$

$$M_k = \sum_{j=0}^{k-1} b_{kj} M_j \quad M_0 = 1 \quad (4)$$

$$a_{ik} = x_{ik} \frac{\varepsilon_{ik}^p}{1 + \alpha_{ik}} \quad (5)$$

$$b_{ik} = x_{ik} \left( 1 - \frac{\varepsilon_{ik}^t}{1 + \alpha_{ik}} \right) \quad (6)$$

$$\sum_{k=0}^{i-1} x_{ik} = 1 \quad (7)$$

The  $N_i^*$ ,  $x_{ij}$ ,  $\alpha_{ij}$ ,  $\varepsilon_{ij}^p$  and  $\varepsilon_{ij}^t$  are the relative intensity of population the level  $i$  (intrinsically by the decay of the parents nucleus), total branching ratio (i.e.  $\gamma$  ray plus conversion) and internal conversion coefficients, full energy peak efficiency and total efficiency, respectively. The  $N_i$  gives the population of the level  $i$  intrinsically and through gamma cascades without detecting the gamma rays in the cascade. The  $A_{ik}$  gives the probability of detection of the full energy difference by detecting the

$\gamma_{ij}$  and through the summing of the cascades between the level  $i,j$ . The  $M_k$  gives the probability that the cascade gamma rays will not be detected during the de-excitation from level  $k$  to the ground state (level 0). McCallum and Coote [2] extended this formalism to calculate the corrected intensity for positron emitters. In the case of the positron emitters, the annihilation gamma rays (2\*511keV) also could cause summing out effect. They have introduced a fictive level above each level, which is populated by positrons. The energy of the level is above the original level by 511 keV and the fictive conversion factor of  $-0.5$  is introduced to simulate the two annihilation-quanta.

### **Matrix formalism**

Another version of the calculation algorithm is presented Semkow et al. [5] using a matrix formalism to calculate the intensity of the gamma rays in the case of the coincidence summing. The observed full-energy peak intensities ( $S_{ik}$ ) for the gamma line emitted from the level  $i$  to level  $j$  are treated as lower triangle elements of the **S** matrix. The intrinsic feeding of the levels from the decay of the parents is marked by the **f** vector and the total branching fraction from the levels are arranged into the lower triangle of the **x** matrix. The elements of **f** and **x** must satisfy the conditions:

$$\sum_{k=0}^n f_k = 1 \quad \sum_{k=0}^{i-1} x_{ik} = 1 \quad i = 1, \dots, n, \quad (8a,b)$$

Other matrices **c**, **a**, **e** and **b** are defined below and their elements are functions of  $x_{ji}$  as well as of the peak efficiencies  $\varepsilon_{ij}^p$ , the total efficiencies  $\varepsilon_{ij}^t$ , and the total  $\gamma$  ray conversion coefficients  $\alpha_{ji}$ :

$$c_{ji} = \frac{x_{ji}}{1 + \alpha_{ji}} \quad a_{ji} = c_{ji} \varepsilon_{ij}^p, \quad e_{ji} = c_{ji} \varepsilon_{ij}^t \quad b_{ji} = x_{ji} - e_{ji} \quad (9a,b,c,d)$$

where  $j > i = 0, \dots, n-1$ .

To take into account the all possible decay paths and coincidences to other matrices, **A** and **B**, are introduces.

$$\mathbf{A} = \sum_{k=1}^n \mathbf{a}^k \quad \mathbf{B} = \mathbf{E} + \sum_{k=1}^n \mathbf{b}^k \quad (10a,b)$$

where **E** is a unit matrix. In addition, two diagonal matrices **N** and **M** are functions of **B**:

$$\mathbf{N} = \text{diag}([\mathbf{fB}]_i) \quad \mathbf{M} = \text{diag}(B_{i0}) \quad (11a,b)$$

The measured  $\gamma$  ray peak intensities, described by the **S** matrix is:

$$\mathbf{S} = \mathbf{R} \mathbf{N} \mathbf{A} \mathbf{M} \quad (12)$$

The scalar quantity **R** is the source disintegration rate. This matrix formula gives the same result as the recursive formula of Andreev et al. [3,4]. Semkow et al. [5] have checked it for  $n=4$  only by expanding the matrices and comparing expressions by the Andreev recursive formula. This formalism was extended for taking into account the contribution of the K X rays emitted during the electron capture and conversion by Korun and Matincic [6]. They have introduced new fictive levels like in the case of positron emitters.

## Combinatorial method

The third approach, presented here, is based on [7], work for calculation the summing out effect in the case of pure gamma emission cascades. The measured count rate  $I_{\gamma_0}$  in the peak of the  $\gamma_0$  line is

$$I_{\gamma_0} = R X_{\gamma_0} \varepsilon_{\gamma_0}^p \kappa_{tc} \kappa_{other}, \quad (13)$$

where  $R$ ,  $X_{\gamma_0}$ ,  $\varepsilon_{\gamma_0}^p$ ,  $\kappa_{tc}$ ,  $\kappa_{other}$  are the parent isotope disintegration rate, emission rate of the  $\gamma_0$  line, the full energy peak efficiency of the detector for the  $\gamma_0$  line, true coincidence correction factor, other correction factors (self absorption, etc.), respectively. The true-coincidence correction factor can be written as factors of the summing out  $\kappa_{tcl}$  and summing in  $\kappa_{tcg}$  corrections ( $\kappa_{tc} = \kappa_{tcl} \kappa_{tcg}$ ). To calculate the summing out correction for the  $\gamma_0$  transition, the decay of the parent isotope have to be separated into independent cascade chains (paths) which contain the investigated  $\gamma_0$  line. A cascade chain contributes to the counts to  $\gamma_0$  line if the  $\gamma_0$  is detected by depositing the full energy, but the other gamma lines have not detected from the chain in any way. (E.g. a cascade chain is shown on Fig. 5. If the gamma line  $\gamma_{21}$  is selected as  $\gamma_0$  than  $\gamma_{21}$  can be detected, while  $\gamma_{43}$  and  $\gamma_{32}$  are not detected.)

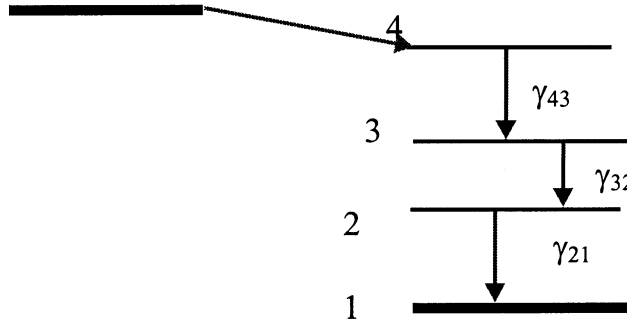


Fig. 5. A cascade chain from decay schema presented on Fig. 1.

Marking with  $\beta_i$  for populating the  $i$ -th cascade chain directly by the parent decay and  $\Gamma_{ij}$  the branching ratio, the contribution of the  $i$ -th cascade chain to the count rate of  $\gamma_0$  line is

$$I_{\gamma_0^i} = R \beta_i \Gamma_{\gamma_0} \varepsilon_{\gamma_0}^p \prod_{j=1, j \neq \gamma_0}^{n_i} \Gamma_{ij} (1 - \varepsilon_{ij}^t)$$

The total intensity of the  $\gamma_0$  line can be got by summing for the all cascade chains.

$$I_{\gamma_0} = R \sum_{i=1}^{n_0} \beta_i \Gamma_{\gamma_0} \varepsilon_{\gamma_0}^p \prod_{j=1, j \neq \gamma_0}^{n_i} \Gamma_{ij} (1 - \varepsilon_{ij}^t) \quad (14)$$

The intensity of the  $\gamma_0$  line with without “summing out” can be get by substituting zero for the total efficiencies in expression 14.

$$I_{\gamma_0}^0 = R \sum_{i=1}^{n_0} \beta_i \Gamma_{\gamma_0} \varepsilon_{\gamma_0}^p \prod_{j=1, j \neq \gamma_0}^{n_i} \Gamma_{ij}$$

The summing out correction factor can be written as

$$\kappa_{tcl} = \frac{I_{\gamma_0}}{I_{\gamma_0}^0} = \frac{\sum_{i=1}^{n_0} \beta_i \prod_{j=1, j \neq \gamma_0}^{n_i} \Gamma_{ij} (1 - \varepsilon_{ij}^t)}{\sum_{i=1}^{n_0} \beta_i \prod_{j=1, j \neq \gamma_0}^{n_i} \Gamma_{ij}}, \quad (15)$$

while  $\Gamma_{\gamma_0}$ ,  $\varepsilon_{\gamma_0}^p$  and R have been eliminated. The eq. (14) is equivalent with the  $N_i M_k$  part of the eq. (1), when  $\alpha_{ik}$  are zero (i.e. there is not internal conversion). The correction was extended for positron emission in [7] by introducing a  $\beta_i S_i$  term in the numerator of eq. (15), where  $S_i$  equal 1 for alpha, negatron and electron capture while  $(1 - 2 * \varepsilon_{511keV}^t)$  when positron feeding the chain.

This model was extended in the framework of this project to take into account the K,L X rays produced during the electron capture and gamma conversion (Fig. 6.). A similar formula that is equivalent with  $A_{ik}$  in eq. (1) was introduced.

The transition from level i to j, in general case, can produce a gamma ray, or electrons by internal conversion. The produced electrons usually can not reach the sensitive volume of the detector. Therefore, they do not cause the coincidence summing. The electron emitted from the atomic level of the atom and a vacancy is produced on the K, L or M level of the atom. The vacancy is filled in by electron from a higher level and the energy difference is given to an X ray, or other electron. The process is repeated until the outer vacancy is filled by a free electron. In point of view of the coincidence correction, the transition goes through gamma ray emission, electrons and X rays starting from the K levels, and/or L1, L2, L3 levels (Fig. 5.), and/or M, N, ... levels. The emitted X ray spectrum depend on where the first vacancy is created. In the case of the higher Z number isotope, the number of the different energy of the X rays can be even ca. 20. Therefore, the earlier applied method, extending the decay schema with fictive levels, seemed to might produce very large matrices which are difficult to handle. This version of formulation of the problem can be extended simpler way.

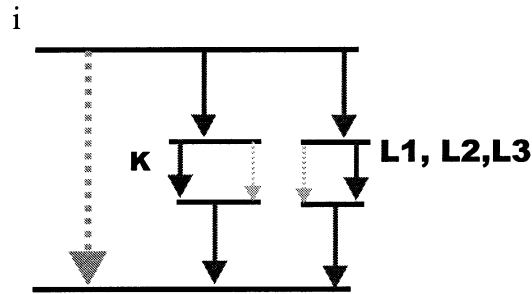


Fig. 6. Decomposition of the transition into path to take into account the electron conversion.

The transition between the level i to j can be divided into different path going through gamma emission, producing vacancy on the K, L1, L2, L3 M, N atomic levels. Filling the vacancy produce partly X rays which could cause coincidence-summing loss. While the transition always go through only one path in one case, there is no coincidence summing between these paths. Therefore the  $\Gamma_{ij}(1 - \varepsilon_{ij}^t)$  should be substitute in eq. (15) with

$$(1 - \varepsilon_{ij}^t) \Gamma_{ij} + \sum_k \Gamma_{ijk} (1 - \omega_k + \sum_l \delta_{kl} (1 - \varepsilon_l^t)) \quad (16)$$

where

$\Gamma_{ijk}$  is the conversion ratio of the j-th transition trough creating vacancy on the k-th atomic shell (K,L1, L2...) in the i-th cascade chain,

- $\omega_k$  is the fluorescence yield of the k-th atomic shell (K,L1, L2...),  
 $\delta_{kl}$  is the emission ratio of l-th x-ray from the k-th atomic shell (K,L1, L2...),  
 $\varepsilon_l^t$  is the product of the total detection efficiency and the self absorption for the energy of the l-th x ray  $\lambda = (\varepsilon_l^t \varepsilon_{sa})_l$ .

The electron capture can handle similar way to the positron emission, introducing new path, including X rays and electron emission. It means that the  $\beta_i S_i$  should be substitute with

$$\beta_i S_i = \sum_k \Delta_{ik} (1 - \omega_k + \sum_l \delta_{kl} (1 - \varepsilon_l^t)),$$

where

- $\Delta_{ik}$  is the branching ratio of the EC transition through generating vacancy on the k-th atomic shell (K,L1, L2...), while populating the i-th cascade chain.

After combining the expression above, the final formula for the summing out correction will be:

$$K_{tcl} = \frac{\sum_{i=1}^{n_0} \beta_i S_i \prod_{j=1}^{n_i} \left[ (1 - \varepsilon_{ij}^t) \Gamma_{ij} + \sum_k \Gamma_{ijk} (1 - \omega_k + \sum_l \delta_{kl} (1 - \varepsilon_l^t)) \right]}{\sum_{i=1}^{n_0} \beta_i \prod_{j=1}^{n_i} \left[ \Gamma_{ij} + \sum_k \Gamma_{ijk} (1 - \omega_k + \sum_l \delta_{kl}) \right]},$$

where

- $n_0$  is the number of cascade chains containing the  $\gamma_0$  transition,  
 $n_i$  is the number of the cascade gamma transitions in the i-th cascade chain ( $i=1,2,\dots,n_0$ )  
 $\beta_i$  is the branching ratio of the  $\beta^-$  (or  $\beta^+$ , EC,  $\alpha$ ) transition populating the i-th cascade chain,  
 $\Gamma_{ij}$  is the branching ratio of the j-th gamma transition in the i-th cascade chain,  
 $\Gamma_{ijk}$  is the conversion ratio of the j-th transition trough creating vacancy on the k-th atomic shell (K,L1, L2...) in the i-th cascade chain,  
 $\omega_k$  is the fluorescence yield of the k-th atomic shell (K,L1, L2...),  
 $\delta_{kl}$  is the emission ratio of l-th x-ray from the k-th atomic shell (K,L1, L2...),  
 $\varepsilon_l^t$  is the product of the total detection efficiency and the self absorption for the energy of the l-th x ray  $\lambda = (\varepsilon_l^t \varepsilon_{sa})_l$ ,  
 $\varepsilon_{ij}^t$  is the product of the total detection efficiency and the self absorption for the energy of the j-th gamma transition in the i-th cascade chain  $\varepsilon_{ij} = (\varepsilon_l^t \varepsilon_{sa})_{ij}$ , (use  $\varepsilon_{ij}=0$  for the  $\gamma_0$  transition)  
 $S_i$   $S_i=1$  for  $\beta$  or  $\alpha$  decay; and  $S_i=[1-2*(\varepsilon_l^t \varepsilon_{sa})_{511keV}]$  for  $\beta^+$  decay while for EC i.

$$\beta_i S_i = \sum_k \Delta_{ik} (1 - \omega_k + \sum_l \delta_{kl} (1 - \varepsilon_l^t))$$

- $\Delta_{ik}$  is the branching ratio of the EC transition through generating vacancy on the k-th atomic shell (K,L1, L2...), while populating the i-th cascade chain.

The calculation of the true coincidence summing in correction can be done similar manner than in the case of the summing out correction. The measured intensity will be proportional with the sum of the original  $\Gamma_{\gamma_0} \varepsilon^p(\gamma_0)$  and the contribution of the paths between the selected level. The intensity gain is proportional with the full energy peak efficiency of the transitions.

$$I \propto \Gamma_{\gamma_0} \varepsilon^p(\gamma_0) + \sum_{i=1}^n \prod_{j=1}^{m_i} \Gamma_{ij} \varepsilon^p(\gamma_{ij})$$

This gives the same result as  $A_{ij}$  in eq. 1 after expanding the sum. Thus the coincidence summing in correction factor will be:

$$\mathcal{K}_{tcg} = 1 + \frac{\sum_{i=1}^n \prod_{j=1}^{m_i} \Gamma_{ij} \varepsilon^p(\gamma_{ij})}{\Gamma_{\gamma_0} \varepsilon^p(\gamma_0)} .$$

The intensity of the alias line can be get as

$$I_{alias,a,b} = \sum_{i=1}^{n_0} \beta_i \prod_{j=1}^{n_i} \left[ \Gamma_{ij} + \sum_k \Gamma_{ijk} (1 - \omega_k + \sum_l \delta_{kl}) \right] R_a R_b \frac{\varepsilon_p(E_a) \varepsilon_p(E_b)}{\varepsilon_p(E_a + E_b)},$$

where  $R_x$  is the branching ratio of the x type of transition to the total transition between the selected level. The calculation is performed only two coinciding lines.

## The “TrueCoinc” program

The aim of the “TrueCoinc” program is to calculate the true-coincidence correction factors for gamma spectrometry using existing database for the input level schema. This calculation is not difficult, but it would need a lot of data preparation. The earlier programs have used own database therefore, the users have to collect and prepare the input data. This program uses available free and commercial databases for the calculation and exempts the user from the time consuming data preparation and calculation. The user has to prepare only the detector efficiencies for the calculation.

### *Hardware, software requirements*

The “TrueCoinc” program runs under the Windows-95/98 operation system on a IBM PC compatible computer, which have enough hardware resource to use the Windows-95/98. The computer should have additional 3-30Mb free space on hard disk, CD drive (optional) for Table of Isotopes CD-ROM, Internet connection (optional).

The program can use the following database of the levels:

- ❑ The CD-ROM version of the Tables of Isotopes (TOI). The CD-ROM contains in the Pcensdf/Pensdf2 directory the parent isotopes files of the ENSDF library in ENSDF-2 format. The files are grouped in subdirectories by mass number 20. The program always try to find the appropriate data file (.enx) in same type of directory structure.
- ❑ Single ENSDF-2 file of the selected parent isotope. The file has to be selected during the database selection, but it can be any directory on a disk. Some samples are attached to the program.
- ❑ Property form of the TrueCoinc program based on the IAEA file format. A selection of the most important isotopes is supplied with the program.

- An ENSDF file of the selected isotope. The original ENSDF file for any isotopes can be downloaded from the Nuclear Data Centers, i.e. National Nuclear Data Center, Brookhaven National Laboratory, <http://www.nndc.bnl.gov/~burrows/ensdf/>. This would give the possibility to use the latest evaluated data for the calculation.

The user should have one of the above-mentioned database.

For calculation of the true coincidence corrections, the knowledge of the total efficiency and full-energy peak efficiency of the used detector, as function of the gamma ray energy, is necessary. The program use the efficiency curves as analytical functions, therefore the measured efficiencies data has to be fitted to an accepted form of the “TrueCoinc” program. It uses the same function as implemented in the GANAAS program

The method of calculation is based on the combinatorial formalism with the following approximations: Gamma-gamma angular correlation is neglected; the effect of the X ray from the M atomic level and bremsstahlung are negligible; the positron-annihilation gamma rays are anti-correlated and originated from the same distance as the other gamma rays.

Using “TrueCoinc” program consist the following steps: Selecting the database, giving the detector parameters, selecting the isotope (A, Z, Symbol, Decay mode, Half-life), starting calculation.

An example for the output of the results is shown on Fig. 7.

The result is arranged in increasing order of the energy or the intensity (selectable) of the emitted gamma rays. The headlines contain:

Total efficiency:                      The identifier of the total efficiency curve  
 Full-energy peak efficiency:        The identifier of the full-energy peak efficiency  
 Parent radioactive isotope, decay mode and half-life:

The data in the columns are the following:

No.                                      Number of the gamma/X ray line  
 E[keV]                                The energy of gamma/X ray line in keV

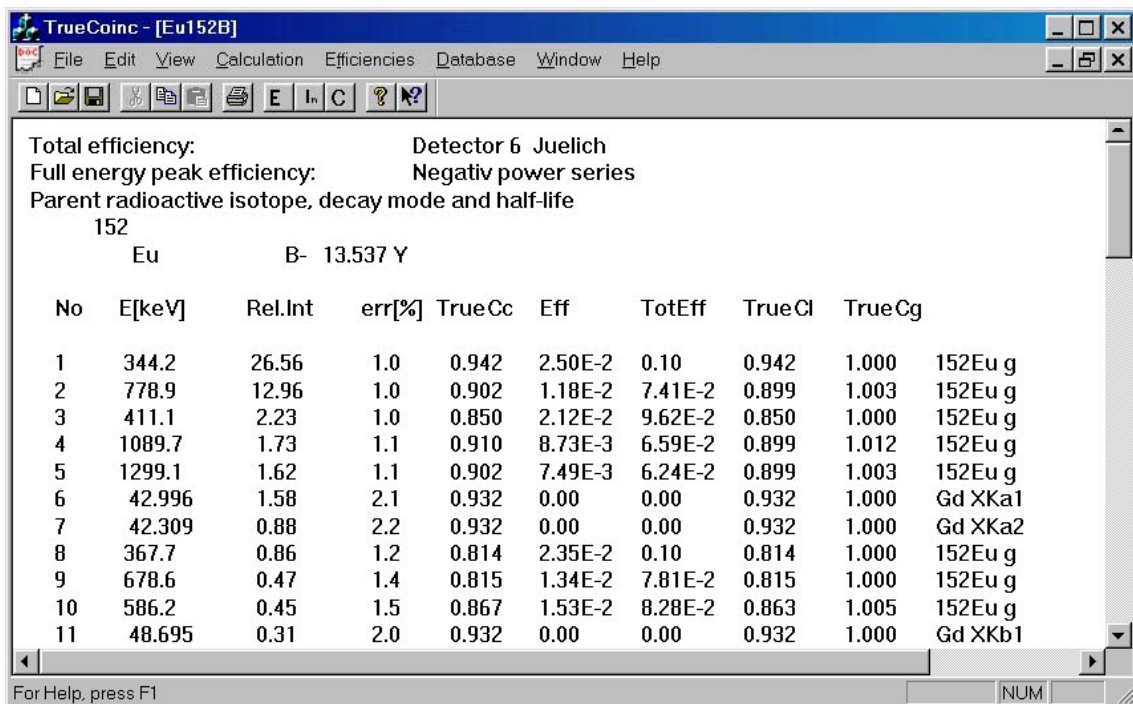


Fig. 7. The output of the “TrueCoinc” program.

Rel.Int.	Intensity of the gamma/X rays. Number of the gamma/X rays emitted for 100 decay of the parent isotope
Err[%]	Relative error of the intensity of gamma ray
TrueCc	True coincidence correction factor. It is the ratio of the measured intensity to the real intensity taking account coincidence corrections.
Eff.	The calculated full-energy peak efficiency for the given energy.
TotEff	The calculated total efficiency for the given energy.
TrueCl	True coincidence loss correction factor. It is always $\leq 1.0$
TrueCg	True coincidence gain correction factor. It is always $\geq 1.0$
	Identifier of the parent of gamma/Xray

The result presented on the screen, can be printed, or write into text file on the disk for further processing by computer programs, or copy the output to the Windows Clipboard, to paste it into other application (e.g. spreadsheets). The options include sorting the output data (energy, intensity), application of intensity limit, taking into account or not the X rays' contribution. Special data library format exists in the IAEA proposed ASCII data format. The program has the capability to read and write data into this text format. This text file can be edited by any text editor to modify the input data without understanding the ENDSF formats. The input data for isotopes used in the energy calibration is attached to the program in this property format.

As an example of the results of the calculation, the data presented on Fig. 3 is shown after application the correction on Fig. 8. The large spread of the data shown on Fig.3 has been removed by the applied correction. The largest applied correction was 35%.

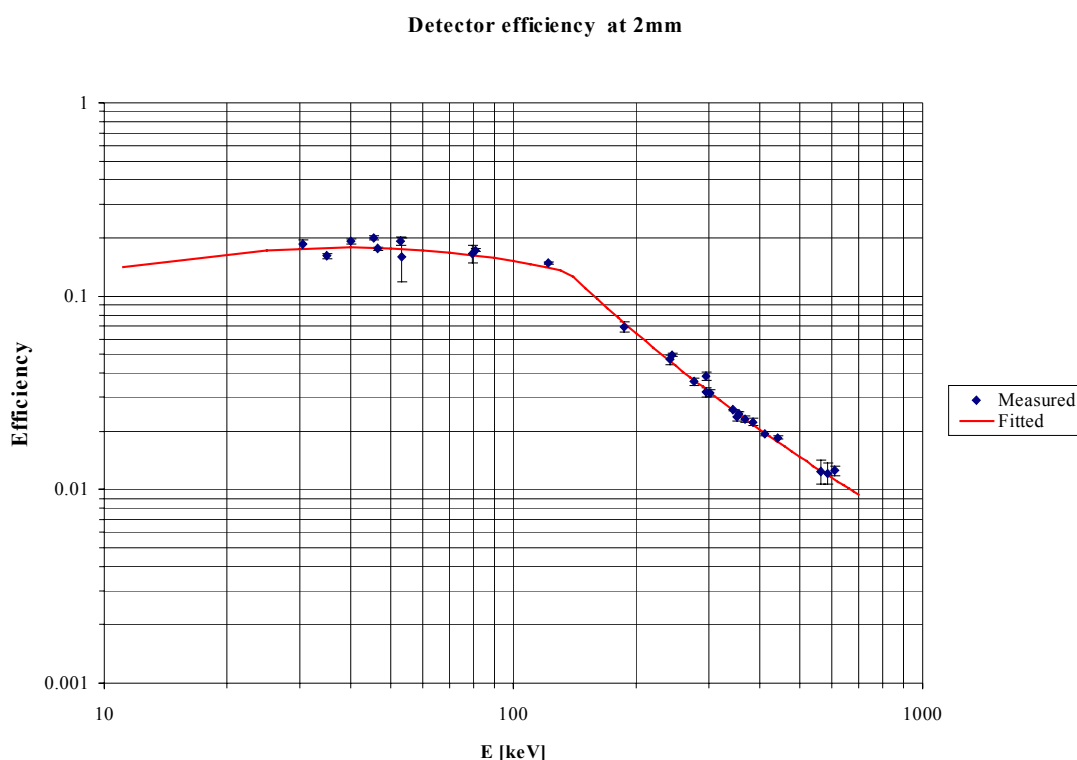


Fig. 8. The corrected efficiency data of Fig. 3.

## Conclusion

The developed “TrueCoinc” program calculates the coincidence correction factors with minimal user effort. The input data for the level parameters and X ray emission are collected from existing databases of the levels. The program is supported with Help and a User Guide

## REFERENCES

- [1] DEBERTIN, K., SCHÖTZIG, U., Coincidence summing corrections in Ge(Li)-spectrometry at low source-to-detector distances, Nucl. Instr. and Meth. **158** (1979) 471.
- [2] MCCALLUM, G.J., COOTE, G.E., Influence of source-detector distance on relative intensity and angular correlation measurements with Ge(Li) spectrometers, Nucl. Instr. and Meth. **130** (1975) 189.
- [3] ANDREEV, D.S., EROKINA, K.I., ZVONOV, V.S., LEMBERG, I.KH., Izv. Akad Nauk, SSSR Ser. Fiz., **37 No.8.** (1973) 1609.
- [4] ANDREEV, D.S., EROKINA, K.I., ZVONOV, V.S., LEMBERG, I.KH., Instr. Expt. Techn. **15** (1972) 1358.
- [5] SEMKOW, T.M., MEHMOD, G., PAREKH, P.P., VIRGIL, M., Coincidence summing in gamma ray spectroscopy, Nucl. Instr. and Meth. in Phys. Res., **A290** (1990) 437.
- [6] KORUN, M., MARTINČIČ, R., Coincidence summing in gamma and X-ray spectrometry, Nucl. Instr. and Meth. in Phys. Res., **A325** (1993) 478.
- [7] DARÓCZY, S., RAICS, P., Laboratory manual IAEA Training Course on Utilization of Neutron Generators, Debrecen, 1982, 16.

# CALCULATION OF THE COUNTING EFFICIENCY FOR EXTENDED SOURCES

**M. Korun, T. Vidmar**

J. Stefan Institute,  
Ljubljana, Slovenia

**Abstract.** A computer program for calculation of efficiency calibration curves for extended samples counted on gamma- and X ray spectrometers is described. The program calculates efficiency calibration curves for homogeneous cylindrical samples placed coaxially with the symmetry axis of the detector. The method of calculation is based on integration over the sample volume of the efficiencies for point sources measured in free space on an equidistant grid of points. The attenuation of photons within the sample is taken into account using the self-attenuation function calculated with a two-dimensional detector model.

## Introduction

Determination of the activities present in samples is straightforward in X-and gamma ray spectrometry if the counting efficiencies are known. The areas of peaks, corrected for counting losses, are proportional to the numbers of radioactive atoms decaying in the sample during the measurement. Neglecting the probability for coincident detection of two or more gamma rays, the factor of proportionality is given by the product of two probabilities: the probability that during the decay a gamma ray with energy E is emitted and the probability that this gamma ray is registered in the spectrum in the full-energy peak.

Whereas the emission probability can be obtained from tables giving the properties of radioactive nuclei, the experimenter himself must extract the detection probability. The detection probability is defined by:

$$\text{probability for detection} = \frac{\text{number of detected photons}}{\text{number of emitted photons}},$$

and is usually referred to as counting efficiency. This efficiency depends on detector properties, sample properties and the relative sample-detector position. For a given detector the efficiency is a function of the sample shape, size, composition, the distance of the sample from the detector and the photon energy.

To calculate the activities of gamma- and X ray emitters from a spectrum measured with a given sample-detector arrangement, the counting efficiency must be known. Usually its uncertainty is the main factor influencing the uncertainty of the calculated activity. Therefore the measurement and/or calculation of the counting efficiency must be done with the greatest care and utmost precision.

The counting efficiency can be extracted by measurement or by calculation. Measurements are performed with calibrated samples, which contain a known activity of one or more gamma ray emitters. If measurements of counting efficiency for a given sample-detector geometry are performed, care must be taken that the calibrated sample resembles the unknown sample in *all the properties influencing the counting efficiency*. If unknown samples come in different sizes, densities and materials the differences between the calibrated sample and the unknown samples must be recognised and appropriate corrections to the counting efficiency applied [1,2]. The uncertainty of the measured efficiency is limited by the uncertainties of the calibrated activities; usually, these amount to 1%.

Alternatively, the counting efficiency can be calculated. The calculations are performed by the Monte-Carlo method or by analytical methods [3-9]. The main disadvantage of calculations is that their results depend on data on the internal construction of the detector that are not very well known.

Usually, therefore, doubt is present as to whether the calculations take the influence of the detector data on the efficiency into account properly. The mentioned disadvantage can be overcome by combining measurements and calculations. The counting efficiency is measured for a specific sample-detector arrangement and the calculation is performed for the same arrangement. The correction extracted from the disagreement is applied to other calculated efficiencies. In this way the calculated efficiencies are corrected, at least in part, for the influence of possible errors in the detector data. The corrected efficiencies are the more reliable the more closely the sample-detector arrangement resembles the arrangement in which the calibration measurement was performed, and the less reliable the less the detector model used in the calculations resembles the actual detector.

The described idea of correction of calculated efficiencies by calibration measurements is used in the calculation of counting efficiencies for extended sources. Many calibration measurements are performed in order to describe the detector properties as thoroughly as possible and a simple detector model is used in order to speed up the calculations.

The spatial dependencies of the point-source efficiencies in the volume where the sample is placed are the detector characterisation data needed to calculate the counting efficiency for an extended source. Measurement of these dependencies at many energies represents a major effort. This effort can be reduced to a large degree by assuming that detectors with similar physical data exhibit similar spatial dependencies of the efficiencies for point sources. Therefore, by choosing one of the supplied detector characterisation data files on the basis of agreement between the corresponding physical properties of the detector they belong to and those of the actual detector, and by replacing the efficiency calibration data for a point source positioned on the detector surface and on its symmetry axis with the data measured for the actual detector, it is possible to avoid the measurement of the spatial dependencies. However, the accuracy of the efficiency calibration curves in this case is best for small samples, positioned on the detector surface.

### Calculation of counting efficiencies for extended sources

It can be shown [3,7,10,11] that the efficiency of an extended source can be described by

$$\varepsilon_V(E) = \frac{1}{V} \int_V \varepsilon_{PS}(E, \vec{r}) F(\mu, E, \vec{r}) dV(\vec{r}) \quad , \quad (1)$$

where  $V$  denotes the sample volume,  $\varepsilon_{PS}(E, \vec{r})$  the efficiency of a point source emitting photons with energy  $E$ , placed at the point  $\vec{r}$  within the sample, and  $F(\mu, E, \vec{r})$  the self-attenuation function. The self-attenuation function describes the amount of radiation with energy  $E$  emitted at point  $\vec{r}$  and prevented from registering in the full energy peak in the spectrum by interaction with the sample material with an attenuation coefficient  $\mu$ . For the case of a homogeneous sample the self-attenuation function can be expressed as [10]:

$$F(\mu, E, \vec{r}) = \frac{\int e^{-\mu s(\vec{r}, \vec{R}) - \mu_w s_w(\vec{r}, \vec{R}) - \mu_G s_i(\vec{r}, \vec{R})} dN(E, \vec{r}, \vec{R})}{\int_{V_D} e^{-\mu_w s_w(\vec{r}, \vec{R}) - \mu_G s_i(\vec{r}, \vec{R})} dN(E, \vec{r}, \vec{R})} \quad . \quad (2)$$

Here,  $V_D$  denotes the sensitive volume of the detector and  $N(E, \vec{r}, \vec{R})$  the number of photons with energy  $E$  emitted at  $\vec{r}$  within the sample volume and interacting in the absence of attenuation within the sample at  $\vec{R}$  within the sensitive volume of the detector in such a way that their full energy  $E$  is absorbed within  $V_D$ .  $s(\vec{r}, \vec{R})$  is the path length these photons traverse in the sample and  $s_w(\vec{r}, \vec{R})$  denotes the path length of the photons through the detector cap or the entrance window.  $\mu_w$  is the attenuation coefficient of the cap or the entrance window material.  $s_i(\vec{r}, \vec{R})$  denotes the path length of

the photons through the inactive layer of the detector crystal (dead layer) and  $\mu_G$  the attenuation coefficient of germanium.

The self-attenuation function depends strongly on sample parameters and much less on the detector parameters, since the influence of the detector partially cancels out in the ratio. Therefore, the calculation of counting efficiencies by Eq. 1, using measured point source efficiencies and a self-attenuation function calculated with a detector model, offers the following advantages:

- Since  $F(0, E, \vec{r}) = 1$ , the efficiency calculation is exact at zero attenuation;
- For sufficiently refined detector models the calculated counting efficiency approaches its exact value.

It follows that for any detector model yielding satisfactory results for the counting efficiency at an attenuation coefficient  $\mu$  in the sample, the results calculated at any  $\mu' < \mu$  are just as good or better.

In the approach implemented the self-attenuation function is calculated using the following simple detector model. The sensitive volume of the detector is represented by a sensitive surface, where the area of the surface equals the area of the front surface of the detector crystal. On top of the sensitive surface is an absorbing, inactive layer of germanium, representing the dead layer of the detector crystal, whose thickness is a parameter supplied by the user and usually obtained from the manufacturer's data sheet.

The surface is positioned within the detector at the depth  $h(E)$ , equal to the sum of the window thickness  $s_w$ , the distance between the crystal and the detector cap  $d_c$ , the thickness of the inactive layer  $s_i$  and the average interaction depth in the germanium crystal  $d_d$ :  $h(E) = s_w + d_c + s_i + d_d$ . The quantity  $d_d$  is calculated as the average interaction depth of photons with energy  $E$  in germanium, impinging on the detector parallel to its axis:

$$d_d = \frac{1}{\mu_G(E)} \frac{1 - e^{-\mu_G(E)l}}{\mu_G(E)l + 1}, \quad (3)$$

Here,  $l$  denotes the crystal length. In the calculation it is assumed that all photons impinging on the sensitive surface are registered in the full energy peak. Then the number of photons impinging at a point  $\vec{R}$  on the detector surface is proportional to the illumination of the surface at that point from a point light source placed at  $\vec{r}$ . The self-attenuation function can be expressed as

$$F(\mu, E, r, h) = \frac{\int_0^{R_c} \int_0^{2\pi} e^{-\mu(E) \frac{h_0}{h(E)} d(\vec{r}, \vec{R}, E) - \mu_w(E) \frac{s_w}{h(E)} d(\vec{r}, \vec{R}, E) - \mu_G(E) \frac{s_i}{h(E)} d(\vec{r}, \vec{R}, E)} R dR d\phi}{\int_0^{R_c} \int_0^{2\pi} e^{-\mu_w(E) \frac{s_w}{h(E)} d(\vec{r}, \vec{R}, E) - \mu_G(E) \frac{s_i}{h(E)} d(\vec{r}, \vec{R}, E)} R dR d\phi} \frac{d^3(\vec{r}, \vec{R}, E)}{d^3(\vec{r}, \vec{R}, E)}, \quad (4)$$

where  $r$  denotes the distance of the source from the detector axis and  $h(E)$  the distance between the point source and the surface representing the sensitive area of the detector;  $h_0/h(E)$  is the part of that distance occupied by the sample material (in the case when the sample is placed on the detector we have  $h(E) = h(E) + h_0$ ),  $s_w/h(E)$  is the part of  $h(E)$  occupied by the window material and  $s_i/h(E)$  is the part of  $h(E)$  occupied by the material of the inactive layer.  $R_c$  denotes the radius of the sensitive surface of the detector,  $R$  and  $\phi$  the co-ordinates of the vector  $\vec{R}$  and  $d(\vec{r}, \vec{R}, E)$  the distance between the source and the point where the illumination is observed:

$$d^2(\vec{r}, \vec{R}, E) = r^2 + R^2 - 2rR \cos(\phi) + h^2(E). \quad (5)$$

The data characterising the detector,  $\varepsilon_{PS}(E, \vec{r})$ , are obtained by measurement [12]. In this way the appropriate detector data such as those on crystal shape, the position of the crystal within the detector cap, the influence of the inactive core etc. are implicitly taken into account.

In the calculation of the counting efficiency a grid of points within the sample is constructed. The self-attenuation function is computed on that grid, thereafter multiplied by the measured efficiencies interpolated to the grid and finally averaged over the sample volume. In this way the material of the sample as well as the sample dimensions are taken into account when calculating the efficiency.

The detector model described well resembles the processes of photon detection at low energies, since there the interaction between the photons and the detector crystal takes place at the crystal surface and the photoeffect is the dominant interaction process. Therefore it is expected that the model will yield good results at low energies. Since attenuation coefficients decrease with energy, it will yield good results at any higher energy as well.

To assure the validity of the model for low energies and high self-attenuation, it is also absolutely necessary to include the dead layer, positioned on top of the active surface, in the model. If the dead layer is absent, the model overestimates the efficiencies at very high self-attenuation, since the inclusion of the dead layer reduces the nominator of Eq. (2) more than its denominator. This is due to the fact that high self-attenuation in the sample causes the gamma rays emitted from a given point within the sample upon exiting the sample to form a beam that is closer to a completely collimated one compared to the beam that results when the sample has low or no attenuation. When such a parallel beam impinges on the dead layer it traverses it on average with a shorter path and is less attenuated than the broader beam with which we are dealing when computing the denominator of Eq. (2), since in that case we have no attenuation in the sample. For the same reason it is also necessary to take into account the absorption in the detector cap, although the effect is usually of lesser importance due to the lower atomic number and density of the cap material as compared to germanium.

## Description of the software

The software is not supplied by a dedicated user interface since it is, in the first case, intended to be used as a building block in automated spectral analysis procedures. It runs unmodified on computers with DOS/WINDOWS, UNIX or VMS operating systems.

The software uses the sample data file, the detector characterisation file and the attenuation data for materials present in the sample and detector as input. The sample data file contains the data on the dimensions of the sample, its distance from the detector, density and composition. The detector characterisation file comprises the data on the detector crystal dimensions and position and the data on the spatial dependence of the efficiencies for point sources at all characterisation energies.

The VOLUME program package is comprised of three programs: VOLUME.EXE that performs the actual computation of the voluminous source full-energy peak efficiency calibration curve, DETECTOR.EXE that checks the adequacy of the detector characterisation input file DETECTOR.DAT, and SAMPLE.EXE that carries out an equivalent task for the sample description input file SAMPLE.DAT. The user, therefore, has to supply the DETECTOR.DAT and SAMPLE.DAT description input files, as well as the attenuation coefficient energy dependence files for all the materials entering the sample matrix composition and the detector cap material.

A typical session with the VOLUME package therefore starts with preparing the input files SAMPLE.DAT and DETECTOR.DAT, proceeds with running a check on them using the SAMPLE.EXE and DETECTOR.EXE files and using the possible error messages they issue as guidelines for the necessary corrections, and ends by computing the efficiencies with the VOLUME.EXE program.

The DETECTOR.DAT input file is used to describe all the geometrical, structural and experimentally obtained data on the detector and its point source efficiencies. Measured efficiencies

are given at a rectangular grid of points, spanning in the axial and radial directions the volume near the detector occupied by the sample. The efficiency  $\varepsilon(E,r,z)$  for the gamma ray energy E at a point (r,z) is given as

$$\varepsilon(E, z, r) = \varepsilon_{00}(E) \varepsilon_z(E, z) \varepsilon_r(E, z, r),$$

where  $\varepsilon_{00}(E)$  denotes the efficiency for a point source positioned on top of the detector on its symmetry axis,  $\varepsilon_z(E,z)$  the axial dependence for the point source at the energy E on the symmetry axis and  $\varepsilon_r(E,z,r)$  the radial dependence at a distance z from the detector.

There should be a minimum of n=3 detector characterisation data records present in the DETECTOR.DAT file. Their number need not be explicitly specified. The efficiencies are computed at all energies where the detector is characterised, at the lower and upper boundary of the detector's useful energy range and at all energies for which the attenuation coefficient of the materials comprised in the sample matrix are given and which fall within the useful energy range.

It should be noted, however, that the characterisation of the detector at just three energies does not assure the calculation of reliable calibration curves over the whole useful energy range of the detector. If the number of characterisation energies is small or if they fall within a narrow energy interval, the calculated efficiency calibration curve is unreliable or reliable only within that energy interval. For reliable calculations at least three energies must lie below the energy where the efficiency reaches its maximum, and at least four above.

Detectors with similar physical data have similar spatial dependencies of their point-source efficiency. Therefore, in order to calculate the counting efficiencies of a specific detector, it is not necessary to measure the spatial dependencies at several energies, since the dependencies given for one of the detectors already characterised can be used instead. Characterisation data files for some detectors can be found on the web site: <http://rubin.ijs.si/vlg/>. These data files must be modified, but apart from the physical detector data, only the absolute efficiencies for a point source placed in the detector cap in the symmetry axis of the detector,  $\varepsilon_{00}(E)$  need be changed.

## Conclusion

The results of the computations stored in the output file bear uncertainties that originate to a large extent in the uncertainties of the input data. Usually, the main sources of uncertainty are the absolute efficiencies  $\varepsilon_{00}(E)$ . The spatial dependence of the efficiency for point sources contributes less to the uncertainty since it is expressed by relative values, where the systematic uncertainties are cancelled out. In detectors sensitive to low energies, the spatial dependence of the efficiency for point sources is almost independent of the energy above 100 keV. Detectors with thick dead layers at the front surface exhibit stronger energy dependence. In any case, the spatial dependence varies smoothly with energy. The uncertainty due to the numerical procedure itself is estimated at 5% for  $E < 20$  keV in the case of an  $\Phi 90 \times 20$  mm  $\text{SiO}_2$  sample with density of  $1.3 \text{ g/cm}^3$ . For samples with smaller self-attenuation this uncertainty is negligible.

The best way to arrive at reliable estimates of the overall uncertainty of the calculated efficiencies is to compare them with measured efficiencies for the same counting geometry. With reliable data sets for the detector properties the relative errors are on average below 5%.

## REFERENCES

- [1] DEBERTIN, K., HELMER, R. G., Gamma and R-Ray Spectrometry with Semiconductor Detectors, North Holland, Amsterdam, 1987.
- [2] GILMORE, G., HEMINGWAY, J. D., Practical Gamma-Ray Spectrometry, John Wiley&Sons, Chichester, 1995.

- [3] NOGUCHI, M., TAKEDA, K., HIGUCHI, H., Nucl. Instr. and Meth. **32** (1980) 17.
- [4] NAKAMURA, T., SUZUKI, T., Nucl. Instr. and Meth. **205** (1983) 211.
- [5] DECOMBAZ, M., GOSTELY, J. J., LAEDERMANN, J. P., Nucl. Instr. and Meth. **A312** (1992) 152.
- [6] HAASE, G., TAIT, D., WIECHEN, A., Nucl Instr. and Meth. **A329** (1992) 483.
- [7] OVERWATER, R. M. W., BODE, P., DE GOEJ, J. M., Nucl. Instr. and Meth. **A324** (1993)209.
- [8] AALTONEN, H., KLEMOLA, S., UGLETVEIT, F., Nucl. Instr. and Meth. **A339** (1994) 87.
- [9] HAASE, G., TAIT, D., WIECHEN, A., Nucl. Instr. and Meth. **A361** (1995) 240.
- [10] KORUN, M., MARTINČIČ, R., Appl. Radiat. Isot. **43** (1992) 29.
- [11] SIMA, O., DOVLETE, C., J. Radioanal. Nucl. Chem. Lett. **200** (1995)191.
- [12] KORUN, M., LIKAR, A., VIDMAR, T., Nucl. Instr. and Meth. **A390** (1997) 203.
- [13] DEBERTIN, K., in IAEA-TECDOC-1045, Software for Nuclear Spectroscopy 1994, IAEA, Vienna 1998.

# LIBRARIAN DRIVEN ANALYSIS OF GAMMA RAY SPECTRA

**V. Kondrashov**

Drew University,  
Los Angeles, California, United States of America

**I. Petersone**

Ellat,  
Riga, Latvia

**Abstract.** For a set of *a priori* given radionuclides extracted from a general nuclide data library, the authors use median estimates of the gamma-peak areas and estimates of their errors to produce a list of possible radionuclides matching gamma ray line(s). The identification of a given radionuclide is obtained by searching for a match with the energy information of a database. This procedure is performed in an interactive graphic mode by markers that superimpose, on the spectral data, the energy information and yields provided by a general gamma ray data library. This library of experimental data includes approximately 17,000 gamma ray energy lines related to 756 known gamma emitter radionuclides listed by the ICRP.

## Introduction

At present there are two different approaches to gamma ray spectra processing. The first approach is based on a traditional peak search routine [1], and the second one on a so-called “librarian” routine. Our approach falls into the second category. The two different approaches are driven by the requirements of two major groups of tasks. The first group deals with analysis of any gamma spectra with randomly distributed gamma peak locations on the energy axis. For example, observations of gamma spectra obtained from any astrophysical experiment, from satellite observations of gamma bursts or gamma-sources on Earth surface, etc. In this case, we have to fix the gamma ray peaks automatically by a routine such as peak-search, by calculating the first or second derivatives from the spectrum acquired with multichannel analyser. The other group is related to the need to identify gamma ray emitting nuclides. In this case peak locations are not distributed randomly but instead they depend on the set of isotopes. Of course, it would be useful to know this set *a priori*. In that is the case, it would not be necessary to check the full energy region for peak locations. This means that we can reduce the number of regions of interest in any real spectrum emitted by radioisotopes.

For the librarian approach, energy calibration should be sufficiently good in a way that deviation between any reference energy and one calculated from the calibration curve should be within one or two channels for the full energy region under scrutiny. Suppose we have a gamma ray line with reference value energy  $E$ . From our energy-channel calibration curve we can calculate the line position  $N_E$  expressed in channels. Following our assumption, we can accept only calibrations with maximum deviation of about  $FWHM/2$  in real line position. This means that we have a real line location within  $N_E \pm \Delta$ , where  $\Delta$  is about  $FWHM/2$  for a gain normally within 0.3-0.7 keV/ch. By using this curve we can estimate a line position with accuracy  $\pm 500$  keV/ch, but that is not enough for reliable nuclides identification.

To adjust the line \ peak \ position we could apply any standard fitting procedures - for example fitting this region by an iterative least-squares procedure using Gaussian shape for the peak area and a linear function for the background representation. In this way we can simultaneously estimate peak parameters more precisely, but that is valid only for peaks with good (just near Gaussian) shape and/or good statistics. To decrease the influence of some distortion factors such as outliers, peak position drift, overlapping with another peaks, etc. it would be reasonable to decrease the number of peak parameters (including those of the background) under scrutiny. We can evaluate resolution as a function of energy by creating the resolution-energy dependence from the calibration routine. Due to the complexity of real spectra we sometimes lose convergence of the iteration procedure. To

overcome these difficulties and adjust the peak position on the analysis interval we apply the median estimate of net peak area with simultaneous calculation of area's dispersion [2,3]. As the reader can see from the above explanation, our approach is based on the interaction of the database of nuclides with spectra processing. The approach has been implemented into the codes DIMEN [2] and WinDIMEN [4] for isotope identification and quantification.

### Median estimate formalism

The definition of the median estimate and the method for its evaluation for gamma-lines processing can be found in [2], while more details on multiplet deconvolution is given in [3]. Only brief introduction to the method will be given here. The central point is to find a more effective way to develop an elementary estimates population that is as large as possible. Our choice is the method of *finite differences* [3], because in this way we can eliminate (or substantially reduce) a linear background influence and obtain a large number of elementary estimates on the Region of Interest (ROI) selected.

We denote the *second finite difference* of any discrete function  $f_i$  as:

$$\Delta^{(2)} f_i = f_{i+2p} - 2f_{i+p} + f_i \quad (1)$$

where,  $i \in (i_1, i_2)$ ,  $i_1$  and  $i_2$  are initial and final numbers of  $f_i$  realization,  $p$  - is an integer size step for a second finite difference.

We will use the following terms and definitions:

- $G_{ij}$  - the Gaussian function (which represents the gamma peak shape) for  $i$ -th channel and  $j$ -th peak in multiplet on ROI selected,  $j=1$  in the case of a single peak.
- $S_j$  - net area of  $j$ -th peak.
- $B_i$  - linear background in the  $i$ -th channel on ROI selected. The background for the entire spectrum can be considered as a set of consecutive linear functions.

The number of pulses in the ROI within  $i \in (i_1, i_2)$  is:

$$\|Y_i\| = \|G_{ij}\| \|S_j\|^T + \|B_i\| + \|\xi_i\| \quad (2)$$

where,  $\|Y_i\|$ ,  $\|S_j\|$ ,  $\|B_i\|$  and  $\|\xi_i\|$  are column matrices with size  $[n \times 1]$  and  $\|G_{ij}\|$  is a matrix with size  $[n \times m]$ ,  $n = i_2 - i_1 + 1$  - number of ROI's channels and  $m$  - numbers of peaks in the multiplet.

$\xi_i$  - is the error of measurement in the  $i$ -th channel, which in general is not described by the Gaussian distribution, but has limited dispersion and a mean value equals to zero.

In order to eliminate the linear background, the second finite difference has been applied for  $Y_i$ :

$$\|\Delta^{(2)} Y_i\| = \|\Delta^{(2)} G_{ij}\| \|S_j\|^T + \|\Delta^{(2)} \xi_i\| \quad (3)$$

To obtain one elementary estimate for peak area we need  $m$  second differences. We can get the total set of elementary estimates by choosing different combinations of  $m$  second differences from the full set of second finite differences.

To achieve the maximum number of second finite differences we can vary the step size of the second difference from  $p=1$  to  $p=\text{int}[n/3]+1$ . For example, the total number of elementary estimates (or combinations) for  $p=1$  is [3]:

$$L = \frac{(i_2 - i_1 - 1)!}{m!(i_2 - i_1 - 1 - m)!} \quad (4)$$

Following [3] we can represent the matrix of net peak area elementary estimates as:

$$\|S_j\|_l = \|\Delta^{(2)}G_{i(k)j}\|^{-1} \|\Delta^{(2)}Y_{i(k)}\| \quad (5)$$

where  $i(k) \in (i_1, i_2)$  and  $k \in (1, m)$ ,  $l$  is the  $l$ -th combination by  $m$  elements on the full set of finite differences for any specified step size  $p$ .

Finally, we can express the median estimate of  $j$ -th peak area  $\tilde{S}_j$ :

$$\|\tilde{S}_j\| = \text{med}_L \|S_j\|_l \quad (6)$$

where  $l \in (1, L)$  or more detailed form:

$$\|\tilde{S}_j\| = \text{med}_L \left( \|\Delta^{(2)}G_{i(k)j}\|^{-1} \|\Delta^{(2)}Y_{i(k)}\| \right)_l \quad (7)$$

We can easily reduce the last formula for singlet and doublet, where:

singlet: 
$$S_{1S} = \text{med}_L \left( \frac{\Delta^{(2)}Y_{i(1)}}{\Delta^{(2)}G_{i(1)1}} \right) \quad (8)$$

doublet ( first peak): 
$$\tilde{S}_{1D} = \left[ \frac{\frac{\Delta^{(2)}Y_{i(1)}}{\Delta^{(2)}G_{i(1)2}} - \frac{\Delta^{(2)}Y_{i(2)}}{\Delta^{(2)}G_{i(2)2}}}{\frac{\Delta^{(2)}G_{i(1)1}}{\Delta^{(2)}G_{i(1)2}} - \frac{\Delta^{(2)}G_{i(2)1}}{\Delta^{(2)}G_{i(2)2}}} \right] \quad (9)$$

## Implementation of the library driven analysis with a graphic user interface as a Windows application

The software package DIMEN, originally developed in Riga Research Radioisotope Institute (Latvia) by V.S. Kondrashov and Z.D. Moroz and initially contributed to Radiation Shielding Information Center (RSIC) at Oak Ridge National Laboratory (USA) in 1996, has been modified and transformed.

The identification of a given radionuclide is obtained by searching for a match with the energy information of a database. This procedure is performed in an interactive graphic mode by markers that superimpose, on the experimental spectra data, the energy information provided by a previously elaborated data library. This library of gamma- and x rays data includes 16712 gamma ray energy lines related to 756 known gamma emitter radioisotopes (749 currently listed by the ICRP and new 7 by C.Lederer and V.Shirley, Table of Isotopes, 7th edn., 1978).

Since DIMEN has been originally developed on Pascal programming language it looks naturally to make above mentioned transformation to Windows environment by object-oriented software platform DELPHI. The translation of analytical part of DIMEN has been mainly carried out by replacing the DOS-functions by the similar Windows-functions and adapting all DIMEN's

algorithms to the new Windows environment. The most significant transformation has been done to create the Graphic User Interface by developing the Main Graphic Window of WinDIMEN. WinDIMEN has been programmed by using the Borland Delphi Professional, Version 4.0 (Build 5.104) Update Pack 2, and Borland Delphi 4.0 for Windows 98,95 and NT. Minimal Computer Requirements are: PC-based machine, 486-processor (100 MHz), 16 Kb RAM, 1 Gb HDD. O/S: Windows 98,95 or NT.

## GUI description

The translation of the Analytical part of DIMEN was realized by replacing DOS-functions with similar Windows-functions and adapting all of DIMEN's algorithms to the new Windows environment.

A view of the GUI is shown on the Figure 1.

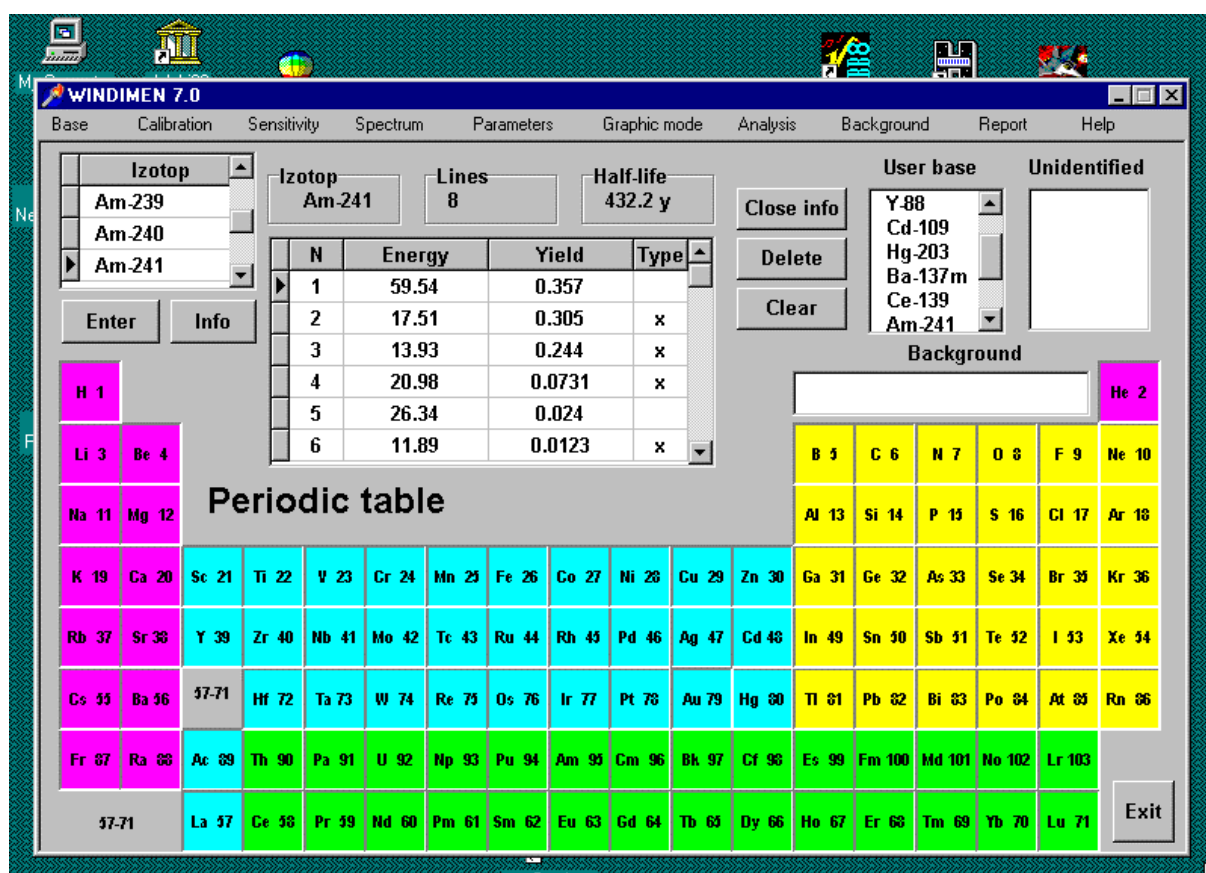


Fig. 1. Main Graphical User Interface (GUI) for WinDIMEN.

The main field of the User Interface is the Periodic Table of Elements. By clicking the left mouse button on the chosen element, the user displays all gamma ray emitted isotopes contained in the WinDIMEN Library in the upper left window. For user reference, the gamma ray lines (energies and yields) of these isotopes are shown in a separate window. On the top of GUI window the reader can find the pop-up menu, which performs the main WinDIMEN's functions and options.

The program has the following steps:

1. Create a nuclide table (user base) according to the preliminary information for the spectrum to be identified.

2. Energy calibration (processing of calibrated peaks and computation of the parameters of the curve "channel number-energy"). The calibration parameters can be kept in a file and then used to process other spectra of the given run. Calibration is recommended before the beginning of each run of measurements by using the spectrum GUI window, see Figure 2.
3. Calibration with respect to absolute sensitivity (efficiency calibration).
4. Processing of the background and storing its parameters to a file.
5. Direct processing of analysed spectrum: identification of analysed lines, computation of peak areas and activities, accounting for the background, printing of the output data.

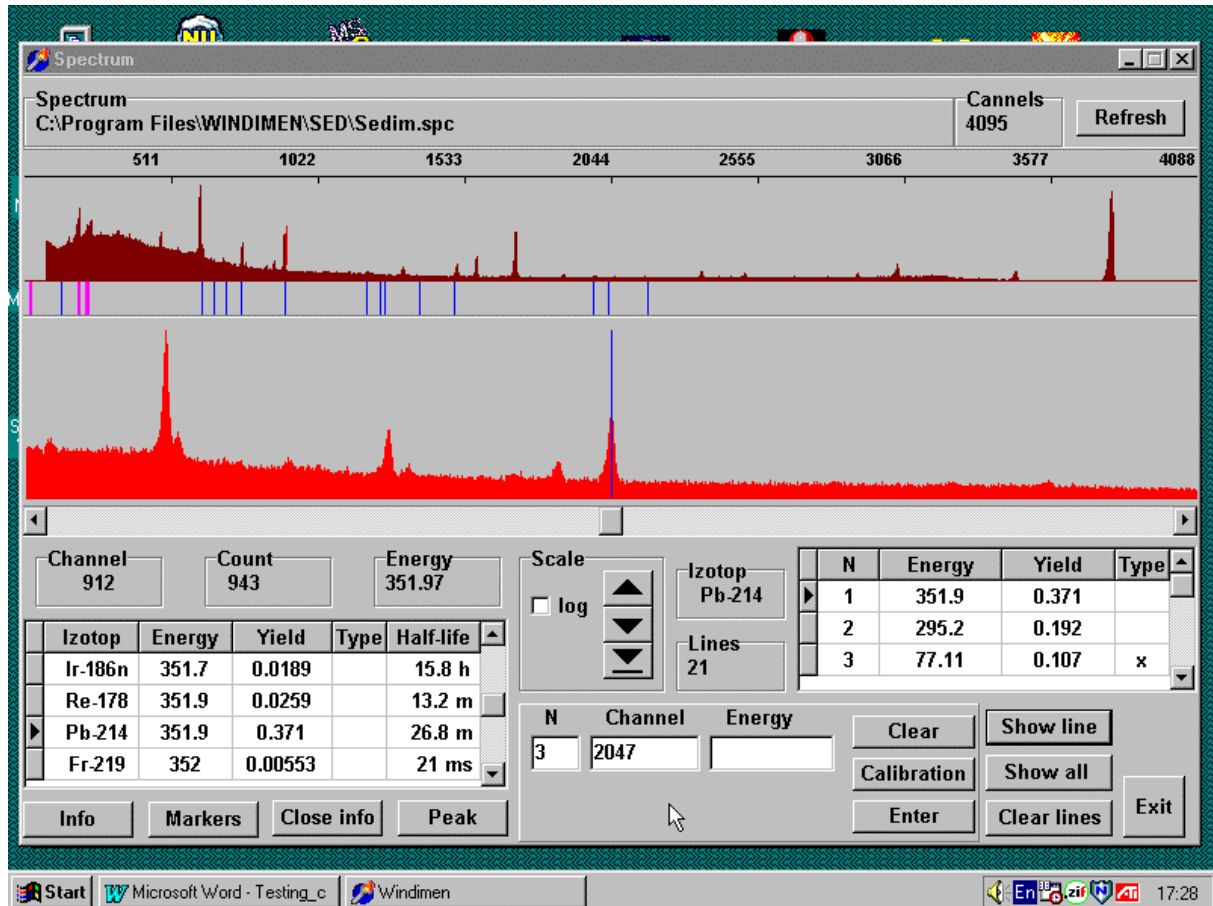


Fig. 2. The spectrum GUI window.

The WinDIMEN reads spectra in two formats: binary (Canberra format) and ASCII (common text format). It reads main parameters such as the file name, energy range, spectrum collecting time, measurement date, probe number, probe mass. Interaction time between WinDIMEN's Data Base and the main program has been optimised and typical program running time is less then for DOS DIMEN version.

Co-operation between the two packages WinDIMEN and ANGES has been elaborated.

- both program use the same spectrum format.
- WinDIMEN graphics option was modified under ANGES spectra performance.
- WinDIMEN can use common ANGES's utilities: energy calibration and efficiency calibration .

In co-operation with National Environmental Health Center in Latvia we have been included in the intercomparison exercise in the BOK 1.1 sub-project, under the Nordic Nuclear Safety Research Programme for 1998-2002, together with a total of 35 laboratories from another countries [5]. The results of intercomparison were discussed at the meeting in Skagen. In the December 2000 the results

of the intercomparison were distributed as NKS-19, ISBN 87-7893-069-3. The intercomparison confirmed that our approach provides a convenient and rapid solution for identifying and quantifying radioisotopes by gamma ray spectra analysis.

## REFERENCES

- [1] ROUTI, J.T., AND PRUSSIN, S.G., Nucl. Instr. and Meth. **72** (1969) 125.
- [2] KONDRASHOV, V. S., MOROZ, Z. D., KOLYSHKIN, A. A., VAILLANCOURT, R., Nucl. Inst. Meth. Phys. Res. **A328** (1993) 542-546.
- [3] KONDRASHOV, V. S., SAJO-BOHUS, L., GREAVES, E. D., Spectrochimica Acta, **49B(9)** (1994) 941-945.
- [4] Kondrashov, V.S., Final Report VEN10239, International Atomic Energy Agency (IAEA), Vienna, 1999.
- [5] KONDRASHOV, V.S., PETERSONE, I., Final Report LAT10883, IAEA, 2000.
- [6] KONDRASHOV, V.S. , et al. "Increasing Reliability in Gamma and X-Ray Spectral Data Analysis. Least Moduli Approach" to be published in Nucl. Instr. and Meth. in Phys. Res. A.
- [7] KONDRASHOV, V.S., ROTHENBERG, S.J., PETERSONE, I., "Database driven analysis for Nuclides quantification by gamma-spectra", Eighth International Symposium on Radiation Physics, Prague, June 5-9, 2000.

# ANALYSIS OF FINE STRUCTURE IN DOPPLER BROADENED ANNIHILATION PEAKS

**L. Calderin, R. Capote**

Center of Applied Studies for Nuclear Development,  
Havana, Cuba

**Abstract.** A Doppler annihilation spectra general unfolding algorithm was developed. This general algorithm has two programs: (i) RESFIT for fitting of the detector system resolution function; and (ii) DPPUNFOL for unfolding the experimental annihilation spectra. It should be mentioned that the asymmetric characteristic of this kind of spectra was considered as a part of the resolution function, instead of including it into the background. Both programs were tested using modeled data with statistical noise from 1- to 3-sigma levels added. A good agreement between the “true” parameters and the unfolded ones was achieved for all studied cases.

## Introduction

For data processing of positron annihilation Doppler spectra exist three different kind of approaches [1-4,7], namely:

- analysis by line-shape parameters,
- fitting to a convolution function model (unfolding),
- model independent deconvolution and after that use of line-shape analysis or fitting to a function model.

A Doppler annihilation spectra unfolding procedure was developed in this work. We also identified models for different components of the spectra, calculated convolutions, integrated them and found the parametric derivatives. Finally, we programmed and tested the code using modelled data.

The general algorithm has two programs:

- RESFIT for fitting of the resolution function.
- DPPUNFOL for unfolding the experimental spectrum.

In the following section we will briefly describe the theoretical background in the used deconvolution method.

## Unfolding model

After a constant background is removed, the real response or spectrum can be represented by the sum of  $np$  inverted parabolas plus  $ng$  gaussians, all normalized:

$$\mu(x) = \sum_{i=1}^{np} p_i(x) + \sum_{j=1}^{ng} g_j(x) \quad (1)$$

given:

$$p_i(x) = \frac{3Ip_i}{4\sigma p_i} \left(1 - \frac{(x - xp_i)^2}{\sigma p_i^2}\right) \theta(|x - xp_i| - \sigma p_i) \quad (2)$$

and

$$g_j(x) = \frac{Ig_j}{\sqrt{\pi}\sigma g_j} \exp\left(-\frac{(x - xg_j)^2}{\sigma g_j^2}\right) \quad (3)$$

where:

- $I_{p_i}$  and  $I_{g_j}$  represent the  $i$ -th parabola and  $j$ -th gaussian intensities respectively,
- $x_{p_i}$  and  $x_{g_j}$  are the  $i$ -th parabola and  $j$ -th gaussian position respectively
- $\sigma_{p_i}$  and  $\sigma_{g_j}$  give the  $i$ -th parabola and  $j$ -th gaussian widths
- step function  $\theta$  is defined as:

$$\theta(z) = 1 \quad z \leq 0$$

$$\theta(z) = 0 \quad z > 0$$

The resolution function in most of the studied cases from the bibliography is assumed as normalized gaussian:

$$G(x) = \frac{1}{\sqrt{\pi}\sigma} \exp\left(-\frac{x^2}{\sigma^2}\right). \quad (4)$$

The background is then assumed as a complementary error function times a intensity parameter [7], to take into account the asymmetry of the peak. Given that the asymmetry of this kind of peak is due to the measurement process itself, we preferred to include such effect in the resolution function using the following expression:

$$C(x) = I_c \text{Cerrf}\left(\frac{x}{\sigma_c}\right) \quad (5)$$

where  $\text{Cerrf}(x)$  is the complementary error function,  $I_c$  is the corresponding intensity and  $\sigma_c$  is a parameter that define the rate which the complementary error function drop from one to zero ( we call this parameter 'width' of  $\text{Cerrf}$ ).

The resolution function is then defined as:

$$R(x) = G(x) + C(x). \quad (6)$$

The measured spectrum at channel  $t$  might be then defined as:

$$\xi_t = \int_{-\infty}^{+\infty} \mu(x) R(t-x) dx + B \quad (7)$$

which can be rewritten in the way:

$$\xi_t = \left[ \sum_{i=1}^{np} (p_i * G)(t) + \sum_{j=1}^{ng} (g_j * G)(t) + \sum_{i=1}^{np} (p_i * C)(t) + \sum_{j=1}^{ng} (g_j * C)(t) \right] + B \quad (8)$$

given the parabolas and gaussian convolutions.  $B$  is a constant background. Calculating the convolutions with the gaussian, we obtained:

$$(p * G)(t) = \frac{3Ip}{8\sqrt{\pi}\sigma p} \left[ \begin{aligned} & \sqrt{\pi} \left( 1 - \frac{\sigma r^2 + 2(xp - t)^2}{2\sigma p^2} \right) (\operatorname{erf}(-xp + \sigma p + t) + \operatorname{erf}(x + \sigma p - t)) \\ & + \frac{\sigma r}{\sigma p^2} \left( \begin{aligned} & (-xp + \sigma p + t) \exp\left(-\frac{(xp + \sigma p - t)^2}{\sigma r^2}\right) \\ & + (xp + \sigma p - t) \exp\left(-\frac{(-xp + \sigma p + t)^2}{\sigma r^2}\right) \end{aligned} \right) \end{aligned} \right] \quad (9)$$

and

$$(g * G)(t) = \frac{Ig}{\sqrt{\pi}\sqrt{\sigma r^2 + \sigma g^2}} \exp\left(-\frac{(xg - t)^2}{\sigma r^2 + \sigma g^2}\right). \quad (10)$$

In the case of the convolutions with  $C(x)$  we work directly with numerical integrals and not with analytical expression. In the case of  $(g * C)(t)$  the integral between  $-\infty$  and zero do not exist. So we have to redefine the lower limit of integration. Given that the gaussian should tend to zero when  $x$  approaches the channel zero we take the lower limit of the integral as the number of channels used to collect the spectrum. The limits of integration became then:

$$(g * C)(t) = \int_{-\infty}^{+\infty} g(x)C(t-x)dx \equiv \int_{LF}^{-LF} g(x)C(t-x)dx \quad (11)$$

where  $LF$  is the extension of  $C(x)$  in its left side. It means for values of  $x$  less than  $LF$   $C(x)$  is zero. We usually take  $LF$  equal to the number of channels. So in this way the infinity for the gaussian convoluted with the function  $C(x)$  is defined. Please, note that this value should be negative.

For the convolution  $(p * C)(t)$  we just have to integrate between  $x_p - \sigma_p$  and  $x_p + \sigma_p$  because outside this region the parabola is zero. Therefore:

$$(p * C)(t) = \int_{-\infty}^{+\infty} p(x)C(t-x)dx = \int_{x_p - \sigma_p}^{x_p + \sigma_p} p(x)C(t-x)dx \quad (12)$$

The necessary parametric derivatives were also calculated. For the fitting of the resolution function and the unfolding procedure we used a Marquardt-Levenberg  $\chi^2$  -minimization subroutine[5,6].

## Tests using modeled data

To test the RESFIT program we modeled 6 resolution functions and introduce three levels of statistical noise in each one of them. So we get 18 sets of modeled data. The levels of the statistical noise correspond to the rule of one, two and three standard deviation for each channel. The Annex 3 shows all the information related to the tests of RESFIT. One more test with asymmetric effect and with the maximum noise added was carried out.

The program DDPUNFOLD was tested using 9 sets of modeled data with maximum statistical noise added (Annex 4). This sets take into account the hardest cases to manage that we found in the bibliography. Like for to test RESFIT we also used a set with asymmetric effect. As initial guessed parameters for the resolution unction we took those fitted by RESFIT.

## Results

Both programs were tested using modelled data with statistical noise added. Some results are shown in the Annexes 4 and 5. Tests using measured data have not been performed yet.

As it shows in the Annexes 4 and 5 the results for the modeled data are very good. There is a very good agreement between the true parameters and the fitted or unfolded ones even in such cases like the one with the narrowest parabolic component. This case is pathologic as it is shown in some references like [2,4] for other kind of unfolding techniques. The standard deviations also show very good behaviour, in all the cases the true value is in the interval given by the corresponding unfolded parameter minus and plus its standard deviation.

## Conclusions

Two codes were developed: one for fitting the resolution function and the other for unfolding Doppler broadened positron annihilation gamma ray spectra. For the first time the asymmetry characteristic of this kind of spectra is considered as a part of the resolution function. Until now the asymmetry was treated as part of the background and it was subtracted from the spectra as the first step [7]. The programs were tested using modeled data and the results are excellent.

## REFERENCES

- [1] KONG, Y., LYNN, K.G., Deconvolution of positron annihilation  $\gamma$  ray energy spectra with the maximum entropy principle, Nucl. Instr. and Meth. **A302** (1991) 145-149.
- [2] BRITTON, D.T., BENTVELSEN, P., DE VRIES, J., VAN VEEN, A., Deconvolution of Doppler-broadened positron annihilation line-shapes by fast Fourier transformation using a simple automatic filtering technique, Nucl. Instr. and Meth. **A273** (1988) 343-348.
- [3] BRITTON, D.T., VAN VEEN, A., Non-iterative fitting of deconvoluted positron annihilation line-shapes. Nucl. Instr. and Meth. **A275** (1989) 343-348.
- [4] DANNEFAER, S., KERR, D. P., Deconvolution of Doppler-broadened spectra of positron annihilation photons. Nucl. Instr. and Meth. **131** (1975) 119-124.
- [5] NASH, J. C., Compact numerical methods for computers: linear algebra and function minimization, Adam Hilger Ltd Bristol (1985).
- [6] PRESS, W. H., FLANNERY, B. P., TEUKOLSKY, S. A., VETTERLING, W.T., Numerical Recipes, Cambridge University Press (1985).
- [7] CHAGLAR, I., et. al., Nucl. Instr. and Meth. **187** (1981) 581.

## Annex 1

### I/O DESCRIPTION FOR RESFIT

This program use the input file with extension CTL (you need to input only input filename) with the following format:

- In the first line a header of until 80 characters of length,
- In the second line the path for the resolution spectrum to fit,
- In the third line the first and last channel for the fitting,
- In the fourth line the scale in keV/channel,
- In the fifth line, separated by space, the initial guess for the parameters:  $I_r$ ,  $x_r$ ,  $\sigma_r$ ,  $I_c$ , and  $\sigma_c$ ,
- In the sixth line five characters of the type F and G for the fixed and guessed parameters respectively,
- In the seventh line the first and last channel to estimate the background constant,
- In the eighth a character F or G to keep the background fixed or to allow to fit it respectively.

The output file is the screen and the information for the initial and fitted parameters with its standard deviations is given.

Example of RESFIT input file (RESFIT.CTL):

```
TEST FOR RESFIT
RESFUN01.997
1 82
1.
1700000. 40.8 4.3 10. 1.
GGGGG
71 82
G
```

## Annex 2

### I/O DESCRIPTION FOR DPPUNFOL

This program use the input file with extension CTL (you need to input only input filename) with the following format:

- In the first line a header of until 80 characters of length,
- In the second line the path for the resolution spectrum to fit,
- In the third line the first and last channel for the fitting,
- In the fourth line the scale in keV/channel,
- In the fifth line the resolution function parameters  $\sigma_g$ ,  $I_c/I_g$ ,  $\sigma_c$  and the left limit of integration for the convolution with the complementary error function,
- In the sixth line tree characters of the type F and G for the fixed and guessed parameters of the resolution function respectively. Note that the left limit of integration is always fixed,
- In the seventh the number of gaussians to unfold ( $n_g$ ),
- In the eighth line the initial parameters for the first gaussian ( $I_g$ ,  $x_g$ ,  $\sigma_g$ ),
- In the ninth line tree characters of type F or G for the each fixed or guessed parameter,
- In the following  $2(n_g-1)$  the same type of information for the rest of the gaussians is given,
- In the  $(7+2n_g)$ -th line the number of parabolic component to unfold appears,
- In the  $(7+2n_g+1)$ -th line the initial parameters for the first parabola ( $I_p$ ,  $x_p$ ,  $\sigma_p$ ),
- In the  $(7+2n_g+2)$ -th line tree characters of type F or G for the each fixed or guessed parameter,
- In the following  $2(n_p-1)$  the same type of information for the rest of the paraboloids is given,
- In the  $(8+2(n_g+n_p))$ -th line the first and last channel to estimate the background constant,
- In the  $(8+2(n_g+n_p)+1)$ -th a character F or G to keep the background fixed or to allow to fit it respectively.

The output file is the screen and the information for the initial and fitted parameters with its standard deviations is given.

Example of input file:

```
TEST FOR DPPUNFOL
SIMDOP01.997
1 150
1.
11.98 0.005 9.57 -150.
FFF
1
440000. 74. 15.
GGG
1
100000. 74. 10.
GGG
141 150
G
```

### Annex 3

#### TESTS FOR RESFIT

( $x_r$ ,  $\sigma_r$  and  $\sigma_c$  in channels.  $I_r$ ,  $I_c$  and B in counts.)

Spectrum file	Control file	True parameters						Initial guessed parameters						Results of the fitting						$\chi^2$
		$I_r$	$x_r$	$\sigma_r$	$I_c$	$\sigma_c$	B	$I_r$	$x_r$	$\sigma_r$	$I_c$	$\sigma_c$	B	$I_r$	$x_r$	$\sigma_r$	$I_c$	$\sigma_c$	B	
RESFUN01.682	resCTL01.682	1000000.	41.	2.5	0.	1.	50.	1700000	40.8	4.3	0.	1.	60	1000281	41.00	2.50	.00	1.F	49.30	23
RESFUN01.954	resCTL01.954							1700000	40.8	4.3	0.	1.	60	1000331	(.00)	(.00)	F	(.85)	48.72	48
RESFUN01.997	resCTL01.997							1700000	40.8	4.3	0.	1.	60	999616	(.00)	(.00)	F	(.85)	47.95	70
RESFUN02.682	resCTL02.682	1000000.	41.	5.0	0.	1.	50.	1700000	40.8	4.3	0.	1.	60	1000132	(.00)	5.0	.00	1.F	49.31	23
RESFUN02.954	resCTL02.954							1700000	40.8	4.3	0.	1.	60	999741	(.00)	5.0	.00	1.F	48.91	47
RESFUN02.997	resCTL02.997							1700000	40.8	4.3	0.	1.	60	999461	(.00)	5.0	.00	1.F	47.92	70
RESFUN03.682	resCTL03.682	1000000.	41.	7.5	0.	1.	50.	1700000	40.8	4.3	0.	1.	60	1000010	(.00)	7.50	.00	1.F	49.28	23
RESFUN03.954	resCTL03.954							1700000	40.8	4.3	0.	1.	60	999363	(.00)	7.49	.00	1.F	49.28	48
RESFUN03.997	resCTL03.997							1700000	40.8	4.3	0.	1.	60	999158	(.01)	7.49	.00	1.F	48.70	67
RESFUN04.682	resCTL04.682	1000000.	41.	10	0.	1.	50.	1700000	40.8	4.3	0.	1.	60	999932	(.01)	10.00	.00	1.F	49.20	23
RESFUN04.954	resCTL04.954							1700000	40.8	4.3	0.	1.	60	999180	(.01)	9.99	.00	1.F	49.19	48
RESFUN04.997	resCTL04.997							1700000	40.8	4.3	0.	1.	60	998872	(.01)	9.99	.00	1.F	48.94	66
RESFUN05.682	resCTL05.682	1000000.	41.	12.5	0.	1.	50.	1700000	40.8	4.3	0.	1.	60	999842	(.01)	12.50	.00	1.F	49.48	23
RESFUN05.954	resCTL05.954							1700000	40.8	4.3	0.	1.	60	999062	(.01)	12.50	.00	1.F	49.52	48
RESFUN05.997	resCTL05.997							1700000	40.8	4.3	0.	1.	60	998658	(.01)	12.49	.00	1.F	49.23	49
RESFUN06.682	resCTL06.682	1000000.	41.	15	0.	1.	50.	1700000	40.8	4.3	0.	1.	60	999724	(.01)	14.99	.00	1.F	50.12	23
RESFUN06.954	resCTL06.954							1700000	40.8	4.3	0.	1.	60	998953	(.01)	14.99	.00	1.F	50.22	48
RESFUN06.997	resCTL06.997							1700000	40.8	4.3	0.	1.	60	998455	(.01)	14.99	.00	1.F	50.24	66
simdata2/ RESFUN01.997	simdata2/ resCTL01.997	1000000.	41.	12.	<b>5000.</b>	<b>10.</b>	<b>50.</b>	1700000	40.8	4.3	10.	1.	<b>71</b>	1000331	(.01)	11.98	5014	14.65	44.23	63
													<b>82</b>	(1271)	(.03)	(.01)	(13)	(.43)	(2.54)	

## Annex 4

### TESTS FOR DPPUNFOL

(all x values,  $\sigma$  values and LF in channels; all I values and B in counts)

Spectrum file	True Parameters										
	$\sigma_r$	$I_c$	$\sigma_c$	LF	$I_g$	$x_g$	$\sigma_g$	$I_p$	$x_p$	$\sigma_p$	B
Simdop01.997	2.5	0.	1.	-81.	1000000	75.	20.	200000.	75.	12.	50.
Simdop02.997	5.	0.	1.	-81.	1000000	75.	20.	200000.	75.	12.	50.
Simdop03.997	7.5	0.	1.	-81.	1000000	75.	20.	200000.	75.	12.	50.
Simdop04.997	10	0.	1.	-81.	1000000	75.	20.	200000.	75.	12.	50.
Simdop05.997	12.5	0.	1.	-81.	1000000	75.	20.	200000.	75.	12.	50.
Simdop06.997	15.	0.	1.	-81.	1000000	75.	20.	200000.	75.	12.	50.
Simdop07.997	10.	0.	1.	-81.	1000000	75.	20.	200000.	75.	5.	50.
Simdop08.997	10.	0.	1.	-81.	1000000	75.	20.	200000.	75.	7.	50.
Simdop09.997	10.	0.	1.	-81.	1000000	75.	20.	200000.	75.	10.	50.
Simdata2/ Simdoppl.997	12.	.005	10.	-150.	1000000	75.	20.	200000.	75.	12.	50.

Control file	Initial guessed parameters										
	$\sigma_r$	$I_c$	$\sigma_c$	LF	$I_g$	$x_g$	$\sigma_g$	$I_p$	$x_p$	$\sigma_p$	B
dppCTL01.997	2.49	0.	1.	-81.	440000.	74.	15.	100000	74.	10.	141 150
dppCTL02.997	5.	0.	1.	-81.	410000.	74.	10.	330000	76.	10.	141 150
dppCTL03.997	7.49	0.	1.	-81.	500000.	76.	10.	100000.	74.	10.	141 150
dppCTL04.997	10	0.	1.	-81.	410000.	76.	10.	330000	74.	10.	141 150
dppCTL05.997	12.49	0.	1.	-81.	410000.	74.	10.	330000	76.	10.	141 150
dppCTL06.997	14.99	0.	1.	-81.	410000.	76.	10.	330000	74.	10.	141 150
dppCTL07.997	10.	0.	1.	-81.	410000.	70.	10.	330000	78.	10.	141 150
dppCTL08.997	10.	0.	1.	-81.	410000.	74.	10.	330000	75.	10.	141 150
dppCTL09.997	10.	0.	1.	-81.	410000.	75.	10.	330000	74.	10.	141 150

Note: In the column B appear the first and last channel to estimate the background.

Output file	Unfolded parameters							
	$I_g$	$x_g$	$\sigma_g$	$I_p$	$x_p$	$\sigma_p$	B	
dpp01OUT.997	998456 (2342)	75.01 (.01)	19.99 (.02)	200587 (2187)	74.98 (.03)	12.08 (.06)	48.21 (1.04)	
dpp02OUT.997	997344 (3546)	75.00 (.02)	20.00 (.03)	201695 (2941)	74.98 (.04)	12.13 (.11)	48.20 (1.08)	
dpp03OUT.997	996880 (4362)	75.00 (.02)	20.00 (.04)	202132 (4309)	74.98 (.05)	12.18 (.18)	48.28 (1.14)	
dpp04OUT.997	998238 (6740)	75.01 (.02)	19.98 (.05)	200714 (6736)	74.96 (.07)	12.12 (.34)	48.49 (1.24)	
dpp05OUT.997	1003147 (10859)	75.02 (.02)	19.95 (.07)	195707 (10903)	74.93 (.09)	11.89 (.64)	48.89 (1.41)	
dpp06OUT.997	1011371 (18085)	75.03 (.03)	19.90 (.12)	187347 (18187)	74.88 (.12)	11.39 (1.27)	49.51 (1.71)	
dpp07OUT.997	997251 (4369)	75.01 (.02)	19.99 (.04)	201707 (4323)	74.97 (.05)	5.41 (.52)	48.40 (1.22)	
dpp08OUT.997	997286 (4772)	75.01 (.02)	19.99 (.04)	201673 (4736)	74.97 (.05)	7.30 (0.42)	48.42 (1.23)	
dpp09OUT.997	997603 (5751)	75.01 (.02)	19.99 (.05)	201354 (5734)	74.96 (.06)	10.19 (.35)	48.45 (1.23)	
Simdata2/ dpp01OUT.997	990408 (12444)	75.02 (.04)	20.06 (.09)	208525 (12483)	74.98 (.11)	12.48 (.62)	47.35 (1.86)	

# QUALITY ASSURANCE AND QUALITY CONTROL IN GAMMA RAY SPECTROMETRY

**K. Heydorn**

Department of Chemistry, Technical University of Denmark,  
Lyngby, Denmark

**Abstract.** The maximum likelihood algorithms for nuclides activities estimation from low intensity scintillation  $\gamma$  ray spectra have been created. The algorithms treat full energy peaks and Compton parts of spectra, and they are more effective than least squares estimators. The factors that could lead to the bias of activity estimates are taken into account. Theoretical analysis of the problem of choosing the optimal set of initial spectra for the spectrum model to minimize errors of the activities estimation has been carried out for the general case of the  $N$ -components with Gaussian or Poisson statistics. The obtained criterion allows to exclude superfluous initial spectra of nuclides from the model. A special calibration procedure for scintillation  $\gamma$ -spectrometers has been developed. This procedure is required for application of the maximum likelihood activity estimators processing all the channels of the scintillation  $\gamma$ -spectrum, including the Compton part. It allows one to take into account the influence of the sample mass density variation. The algorithm for testing the spectrum model adequacy to the processed scintillation spectrum has been developed. The algorithms are realized in Borland Pascal 7 as a library of procedures and functions. The developed library is compatible with Delphi 1.0 and higher versions. It can be used as the algorithmic basis for analysis of highly sensitive scintillation  $\gamma$ - and  $\beta$ -spectrometric devices.

## Introduction

Since the appearance of the ISO Guide [1] in 1993 the BIPM philosophy [2] has become the fundament for all analytical quality control and quality assurance. Quality assurance today is based on an *uncertainty budget*, and statistical control means that the uncertainty of data predicted by the uncertainty budget is consistent with the actually observed variability of replicate measurements.

Validation of an analytical method based on  $\gamma$ -spectrometry requires that

- a) all systematic errors are eliminated or appropriately corrected for,
- b) all sources of variability are identified and their contribution to the analytical uncertainty accounted for in the uncertainty budget,
- c) analytical results are found to be in statistical control.

The key to validation is the last point, which expresses that the estimated standard deviation  $\sigma_i$  and observed variability among  $n$  replicate analytical results  $y_i$  be in complete agreement. This is tested by the statistic

$$T = \sum_i^n \frac{(y_i - \hat{\mu})^2}{\hat{\sigma}_i^2} \quad (1)$$

where  $\hat{\mu}$  is the weighted mean of  $n$  individual results

$$\hat{\mu} = \frac{\sum \omega_i y_i}{\sum \omega_i} \quad (1a)$$

and the weights

$$\omega_i = \frac{1}{\hat{\sigma}_i^2} \quad (1b)$$

When results are in statistical control the statistic  $T$  is closely approximated by a  $\chi^2$ -distribution with  $n-1$  degrees of freedom.

For  $m$  duplicates ( $n = 2$ ) these formulae are simplified

$$T = \sum_1^m \frac{(y_1 - y_2)^2}{\hat{\sigma}_1^2 + \hat{\sigma}_2^2} \quad (2)$$

with m degrees of freedom.

In neutron activation analysis and other radioanalytical methods the variability of results cannot be explained only from an *a priori* precision because of the significant contribution from counting statistics. It has been shown unequivocally [3] that, when the *a priori* variance estimate is compounded with the variance contribution from counting statistics in the uncertainty budget, the resulting combined  $\hat{\sigma}$  should be used in Eq. (1) without any significant change in the distribution of T. Therefore, also in these methods the statistic T is the most suitable test for the presence or absence of significant unknown or unexpected sources of variability.

## Uncertainty budget

The propagation of uncertainty is represented by the Gauss-Laplace equation [4]

$$\hat{\sigma}_y^2 = \sum_{i=1}^p \left( \frac{\partial y}{\partial x_i} \right)^2 \hat{\sigma}_i^2$$

where the combined standard uncertainty of the final analytical result  $y = f(x_1, \dots, x_p)$  is calculated from the uncertainties  $\sigma_i$  of the individual variables  $x_i$  using the partial derivatives as sensitivity coefficients.

In simple arithmetic expressions the propagation of uncertainty is just the addition of variances, and in logarithmic expressions uncertainty is propagated in the form of the relative uncertainties; it is therefore expedient to separate absolute and relative contributions in the calculation of the combined uncertainty.

In neutron activation analysis and other radioanalytical methods the uncertainty budget is an evaluation of the contribution from all possible sources of variability to the distribution of replicate analytical results. Sources of variability with no significant contribution need not be accurately accounted for, while the most significant sources of variability must be carefully evaluated, often by conducting a series of experiments to determine the standard deviation of the distribution.

Identification of all sources of variability in an analytical method is possible only for the professional practitioner of the art. Significant sources of variability in radioanalytical methods may, however, be associated with all stages of the analysis and should be studied separately for each of several types:

- Sample characteristics;
- Irradiation conditions, if applicable;
- Radionuclide properties;
- Radiochemical separation, if applicable;
- Counting conditions.

When the uncertainty budget is complete, there are no unknown sources of variability, and statistical control is maintained under all conditions. In that case the distribution of the statistic T in Eq. (1) is indistinguishable from a  $\chi^2$ -distribution and well suited for continuous quality control. When this stage has been reached it is usually practical to pool all relative uncertainties  $\hat{\sigma}_r^2$ , all absolute uncertainties  $\hat{\sigma}_a^2$ , and obtain the following expression for the expected standard uncertainty of the result

$$\hat{\sigma}^2 = \hat{\sigma}_a^2 + \bar{y}^2 \hat{\sigma}_r^2 + \sigma_c^2 \quad (3)$$

where  $\sigma_c^2$  is the contribution from counting statistics.

However, Eq. (1) is applicable **only** if the individual results  $y_i$  and their corresponding standard deviations  $\sigma_i$  are correctly estimated! Verification of the computer programs used for the analysis therefore has to be carried out **before** any serious attempts to validate the analytical method are begun.

## Verification

Experience has shown that it is possible to achieve statistical control in neutron activation analysis on the basis of an uncertainty budget with significant contributions to the uncertainty of the final analytical result being only irradiation exposure, and counting statistics, and that it is possible to calculate the standard deviation of the distribution of irradiation exposures around their mean from knowledge of the irradiation geometry [5] and the counting statistics from the assumption of an underlying Poisson statistic [6].

In this case the combined uncertainty of a result  $\hat{\sigma}$  from Eq. (3) is reduced to

$$\hat{\sigma} = \sigma_{ir}^2 + \sigma_c^2 \quad (4)$$

where

$$\sigma_{ir}^2 = \bar{y}^2 \hat{\sigma}_r^2$$

$\hat{\sigma}_r^2$  and  $\hat{\sigma}_r$  could be determined for each separate irradiation facility by Monte Carlo calculations, while  $\sigma_c^2$  is calculated by a suitably validated computer program for propagation of statistical variation.

According to this simple budget the parameters listed in Table 1 should have no influence on the uncertainty of the analytical result. This means that the data processing program should be capable of correcting accurately for all parameters listed without introducing any excess variability not accounted for in Eq. (4) — in other words the contributions from all these variables are covered by counting statistics.

TABLE 1. PARAMETERS ASSUMED TO HAVE NO DIRECT INFLUENCE ON THE UNCERTAINTY OF RESULTS OBTAINED BY RADIOANALYTICAL METHODS, INCLUDING NAA

Method	Sample
Variables	
Irradiation time	Quantity
Neutron flux density	Activity
Decay time	Concentration
Counting time	$\gamma$ -energy
Dead time	Half-life
Peak width	
Factors	
Detector	Determinand
Counting position	Matrix
Counting equipment	Indicator

The experimental justification of these assumptions should be based on the verification of complete statistical control for real sample materials under all conceivable conditions of practical analysis, in order to show that variations in all these parameters are adequately accounted for by Eq. (4). Since some of the corrections are not completely accountable [7], some of the variable parameters should not go beyond certain limits.

This applies particularly to corrections for losses during counting, which have to include not only dead time, but also the effects of pile-up at higher count rates. In specialized gamma-spectrometry, we found that the introduction of loss-free counting (LFC) systems resulted in significant deviations from the undisturbed Poisson statistics, leading to a loss of statistical control of the analytical results. This led to a special study of the statistics of LFC spectra at the Belgian Nuclear Research Center in Mol [8].

Deviations from Poisson statistics were also expected in other types of corrected spectra, such as those produced under Compton suppression. A special study in co-operation with the University of Illinois and based on their Compton-suppression system is reported at this meeting [9].

Highly standardized methods with fixed irradiation times, decay times, counting positions *etc.* result in almost constant corrections, which may very well be erroneous. Such methods may therefore give reproducible, but biased results. Reliable analytical methods are robust against changes in normal operating conditions and should not be rigidly standardized. In NAA it should be sufficient to specify the maximum permissible dead time during counting, and the irradiation and counting geometries that should be used.

### ***Validation of the uncertainty budget***

Experimental verification of our data processing software is carried out by replicate countings of the same sample in a very simple detector assembly [10], but under such different conditions that many effects need different corrections. Most correction methods fail when there is a significant change of count-rate during the counting period, and therefore the relevant limitations of the method should be stated in the description of the method.

The validation procedure proceeds stepwise through the following stages:

1. *Data processing*, checking the adequacy of corrections for decay, counting losses etc.
2. *Counting conditions*, checking the reproducibility of counting geometry for different materials at a full range of  $\gamma$ -energies.
3. *Irradiation conditions*, checking the adequacy of the *a priori* estimate of variability among duplicates.
4. *Radiochemical separation*, checking the adequacy of correction for losses during separation
5. *Sampling*, determining the variability among duplicate samples of relevant types of environmental materials.

Validation refers only to the particular equipment and conditions specified in the analytical procedure and has to be repeated whenever the procedure is modified. The data reported in the following from the author's own laboratory therefore serve merely to illustrate the method and to demonstrate that statistical control can be achieved in practice.

By allowing many factors and variables to change at the same time, but independently of each other, it is possible to validate Eq. (4) with a relatively small number of experiments.

**Experiment 1.** One sample of each of three different environmental materials were irradiated consecutively and counted immediately after the end of irradiation for 2, 5 and 10 minutes in succession at a counting position giving a dead time close to, but not exceeding 25%.

Using BCR certified reference materials for hay powder, fly ash and aquatic plant, irradiated for 10 s at a neutron flux density of  $2.5 \times 10^{13}$  n/cm<sup>2</sup>s, we were able to investigate the influence of:

decay	from 1–0.002
counting time	from 2–10 min
dead time	from 2–25%
half life	from 2.2–900 min
$\gamma$ -energy	from 0.62–2.75 MeV
determinands	Al, Br, Cl, K, Mn, Na
concentrations	70 $\mu\text{g.g}^{-1}$ –35 $\text{mg.g}^{-1}$
matrices	3 different

Data from the 3 successive countings were tested by the T-statistic in accordance with Eq. (1), and results are presented in Table 2 for each element and type of material. With 2 degrees of freedom for each characteristic  $\gamma$ -line identified in all three countings, we find that for all three materials the variability of results for the elements determined could be entirely attributed to counting statistics. When all results are pooled, we obtain  $T = 43.5$  for 40 degrees of freedom, which has a probability  $P(\chi^2 \geq T) = 0.33$ .

This means that corrections for decay, counting time and dead time, as well as pulse pile-up etc., do not give rise to additional variability of results within the range of conditions covered in the experiment. Longer half-lives give rise to smaller corrections, so that there is no need to make additional experiments with other determinands. Neither the elemental concentrations nor the matrix composition had any influence on the variability of results within the range of  $\gamma$ -energies covered by the experiment.

TABLE 2. STATISTICAL CONTROL IN TRIPLE COUNTINGS\* OF THREE DIFFERENT ENVIRONMENTAL SAMPLES, CORRECTED FOR DEAD-TIME LOSSES AND RADIOACTIVE DECAY

Irradiated material and code		Fly ash BCR 38			Aquatic plant BCR 61			Hay powder BCR 129			
% dead time		start = 26% finish = 2%			start = 21% finish = 6%			start = 24% finish = 17%			
Radio-nuclide symbol	Half-life min	Number of $\gamma$ -lines	Precision %	Statistic T	Number of $\gamma$ -lines	Precision %	Statistic T	Number of $\gamma$ -lines	Precision %	Statistic T	
<sup>28</sup> Al	2.2	2	0.8	4.21	2	1.0	1.97	-			
<sup>56</sup> Mn	155	1	2.5	1.84	3	0.5	8.65	2	0.7	10.89	
<sup>24</sup> Na	900	-			1	8.5	5.06	2	1.0	3.34	
<sup>38</sup> Cl	37	-			1	7.5	0.54	4	0.5	2.05	
<sup>42</sup> K	722	-			-			1	3.2	1.77	
<sup>80</sup> Br	18	-			-			1	2.1	3.14	
Degrees of freedom		3 × 2 = 6 d.f.			6.05	7 × 2 = 14 d.f.		16.22	10 × 2 = 20 d.f.		21.19

\* 2 min, 5 min, and 10 min

TABLE 3. REPRODUCIBILITY OF COUNTING GEOMETRY IN FOUR DIFFERENT POSITIONS

Precision %	Position 257 mm		Position 175 mm	
	d.f. <sup>a</sup>	T	d.f. <sup>a</sup>	T
<2%	12	13.15	14	18.25
2–8%	15	17.46	7	8.56
>8%	17	11.72	7	5.46
Total	44	42.33	28	32.27
$P(\chi^2 \geq T)$	0.54		0.26	
Precision %	Position 117 mm		Position 76 mm	
	d.f.	T	d.f.	T
<2%	6	6.05	9	12.77
2–8%	13	11.21	13	8.96
>8%	8	9.62	3	0.53
Total	27	26.88	25	22.26
$P(\chi^2 \geq T)$	0.47		0.62	

<sup>a</sup> Degrees of freedom = number of pairs of identified spectral peaks

**Experiment 2.** Two samples of each of three different environmental materials were irradiated together and counted alternately 1 hour after irradiation for 20 min and 1 h at the same counting position. Each pair was counted again in another position the following day.

Using BCR CRMs for cod muscle, aquatic plant, and beech leaves, irradiated between 10 s and 2 min, we were able to investigate the influence of:

decay	from 1 h–24 h
counting time	from 20 min–1 h
half-life	from 0.63 h–35.3 h
counting position	76–257 mm from detector
precision	from 0.35–30%
$\gamma$ -energy	from 0.06–3.08 MeV
matrices	3 different

Data from duplicate countings in 4 different counting positions were tested by the T-statistic in accordance with Eq. (2), and results are presented in Table 3 for each counting position, grouped according to the counting precision.

In order to cover as thoroughly as possible the range of  $\gamma$ -energies, as well as different levels of precision, all unequivocally identified peaks present in duplicate spectra were used for the test, with the exception of:

- single escape peaks, which — unlike double escape peaks — tend to be asymmetric [11], and therefore cannot be evaluated properly by the photo-peak integration program.
- annihilation peaks, which also tend to be asymmetric, and whose intensity is determined by high-energy  $\gamma$ -lines with different half-lives, so that a correct decay correction is not possible.
- 1293 keV  $\gamma$  ray from <sup>41</sup>Ar originating from the air in the irradiation container, and not from the sample.

Results in Table 3 demonstrate the absence of excess variability under all conditions of the experiment, even at the best precision. With a total  $T = 123.74$  at 124 d.f. the reproducibility of counting geometry in all 4 positions investigated does not contribute to the uncertainty for any of the environmental materials included in the investigation.

**Experiment 3.** Irradiation conditions may now be tested by simultaneous irradiation of several samples from the same homogeneous material, and examples of this have been presented earlier in reference [4].

**Experiment 4.** The contribution of a radiochemical separation to the uncertainty budget is associated with the correction for chemical yield and how this is determined; it has to be taken into account by its own appropriate budget for the uncertainty of the yield determination. An example of this is presented in a monograph on analytical chemistry [12].

**Experiment 5.** Two large samples of an environmental material with a very high degree of homogeneity were irradiated together and counted in the same counting geometry after several days of decay. A sub-sample of approx. 10% should be taken of each sample and counted in the same counting position for a correspondingly longer period.

Using a BCR certified reference material of river sediment [13] with a minimum recommended sample size of 100 mg, we irradiated one-gram samples for 3 hours in a thermal neutron flux density of  $4 \times 10^{13}$  n/cm<sup>2</sup>s. After a decay of 10 days each sample was divided into approximately 900 and 100 mg in separate counting vials, and counted for 30 min and 5 h respectively. This enabled us to check the influence of:

sample size	from 0.1–0.9 g
counting position	26–257 mm from detector
counting time	from 30 min–5 h
half-life	900 min–5.3 y

Results in Table 4 for 2 sets of samples at 2 different counting positions are shown to be independent of sample size at these two counting geometries, when compared by a T-value obtained from Eq. (2) at a counting precision of less than 1%. Only for the element Sc a high value of T shows that results are not identical at a level of 0.3%, indicating an uneven distribution among the samples in spite of its status as certified; the same lack of agreement could be observed for other trace elements for which no certification had been attempted.

TABLE 4. COMPARISON OF RESULTS OBTAINED FOR 100 MG AND 900 MG SAMPLES OF RIVER SEDIMENT CRM 320 AFTER 1–2 WEEKS' DECAY

Element symbol	Concentration mg/kg	Relative precision	Number of comparisons	Statistic T
Fe	40 000	0.6%	6	7.06
Ca	20 000	7.5%	4	6.01
Na	17 000	1.1%	6	4.75
Rb	150	5.5%	4	1.35
Cr	138 <sup>b</sup>	1.4%	4	4.99
Co	17	1.7%	6	6.07
Cs	5	6.5%	8	7.48
P( $\chi^2 \geq T$ ) = 0.48 for degrees of freedom =			38	37.71
Sc	15 <sup>b</sup>	0.3%	8	28.68
P( $\chi^2 \geq T$ ) < 0.03 for degrees of freedom =			46	66.39

<sup>b</sup>Certified value

## Nuclear interference correction

An important source of systematic error in neutron activation analysis with, as well as without radiochemical separation, is the formation of the same indicator nuclide from several elements possibly present in the sample, usually referred to as *nuclear interference*. Unless it can be proven by calculation that the interference can be disregarded, it is necessary to correct the result for it and to include the uncertainty of the correction in the uncertainty budget.

Such correction relies on the determination of the quantity of interfering elements present in the sample, which is properly done also by the use of gamma-spectrometry. The combination of several gamma-spectra to calculate the corrected value of the determinand calls for a more complicated composition of the uncertainty budget.

Actual examples of nuclear interference are listed in Table 5. [14] In principle all these interferences can be accounted for in the same manner, and a spreadsheet calculation of their contribution to the uncertainty has been developed. Naturally, the interference is most important at the lowest levels of the determinand, where radiochemical separation is needed, and the recovery of the indicator radionuclide must be taken into account.

### Example

As an example let us pretend that we have carried out RNAA for two determinands in the same sample, and for simplicity let us assume that both can be determined from the same  $\gamma$ -spectrum, but with some interference from one indicator to the other. We also assume that comparators of both determinands were irradiated together with the sample. The data needed for calculating the concentration of determinands in a sample may be organized in a spreadsheet as shown in the following Tables 6 and 7.

*Calculations* are now carried out in the following sequence, and results are organized as shown in Table 8.

1) Photopeak counts are corrected to count rates at the time of pile-out by multiplication with a decay correction for

$$t_c = L - C = \text{Date and time of counting} - \text{Date and time of pile-out}$$

$$t_m = K$$

$$\text{decay correction} = \lambda * e^{\lambda t_c} / (1 - e^{-\lambda t_m})$$

where  $\lambda$  is the decay constant for the radionuclide associated with the photopeak in question. Decay corrections are conveniently placed in the columns immediately after the counting data.

2) The uncorrected content of 1. determinand in the separated sample and its corresponding standard deviation are calculated as

$$\text{content} = AD * M/AM * O/AO \quad \text{and placed in column CA}$$

$$CV^2 = (N/M)^2 + (AN/AM)^2$$

$$\text{standard deviation} = \text{SQRT}(CV^2) * \text{content} \quad \text{and placed in column CB}$$

3) The uncorrected content of 2. determinand in the separated sample and its corresponding standard deviation are calculated as

$$\text{content} = BD * Q/BQ * S/BS \quad \text{and placed in column CC}$$

$$CV^2 = (R/Q)^2 + (BR/BQ)^2$$

$$\text{standard deviation} = \text{SQRT}(CV^2) * \text{content} \quad \text{and placed in column CD}$$

TABLE 5. NUCLEAR INTERFERENCES IN NEUTRON ACTIVATION ANALYSIS

Determinand	Indicator	Interferent
Vanadium	<sup>52</sup> V	Chromium Manganese
Chromium	<sup>51</sup> Cr	Iron
Manganese	<sup>56</sup> Mn	Iron
Cobalt	<sup>60</sup> Co	Copper
Arsenic	<sup>76</sup> As	Bromine
Selenium	<sup>81m</sup> Se	Bromine Uranium
Bromine	<sup>82</sup> Br	Rubidium
Molybdenum	<sup>99</sup> Mo	Uranium
Ruthenium	<sup>105</sup> Ru	Uranium
Tellurium	<sup>131</sup> I	Uranium
Lanthanum	<sup>140</sup> La	Uranium
Neodymium	<sup>149</sup> Nd	Uranium
Platinum	<sup>199</sup> Au	Gold

4) Correction of the influence of 2. determinand on the result for the 1. determinand requires the calculation of the effective value

effective value =  $AD/BD * BM/AM * BO/AO$  and placed in column CE

$$CV^2 = (AN/AM)^2 + (BN/BM)^2$$

standard deviation =  $SQRT(CV^2) * \text{effective value}$ , placed in column CF

5) The corrected content of the 1. determinand in the separated sample is now calculated as

content =  $CA - CC*CE$  and placed in column CG

$$CV^2 = (R/Q)^2 + (BR/BQ)^2 + (BN/BM)^2$$

standard deviation =  $SQRT[(CA*N/M)^2 + CV^2*(CC*CE)^2 + (CG*AN/AM)^2]$   
and placed in column CH

At this stage it should be checked whether CG is negligible in comparison with the quantity of added carrier; if not the recovery E should be reduced by subtracting their ratio.

TABLE 6. ORGANIZATION OF DATA FOR RNAA

Parameter	Column
Identification of sample	A
Irradiation time	B
Pile-out time	C
Quantity	D
Recovery 1 ± SD	E±F
Recovery 2 ± SD	G±H
Identification of determinand 1	AA
Half-life of indicator 1	AB
Quantity of determinand 1	AD
Identification of determinand 2	BA
Half-life of indicator 2	BB
Quantity of determinand 2	BD

6) The real concentration of determinand in the sample material and its uncertainty are finally calculated from the original sample weight and the recovery of the appropriate carrier in the separated sample:

$$\begin{aligned} \text{concentration} &= CG/(D \cdot E) && \text{is placed in column CK} \\ CV^2 &= (F/E)^2 + (CH/CG)^2 \\ \text{standard deviation} &= \text{SQRT}(CV^2) \cdot \text{ABS}(CK) && \text{and placed in column CL} \end{aligned}$$

TABLE 7. ORGANIZATION OF DATA FOR RNAA

Identification	Quantity g	Indicator 1 counts±SD	Decay Correction 1	Indicator 2 counts±SD	Decay Correction 2	Time of Counting	Counting time	Decay time
A Sample	D	M±N	O	Q±R	S	L	K $t_m$	L-C $t_c$
AA Comparator 1	AD	AM±AN	AO	AQ±AR	AS	AL	AK $t_m^*$	AL-C $t_c^*$
BA Comparator 2	BD	BM±BN	BO	BQ±BR	BS	BL	BK $t_m^\#$	BL-C $t_c^\#$

TABLE 8. ORGANIZATION OF RESULTS FROM RNAA

Parameter	Column
Content of determinand 1	CA
Standard uncertainty of content	CB
Content of determinand 2	CC
Standard uncertainty of content	CD
Effective value	CE
SD of effective value	CF
Corrected content 1	CG
SD of corrected content	CH
Result for determinand 1	CK
Standard uncertainty of result	CL

TABLE 9. DETERMINATION OF THE PLATINUM CONTENT IN BCR 186 PIG KIDNEY BY RNAA [15]

Sample size in g	Recovery %	Apparent Platinum ng ±SD	Observed Platinum ng ±SD	Gold ng ±SD	Effective value ratio ±SD	Actual Pt ng ±SD
2.23	76.4	13.6 ±0.8	3.206 ±0.004	4.50 ±0.04	-0.9 ±0.8	
2.38	92.5	13.6 ±0.5	3.713 ±0.004	3.50 ±0.03	0.6 ±0.5	
2.19	72.2	10.7 ±0.9	3.161 ±0.003	3.84 ±0.03	-1.4 ±0.9	
2.25	95.7	18.5 ±0.9	4.436 ±0.005	4.36 ±0.05	-0.8 ±0.9	
D	E	CA ±CB	CC ±CD	CE ±CF	CG ±CH	

An example of actual results obtained from the determination of Pt in a reference material BCR 186 Pig Kidney [15] is shown in Table 9, indicating also the spreadsheet columns, from where these results are taken. The indicator for Pt is  $^{199}\text{Au}$ , formed by the decay of  $^{199}\text{Pt}$ , but also from neutron capture in  $^{198}\text{Au}$ , the indicator for gold. The correction for nuclear interference is in this case comparable to the total amount of  $^{199}\text{Au}$  and therefore leads to very large final uncertainties in the results for Pt.

In spite of the extended and complicated line of propagation of the uncertainty based only on the correct estimation of counting statistics, the results and their associated combined standard uncertainty are found to be in a condition of satisfactory statistical control. The mean value is not

significantly different from zero, and the T-test from Eq. (1) gives  $T = 5.55$  with 3 degrees of freedom, which is not significant at the 5% level of confidence.

Corrections for nuclear interference from uranium in the determination of the rare-earth elements, Mo, Ru, Se, and Te may be carried out in a similar way. [14] The concentration of U in the sample, however, has to be determined separately, and the recovery must include the fission yield of the indicator.

## REFERENCES

- [1] Guide to the Expression of Uncertainty in Measurement, International Organization for Standardization, Geneva (1993).
- [2] GIACOMO, P., *Metrologia* **17** (1981) 73.
- [3] HEYDORN, K., "Quality assessment of software for gamma ray spectrum analysis", Software for Nuclear Spectrometry, IAEA-TECDOC-1049, International Atomic Energy Agency, Vienna (1998) 50-61.
- [4] HEYDORN, K., "Validation of Neutron Activation Analysis Techniques", in *Quality Assurance for Environmental Analysis*, ed. by Ph. Quevauviller et al., Elsevier (1995) 89-110.
- [5] HEYDORN, K., DAMSGAARD, E., *J. Radioanal. Nucl. Chem.* **110** (1987) 539-553.
- [6] HEYDORN, K., *Mikrochim. Acta*, III (1991) 1-10.
- [7] HEYDORN, K., *Fresenius J. Anal. Chem.*, **337** (1990) 498-502.
- [8] POMMÉ, S., et al., *Nucl. Instr. and Meth. A* **422** (1999) 388-394.
- [9] LANDSBERGER, S., HEYDORN, K., ISKANDER, F.Y., NISSET, M., "Compton suppression gamma-ray spectrometry", this TECDOC, p. 77-89.
- [10] HEYDORN, K., *Neutron Activation Analysis for Clinical Trace Element Research*, CRC Press, Boca Raton **1** (1984) 136.
- [11] HEYDORN, K., RHEE, S.K., *Trans. Am. Nucl. Soc.* **60** (1989) 3-4.
- [12] HEYDORN, K., "Radiochemical neutron activation analysis", in *Encyclopedia of Analytical Chemistry*, ed. by Robert A. Meyers, Wiley (2000) p. 12762-12782.
- [13] GRIEPINK, B., MUNTAU, H., EUR Report, **11850** (1988)
- [14] HEYDORN, K., *Neutron Activation Analysis for Clinical Trace Element Research*, CRC Press, Boca Raton **2** (1984) 42-45.
- [15] RIETZ, B., HEYDORN, K., *J. Radioanal. Nucl. Chem.* **174** (1993) 49-56.



# COMPTON SUPPRESSION GAMMA RAY SPECTROMETRY

**S. Landsberger, F.Y. Iskander, M. Niset**

Nuclear and Radiation Engineering Program, Nuclear Engineering Teaching Laboratory,  
University of Texas at Austin,  
Austin, Texas, United States of America

**K. Heydorn**

Department of Chemistry, Technical University of Denmark,  
Lyngby, Denmark

**Abstract.** In the past decade there have been many studies to use Compton suppression methods in routine neutron activation analysis as well as in the traditional role of low level gamma ray counting of environmental samples. On a separate path there have been many new PC based software packages that have been developed to enhance photopeak fitting. Although the newer PC based algorithms have had significant improvements, they still suffer from being effectively used in weak gamma ray lines in natural samples or in neutron activated samples that have very high Compton backgrounds. We have completed a series of experiments to show the usefulness of Compton suppression. As well we have shown the pitfalls when using Compton suppression methods for high counting deadtimes as in the case of neutron activated samples. We have also investigated if counting statistics are the same both suppressed and normal modes. Results are presented in four separate experiments.

## **Influence of dead time in Compton suppression NAA**

### ***Background***

Compton suppression spectrometry has developed into an established position in low-level counting. It is attractive because of the reduction in the Compton continuum, and cosmic and natural background. Usually Compton suppression methods have been used in environmental studies with low-level activities and subsequent low dead times. In neutron activation analysis (NAA), Compton suppression can help to improve precision and accuracy for isotope identification and also substantially reduce spectral interferences. In general, NAA deals with a much broader range of dead times. The principle of the system is based on the Compton effect described as follows. When a gamma ray interacts with the main detector, the Compton effect may occur, in which a recoil electron and a scattering photon are created sharing the initial gamma ray energy. The recoil electron has a short range and deposits its energy in the main detector, while the scattered photon is more likely to escape the main detector. In a normal detection system, the signal from the recoil electron is recorded as a contribution to the baseline since the energy of the recoil electron is lower than the original gamma ray energy. In the Compton system, photons passing the main detector are detected by the surrounding NaI(Tl) detector. If both the main and NaI(Tl) detectors record the signals within a specific time interval, the signal is eliminated under the assumption that the signals result from Compton scattering. Through this procedure, the baseline of Compton continuum in the spectrum is reduced to a level much lower than in a normal spectrum, and the analytical sensitivity is drastically improved.

### ***Experimental***

The Compton suppression gamma ray detection system used in the study consists of a main germanium detector which has an 18% relative efficiency with 1.9 keV resolution for a 1332 keV photopeak of  $^{60}\text{Co}$ , a large NaI(Tl) crystal ring detector outside the main detector, and an ORTEC ADCAM PC based multi-channel analyzer. The diagram of the system is shown in Figure 1 and a detailed description of the system has been presented elsewhere [1]. The detection system can measure a sample in both normal and Compton modes simultaneously.

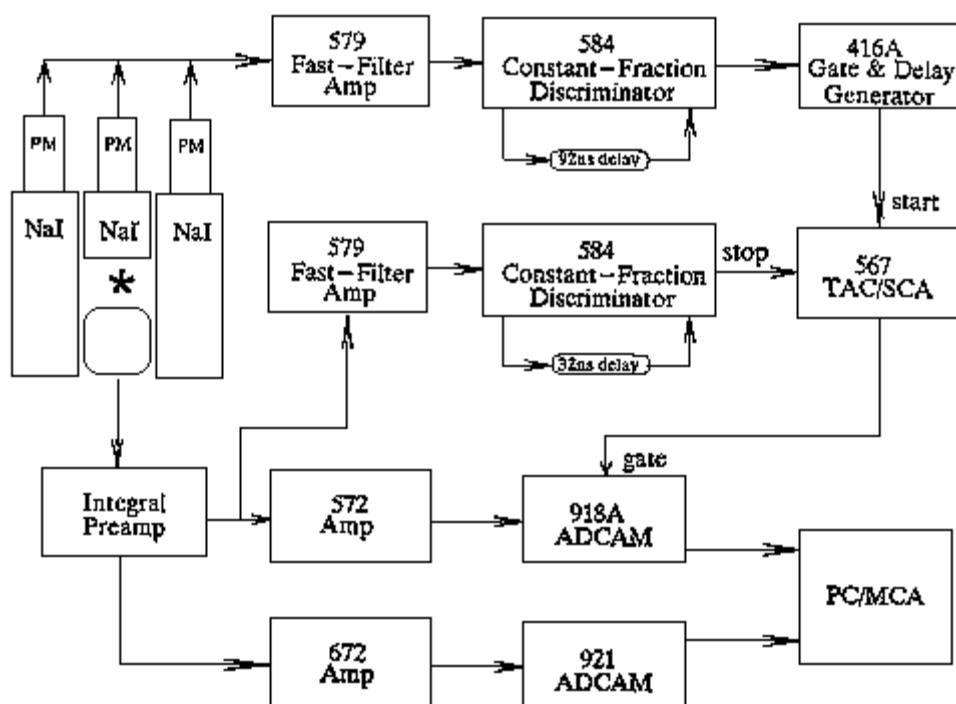


Fig. 1. Schematic diagram of the Compton suppression gamma ray counting system.

The Compton suppression system can reduce the continuum quite significantly, usually by a factor of 5 to 10. This is useful especially for low level elemental analysis. However, this advantage can only be taken if the radionuclide has a single or one major gamma ray, such as  $^{65}\text{Zn}$ (1115keV), and  $^{58}\text{Co}$ (810keV) for Ni analysis, and gamma rays which are not coincident with each other. The Compton suppression system can significantly improve the detection limit and minimize the statistical error of the peak detection. Some radionuclides with more than two coincident gamma rays can not be effectively determined by Compton suppression. For example, the radionuclide  $^{46}\text{Sc}$  has two gamma rays with energies 889 keV and 1120 keV. These two photopeaks are coincident with each other in the Compton spectrum. The count rates of two peaks in this case are no longer proportional to amount of the scandium. The peak counting rates vary with deadtime that can not be adequately corrected using the usual procedures. An example of  $^{46}\text{Sc}$ -1120 keV photopeak measured in the Compton mode is presented in Figure 2. This experiment was done by using a fixed  $^{46}\text{Sc}$  source and another removable gamma ray source (without 1120 keV peak) to adjust the dead time. In normal mode, the peak rate decreases with dead time, which can be compensated by using pulser, two-source correction or internal ADC correction. However, the count rate in the Compton mode increases with dead time, and this phenomenon depends on the individual radioisotope. Ratio of the peak rates, also shown in Figure 3, decreases significantly with dead time. This means that detection of two coincident gamma rays from the same isotope depends on dead time of the Compton system. The higher the deadtime, the less effective the Compton suppression, due to higher random coincidences being detected. Millard [2] did a study on this subject for dead times up to 18%. It was concluded that the results obtained with Compton suppression counting depended not only on the physical arrangement of the detectors and the performance characteristics of the electronic equipment but also on the decay characteristics of the nuclides analyzed. The ratio of the count rate in a gamma line in anti-coincident and coincident modes was used to monitor the proper quantification of the activity measured. Therefore, for successful and reliable implementation of Compton suppression in NAA, a detailed investigation on the change in activity quantification is warranted. In this work a different approach was used. A 1% standard liquid solution of manganese was irradiated to produce  $^{56}\text{Mn}$  with a half-life of 2.6 h. The same activated sample was counted repeatedly so that as the overall activity decreased,

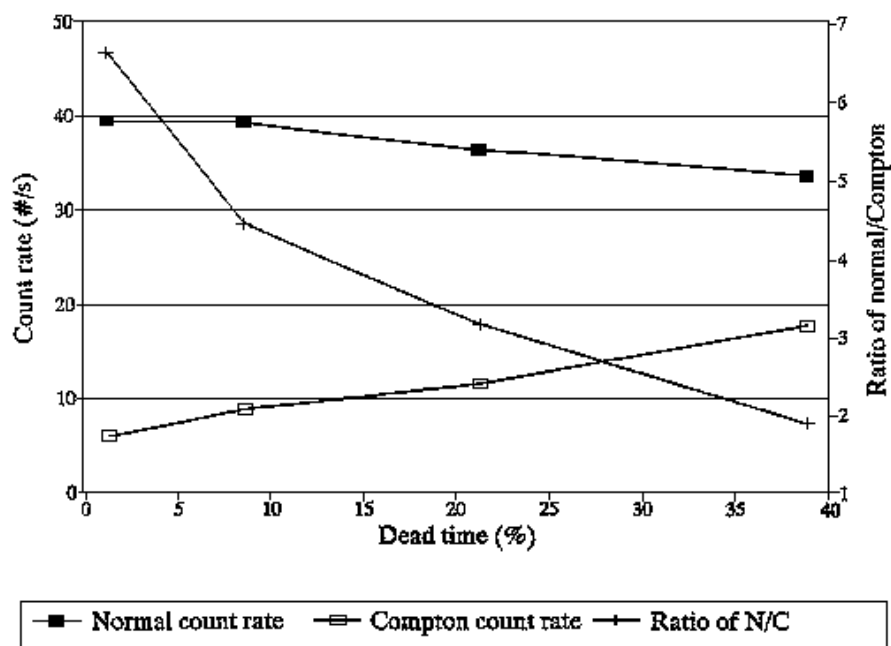


Fig. 2. Count rate of  $^{46}\text{Sc}$  1120 keV peak as a function of dead-time in normal and Compton counting modes.

there was a decrease in the dead time of the measurement. The analysis was done exactly like routine NAA. The irradiated solution had predominantly  $^{56}\text{Mn}$  activity. The three gamma lines at 846.8, 1810.7, and 2113.2 keV were evaluated. The first one has a 50% coincident rate, while the other two are 100% coincident. Both Compton suppressed and unsuppressed spectra were collected and analyzed. The results for a 96% and 19 per cent deadtime are shown in Figure 3 and 4, respectively. Corrections for the dead time by means of a pulser were applied in both suppressed and unsuppressed modes. The figures presented can be interpreted as the departure of the efficiency of detection present because of an increase in the overall dead time of the measurement. As the dead time increases, the Compton suppression becomes less effective; therefore, photons that are suppressed because they are coincident become less suppressed as the dead time increases. The Compton suppressed mode, on the other hand presents an increase in the overall count rate for the gamma lines with 50 and 100% coincidence rate. The exact difference in the detector efficiency with variations in the dead time will depend on the coincident rates of the various gamma lines, among other factors. It is not feasible that such differences can be exactly calculated and corrected for individual isotopes; therefore, reliable analysis with Compton suppression is best applied when the dead times are low involving non-coincident or mostly non-coincident gamma lines. More recently Westpahl et al. [3] have introduced loss-free counting techniques to Compton suppression methods but it has seen only limited use. As well Westpahl [4] also reported on the real-time correction of chance coincidence losses in high count rate Compton spectrometry.

## Influence of Compton suppression on counting statistics

### Background

It has been pointed out by Pomme et al. (2000) that although nuclear emission does indeed often show Poisson statistical behavior, nuclear spectroscopy counting may not. This is primarily due to non-random counting losses due to deadtime and and/or pulse pileup, which can transform some of the Poisson statistical characteristics. Furthermore, Pomme et al. (1999) showed that pileup rejection causes an enhanced count scatter when applying loss free counting. We investigated if Compton suppression did alter any of the normal statistical fluctuations observed seen in routine gamma ray counting.

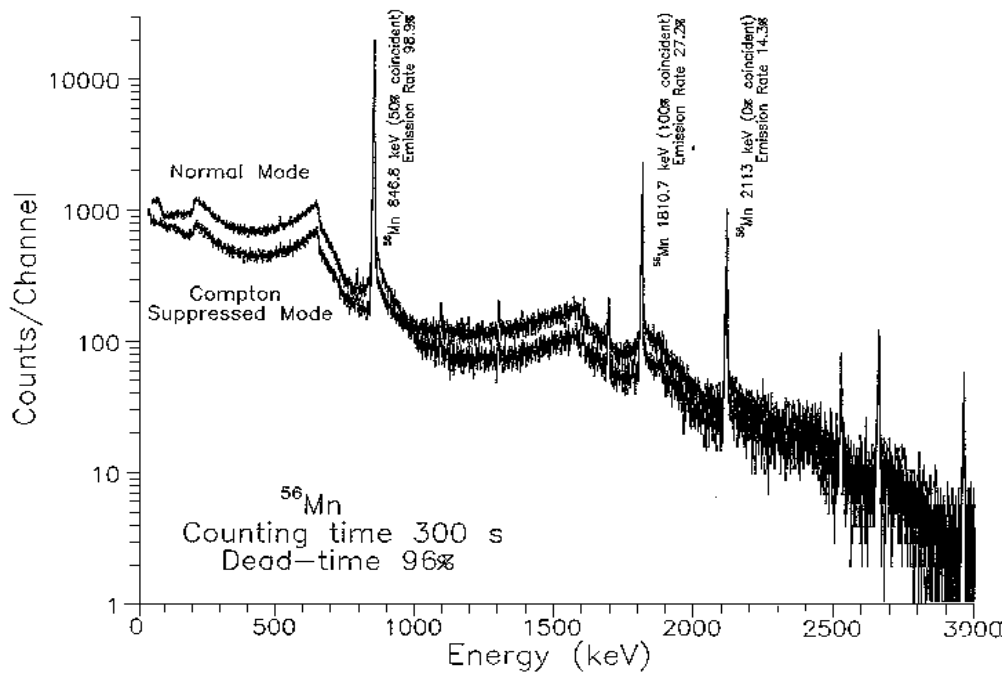


Fig. 3. Spectra of  $^{56}\text{Mn}$  measured in normal and Compton counting modes with dead time 96%.

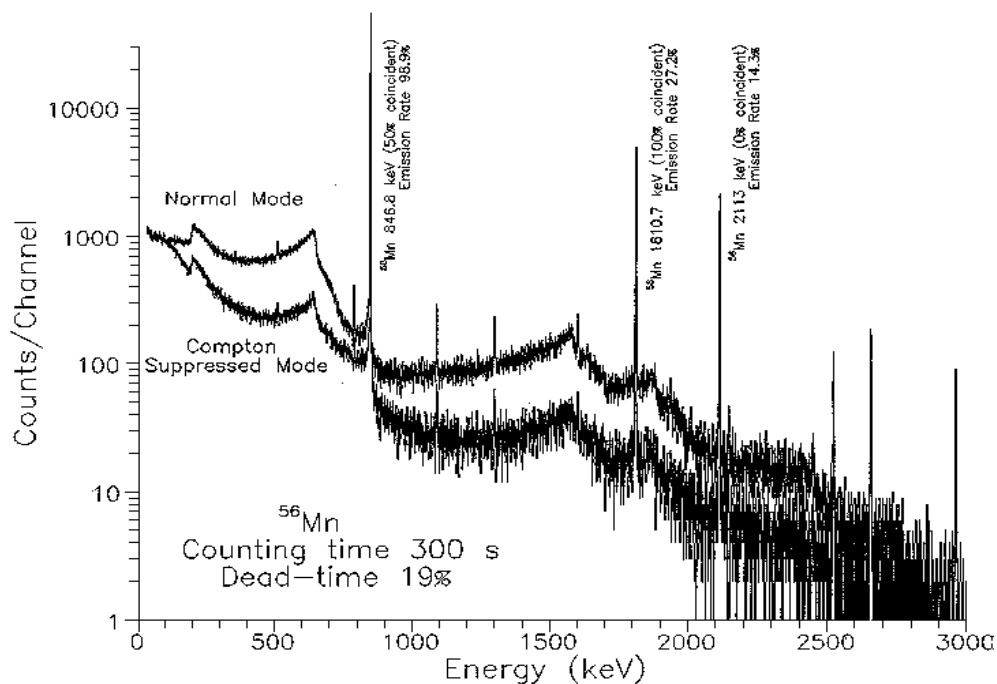


Fig. 4. Spectra of  $^{56}\text{Mn}$  measured in normal and Compton counting modes with dead time 19%.

### Experimental

We counted a  $^{60}\text{Co}$  source in a normal and Compton mode. A counting position was chosen to give a deadtime of less than 2%. Both the 1173 and 1332 keV photopeaks are in 100% coincidence with each other. This results in a counting efficiency being reduced almost by factor of eight which is ideal since this is using the Compton effect to its fullest. We acquired almost 250 spectra both in the normal and Compton mode having average net peak areas of 59,640 and 8,356 counts.

Normal Acquisition (1332 keV photopeak):

mean = 5.964 E+4 counts  
std (exp) = 230.2 (experimental result)  
sqrt (mean) = 244.2 (Poisson theoretical std)

Compton Suppression (1332 keV photopeak):

mean = 8.356 E+3 counts  
std (exp) = 99.0 (experimental result)  
sqrt (mean) = 91.4 (Poisson theoretical std)

Results for the normal and Compton data were statistically treated and graphically represented in Figures 5 and 6. As can be seen there appears to be virtually no significant statistical differences between the normal and Compton modes.

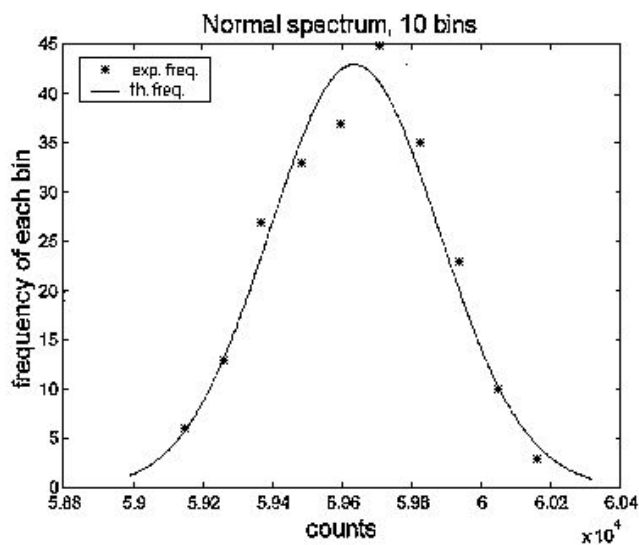


Fig. 5. Normal spectrum, 10 bins.

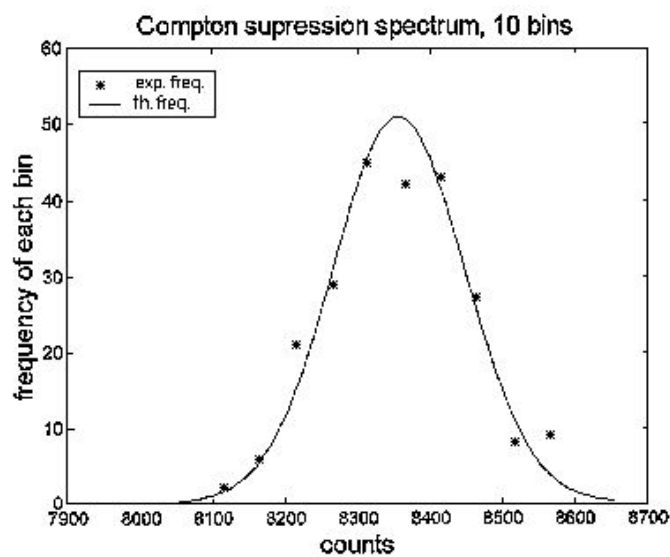


Fig. 6. Compton Suppression spectrum, 10 bins.

## Determination of $^{137}\text{Cs}$ in soil samples by low-level Compton suppression gamma counting

### *Background*

Ever since the advent of atmospheric nuclear testing, there have been intense studies into the environmental and medical consequences of  $^{137}\text{Cs}$ , which is a major product of the fission process.  $^{137}\text{Cs}$  has a half-life of 30 years and has become ubiquitous in the northern hemisphere due to atmospheric tests conducted primarily by the United States and the Former Soviet Union. Atmospheric tests were also conducted to a much lesser degree by the French and later on by the Chinese. The British mainly conducted their tests in the southern hemisphere. Although atmospheric testing was halted in 1963 with the advent of the partial test ban treaty,  $^{137}\text{Cs}$  was again widely released as a direct result of the Chernobyl nuclear reactor accident in 1986. Large areas of the Ukraine, and other Former Soviet Union Republics were contaminated with  $^{137}\text{Cs}$  and other radionuclides. Furthermore, areas in various parts of Europe received the radioactive fallout. Thus, one can expect that  $^{137}\text{Cs}$  will remain in the environment at measurable quantities for the next two-three centuries. In fact  $^{137}\text{Cs}$  is now considered to be part of the "natural background" in naturally occurring radioactive materials (NORM).  $^{137}\text{Cs}$  is readily absorbed onto clay particles, for those size fractions less than 2 micrometers ( $< 2 \mu\text{m}$ ). Because of this phenomenon one can derive a historical dating (1945 onwards) of soils by sampling up to one meter below the surface.

One area of continued research is in soil erosion, which can be modeled using the  $^{137}\text{Cs}$  data collected in soil samples. One can also measure the on-site distribution of soil erosion, deposition within several watersheds, determine annual average soil loss, and ultimately evaluate the consequences for plant productivity and loss. The US Army conducts its training and various maneuver exercises on land. At present the Army Training and Testing Area Carrying Capacity (ATTACC) model is currently the only officially sanctioned tool to determine the capacity of military lands to support training and testing missions. Special consideration is given to land rehabilitation and maintenance including carrying capacity.

As a result of this need, the US Construction Engineering and Research Lab contracted the Nuclear Engineering Teaching Laboratory to measure  $^{137}\text{Cs}$  in two soil environments. One in an undisturbed place for background information and the other in general areas of a US Army training facility. Forth Hood, Texas was chosen for sampling site.

### **Sampling and sample preparation**

In the first expedition undisturbed samples were collected at two gravesites; Walker (W) and Spring Hill (S) Cemetery at Fort Hood. Two locations (1 and 2) several meters apart were chosen at each gravesite. Four separate pits about one meter apart in a circle were dug at each location. Very careful sampling was done to ensure accurate depth profile. From each pit 3 cm slabs sections down to 24 cm were collected, placed into polyethylene bags and labeled. Therefore for each specific location there were 4 sub-samples at every depth. These sub-samples were mixed together, to ensure maximum representation of the locations, making a total of eight samples per location. This procedure was repeated several meters away at the second location. Samples were identically collected from another two locations in the second gravesite. The total number of composite samples collected was 32. Once the samples delivered to the laboratory, they were sieved using a standard ASTM 1.18 mm to remove small stones and other types of debris. The sieving significantly helped in homogenizing the soil samples. The average final combined weight was about 0.4–0.6 kg. In the second expedition, 86 grab samples were taken from various sites at Fort Hood (these results will be reported in a future communication).

## Experimental

From each bag 100 grams of soil was placed into a 250-mL glass beaker. The Compton suppression gamma ray spectrometer was used to detect the 662 keV photon decaying from  $^{137}\text{Cs}$ . This system greatly reduces the background from naturally occurring radiation such as the multitude of radioactive decay products from the uranium series and  $^{40}\text{K}$ . Ultimately, the signal to noise ratio significantly improves making the detection of small peaks easier. A complete technical description of the set-up and review of Compton suppression is given elsewhere (Landsberger and Peshev, 1996). A list of the major gamma rays found in our laboratory environment and their reduction factors are shown in Table 1. Samples were typically counted for 0.6–1 day. A partial spectrum between 600–700 keV with and without Compton suppression is seen in Figure 7. A comparison between Figs. 8 and 9 reveals that for high  $^{137}\text{Cs}$  concentrations there is little advantage of using Compton suppression. However, for low  $^{137}\text{Cs}$  concentrations the signal to noise ratio improves to reduce the error on the photopeak significantly. The advantage of using Compton suppression is the ability to achieve good sensitivity for  $^{137}\text{Cs}$  using relatively small sample sizes; from 100–200 grams.

Accurate radioactive counting of low-levels of contaminated or environmental soils is one of the most difficult analytical procedures to undertake. Firstly, one needs to have enough material to count for a reasonable amount of time. On the other hand, one needs to limit the amount of material so that matrix effects in the form of gamma ray attenuation is reduced or minimized. In the second requirement matrix matching of samples and calibration material is crucial. Not all soils have the same major matrix composition and density. Thus, a soil that is denser and has higher amounts of potassium and calcium may attenuate the gamma ray signal more substantially than a soil that is less dense and may have a typical aluminum-silicate base.

TABLE 1. SUMMARY OF MAJOR NUCLIDES FOUND IN LABORATORY BACKGROUND AND THE REDUCTION FACTOR WHEN USING COMPTON SUPPRESSION (CPD = COUNTS PER DAY)

Energy KeV	Nuclide	Source	cpd without Compton	cpd with Compton	cpd without Comp/ cpd with Comp
186.2	$^{226}\text{Ra}$	$^{226}\text{Ra}$ series	5604	1935	2.90
238.6	$^{212}\text{Pb}$	$^{232}\text{Th}$ series	3609	2264	1.59
295.4	$^{214}\text{Pb}$	$^{226}\text{Ra}$ series	2635	1065	2.47
352.0	$^{214}\text{Pb}$	$^{226}\text{Ra}$ series	2250	1033	2.18
511.0		annihilation	2317	466	4.97
583.1	$^{208}\text{Tl}$	$^{232}\text{Th}$ series	999	318	3.14
609.3	$^{214}\text{Bi}$	$^{226}\text{Ra}$ series	1252	444	2.82
911.0	$^{228}\text{Ac}$	$^{232}\text{Th}$ series	546	225	2.43
968.8	$^{228}\text{Ac}$	$^{232}\text{Th}$ series	447	159	2.81
1120.0	$^{214}\text{Bi}$	$^{226}\text{Ra}$ series	419	132	3.17
1460.8	$^{40}\text{K}$	primordial	1229	1042	1.18
2614.3	$^{212}\text{Pb}$	$^{232}\text{Th}$ series	236	139	1.70

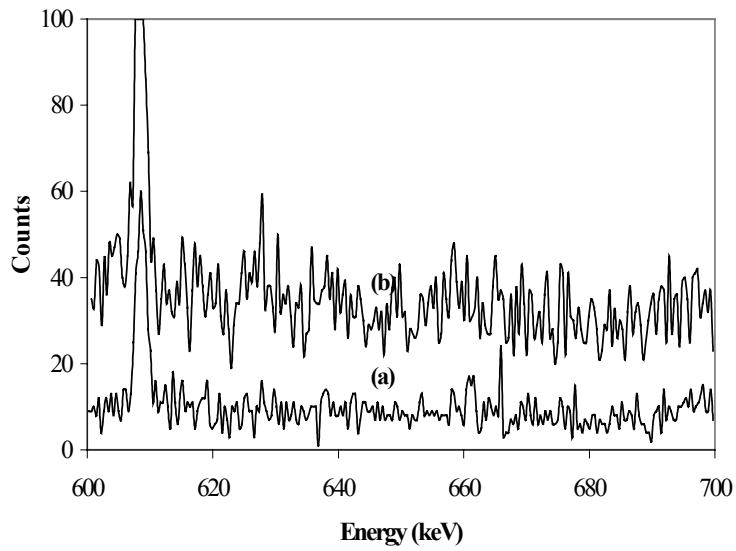


Fig. 7. Comparison of laboratory background. (a) with and (b) without Compton suppression.

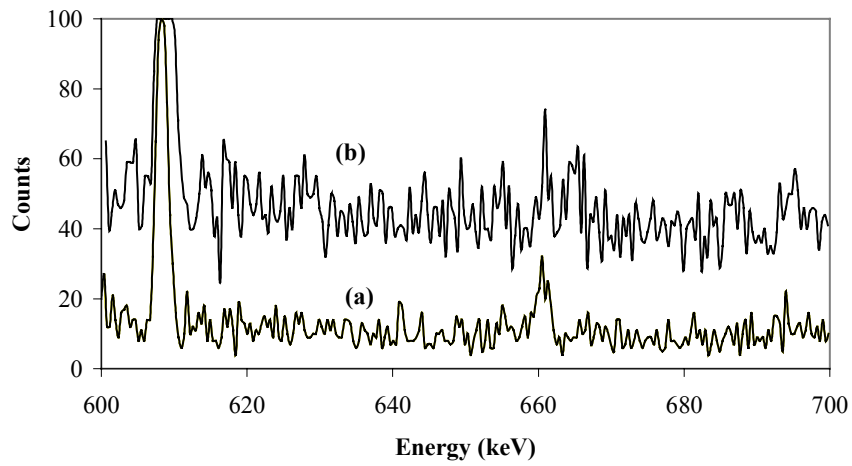


Fig. 8. Low concentration of  $^{137}\text{Cs}$  (0.7 Bq/kg). (a) with and (b) without Compton suppression.

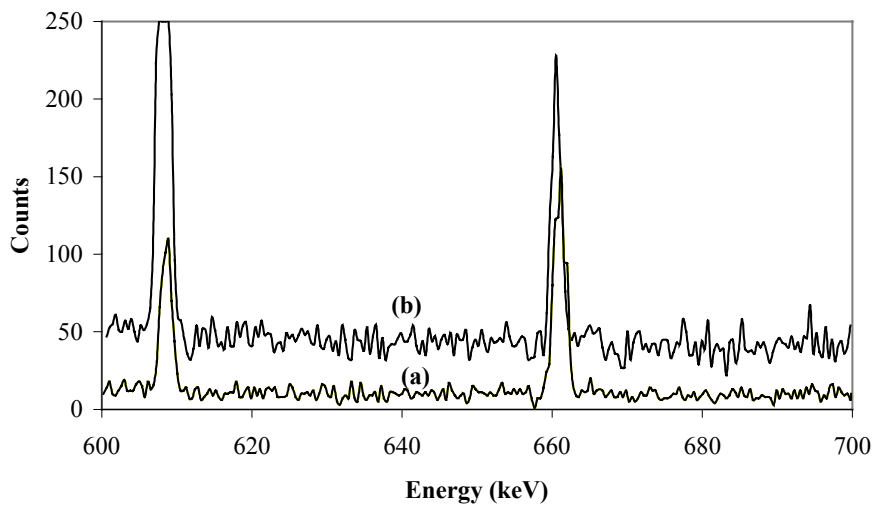


Fig. 9. High concentration of  $^{137}\text{Cs}$  (12 Bq/kg). (a) with and (b) without Compton suppression.

In this work two International Atomic Energy Agency (IAEA) standard reference materials were used to calibrate the system and perform quality assurance. IAEA (375) sample with a concentration of 5280 Bq/kg (with a confidence interval of 5200–5360 Bq/kg) was used as the calibration source and IAEA Soil 6 with a concentration of 53.65 Bq/kg (with a confidence interval of 51.43–57.91 Bq/kg) was used as an unknown. The result was within 10% of the certified value. We suspected that the difference in soil density mainly attributed to this error. To test our hypothesis we used only five grams of IAEA Soil 6 as the standard and five grams of IAEA 375 as the unknown. Five separate measurements were performed with results all lying between  $\pm 3.5\%$  of the mean value of 5280 Bq/kg. The results are shown in Table 2.

We performed a T-test [7] to evaluate statistical control with 4 degrees of freedom and  $P \geq 0.20$  and found the results to be acceptable.

The next set of experiments was to obtain a soil profile of the four sites, two each from the same cemetery. These results are seen in Table 3 and are plotted in Figure 10. The reproducibility of locations S-1 and S-2 from the first cemetery are in very good agreement, while the W-1 and W-2 locations do not agree as well. However, the general  $^{137}\text{Cs}$  profile of all sites shows an exponential drop from top soil to a depth of 24 cm.

TABLE 2. QUALITY CONTROL REPORT FOR MEASURING  $^{137}\text{CS}$  USING IAEA SOIL 6

Measured Activity (Bq/kg) $\pm$ Std. Dev.	% Agreement
5102 $\pm$ 86.8	96.5
5299 $\pm$ 89.9	100.3
5191 $\pm$ 80.0	98.3
5200 $\pm$ 88.2	98.5
5388 $\pm$ 93.8	102.0

TABLE 3. MEASUREMENT OF  $^{137}\text{CS}$  IN SOIL SAMPLES AT VARIOUS DEPTHS

ID	Depth cm	S-1 Bq/kg	S2 Bq/kg	W1 Bq/kg	W2 Bq/kg
A	3	13.81 $\pm$ 0.77	16.58 $\pm$ 0.54	17.74 $\pm$ 0.76	24.57 $\pm$ 0.52
B	6	13.22 $\pm$ 0.67	16.66 $\pm$ 0.84	14.79 $\pm$ 0.65	19.84 $\pm$ 0.73
C	9	8.46 $\pm$ 0.58	9.79 $\pm$ 0.71	8.17 $\pm$ 0.75	11.44 $\pm$ 0.59
D	12	6.94 $\pm$ 0.36	5.64 $\pm$ 0.33	3.51 $\pm$ 0.45	5.66 $\pm$ 0.30
E	15	3.18 $\pm$ 0.31	3.52 $\pm$ 0.23	2.09 $\pm$ 0.21	4.42 $\pm$ 0.32
F	18	2.96 $\pm$ 0.27	2.82 $\pm$ 0.27	1.24 $\pm$ 0.20	3.03 $\pm$ 0.24
G	21	2.02 $\pm$ 0.20	1.69 $\pm$ 0.18	1.16 $\pm$ 0.20	2.04 $\pm$ 0.20
H	24	1.93 $\pm$ 0.20	1.02 $\pm$ 0.16	1.06 $\pm$ 0.18	1.66 $\pm$ 0.19

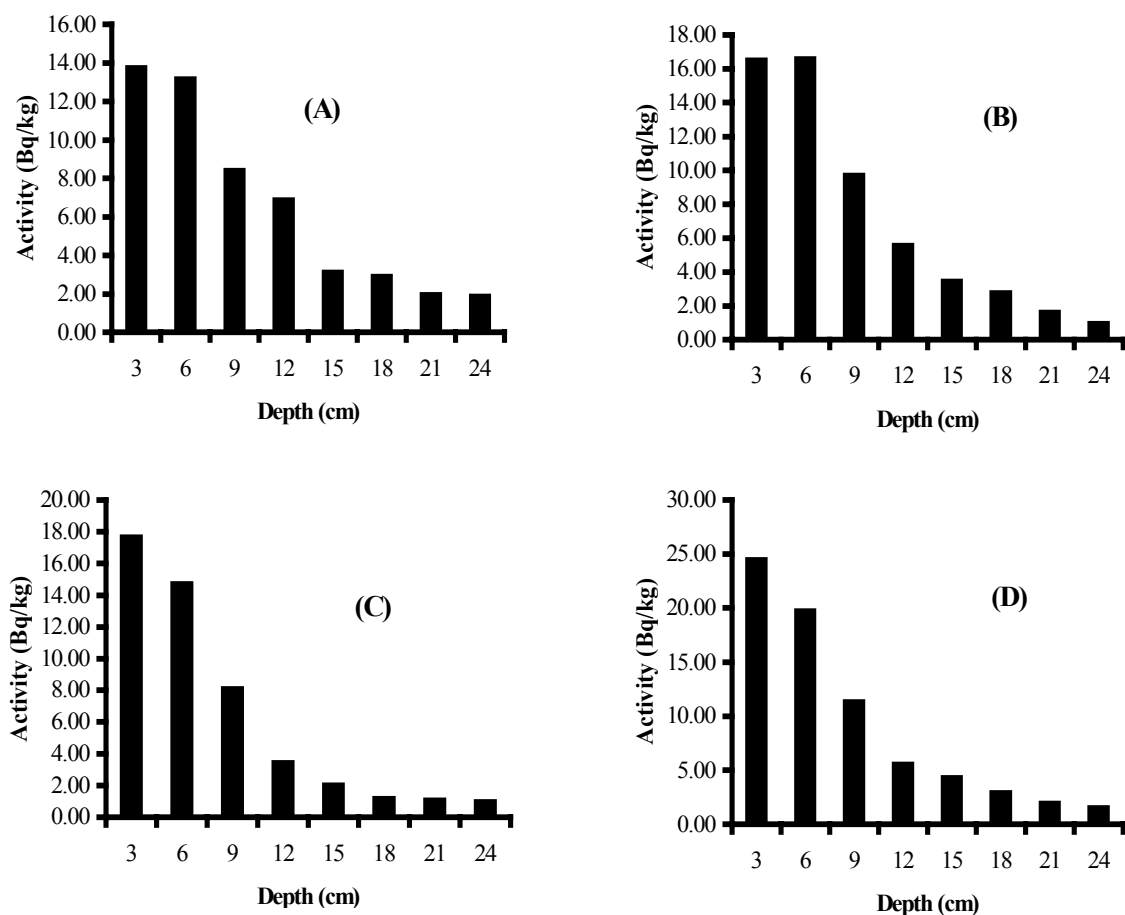


Fig. 10. Graphical interpretation of  $^{137}\text{Cs}$  in soil samples at various depths from the four sampling locations; (A) Spring Hill-1; (B) Spring Hill-2; (C) Walker-1 and (D) Walker-2.

In the second set of experiments we investigated the effect of counting time on the counting statistical error. For samples with high  $^{137}\text{Cs}$  concentrations greater than 10 Bq/kg, we found no statistical difference between the normal and Compton suppression gamma counting mode for counting periods of 0.5, 1, 1.5, 2, and 3 days (Table 4). However, for  $^{137}\text{Cs}$  concentrations less than one Bq/kg, the error significantly drops when using the Compton mode after one day of counting (Table 5).

TABLE 4. COMPARISON BETWEEN COUNTING STATISTICS UNDER COMPTON VS NORMAL COUNTING MODE FOR A SAMPLE WITH ACTIVITY OF 12.59 Bq/Kg

Count Time (Days)	% Counting Statistics Normal Mode	% Counting Statistics Compton Mode
0.5	9.4	10.9
1	6.5	6.8
1.5	5.8	5.3
2	5.5	4.6
3	4.3	4.9

TABLE 5. COMPARISON BETWEEN COUNTING STATISTICS UNDER NORMAL VS COMPTON COUNTING MODE FOR A SAMPLE WITH ACTIVITY OF 0.73 Bq/Kg

Count Time (Days)	% Counting Statistics Normal Mode	% Counting Statistics Compton Mode
0.5	31.0	32.6
1	27.9	20.0
1.5	27.9	20.0
2	28.8	16.7
3	25.6	7.2

## Conclusions

We have demonstrated that Compton suppression gamma ray spectrometry is ideal to determine  $^{137}\text{Cs}$  in soil samples as low as 100 grams. The main advantage of the system is in determining  $^{137}\text{Cs}$  concentration concentrations at levels between 1–3 Bq/kg. Typical counting statistical errors are 10% at 5 Bq/kg and 20% at 1 Bq/kg. Below 1 Bq/kg the errors rise to 30-35% for a one-day count. It is recommended that for a large sampling program the amount of sample be increased to 200 grams to reduce the counting time for lower  $^{137}\text{CS}$  concentrations and acquire a much higher efficiency detector (> than 50%) which would further reduce the counting time. As well for such larger sampling programs a specific sample changer and dedicated Compton suppression system should be allocated.

## REFERENCES

- [1] PETRA, M., G. SWIFT, S. LANDSBERGER, Nucl. Instr. Meth., **A 299** (1990) 85.
- [2] MILLARD, H. T., Jr., Nucl. Instrum. Meth., **223** (1984) 416.
- [3] WESTPHAL G. P., JOSTL, K., SCHRODER, P., LAUSTER, R., HAUSCH E., Nucl. Instr. Meth., **A 422** (1999) 347.
- [4] WESTPAHL, G. P. Nucl. Instr. Meth., **A 416** (1999) 536.
- [5] POMME, S., HARDEMAN, F., ROBOUCH, P., ARANA, G., EGUSKIZA, M., "Is it Safe to Use Poisson Statistics in Nuclear Spectroscopy", Tenth Modern Trends in Activation Analysis, Gaithersburg, USA. J. Radioanal. Nucl. Chem. (2000, in press).
- [6] POMME, S. et al. Nucl. Instr. Meth., **A 432** (1999) 456.
- [7] HEYDORN, K., Mikrochimica Acta 3 (1991) 1.
- [8] LANDSBERGER, S., S. PESHEV, J. Radional. Nucl. Chem., 202 (1996) 203.



# EXPERT SYSTEM SHAMAN AND VERIFICATION OF THE COMPREHENSIVE NUCLEAR TEST BAN TREATY

**P.A. Aarnio, J.J. Ala-Heikkilä, T.T. Hakulinen, M.T. Nikkinen**

Helsinki University of Technology,  
Helsinki, Finland

**Abstract.** SHAMAN is an expert system developed at Helsinki University of Technology for carrying out the nuclide identification and peak interpretation in gamma spectrum analysis. SHAMAN utilizes a comprehensive reference library with 2600 radionuclides and 80,000 gamma lines, as well as a rule base of sixty inference rules. The code has to be interfaced with advanced peak analysis software like UniSAMPO, for example. SHAMAN takes the spectrum, calibration information, and peak analysis results and applies the rules and the library to produce comprehensive quantitative information of the radionuclides present and full interpretation of the peaks. SHAMAN has been tested and compared with other programs using the air filter spectra obtained within the framework of the Comprehensive Nuclear Test Ban Treaty. The results of the comparison show that SHAMAN outperforms the programs having highly optimised nuclide libraries.

## Introduction

In the Comprehensive Nuclear Test Ban Treaty (CTBT) monitoring network, gamma spectrometry is used daily for the analysis of air filter samples from 80 radionuclide monitoring stations positioned around the globe. The measured gamma spectra are sent to the International Data Center (IDC) to be analyzed. Usually only naturally occurring radioactivity is detected, but the sample may also contain some man-made radionuclides due to, e.g., releases from civilian nuclear plants or other sources. In the CTBT framework the aim is to detect radioactivity caused by nuclear weapons tests.

The Comprehensive Nuclear Test Ban Treaty requires that the IDC applies “on a routine basis automatic processing methods and interactive human analysis to raw International Monitoring System data” [1, Part I.18], and “the verification activities shall be based on objective information” [1, Article IV.2]. These procedural and quality requirements mean that the analysis results of the verification activities have to be correct. In gamma spectrometry, particular emphasis must be placed on radionuclide identification.

In the CTBT monitoring system, the measured gamma spectra go through an *event screening* process, where they are classified according to the radionuclides present in the sample. Samples containing only natural or benign man-made radionuclides receive low classifications and are automatically excluded from further analysis. Anomalous findings yield high classifications depending on the detected radionuclides. All automatically processed spectra are manually reviewed by human analysts.

Accurate and complete analysis of a typical air filter gamma spectrum, let alone one that contains fresh fission debris, is a very demanding task due to the large number of peaks in the spectrum and the uncertainties inherently present in the measurement process. For the results to be reliable, the analysis must be in statistical control throughout. This means, among other things, that all statistically significant gamma peaks are explained. This sets high requirements for the entire radionuclide measurement and analysis system. Within the CTBT network, a high-quality automated gamma spectrum analysis is essential for several reasons:

Successful event screening requires that fission products are correctly identified. If this cannot be done reliably in the automated routine analysis, the spectrum may not draw the immediate and appropriate attention of the analysts. If the detection of fission products is left for the analysts, there is a higher risk for an evasive sample to pass the review and to be left without a further analysis.

Event timing is based on ratios of radionuclide concentrations, and thus, it is highly dependent on the accuracy of the spectrum analysis results. Accurate event timing is essential for the “fusion”

with the other monitoring technologies, as well as for the backtracking of plume transport. Large uncertainties in the nuclide concentrations lead to large uncertainties in event timing.

If a complete interpretation of gamma spectra is the objective, every gamma peak left unidentified in the automatic processing has to be manually analyzed. Thus, reducing the number of false identifications and unexplained gamma peaks speeds up analysis and reduces labor costs.

At the International Data Center (IDC) in Vienna, Austria, the automated gamma spectrum analysis is currently accomplished with software that uses algorithms from the commercial Canberra Genie-PC package [2]. Its performance has been tuned into the IDC environment by tailoring the processing parameters and the reference library, in addition to implementing a connection for input data and results into an Oracle database. The performance of this software is discussed in Refs. [3–6], for example.

As an alternative radionuclide identifier, the expert system SHAMAN [7–12] was integrated into an IDC research pipeline through the Provisional IDC in Arlington, and its performance was evaluated in this environment. These results were published in detail in three reports [13–15]. In this review paper, we present the most essential findings.

## Expert system SHAMAN

The analysis of a gamma spectrum can be divided into two separate phases. The first phase is the *quantitative analysis*, in which the energies and intensities of gamma peaks in the gamma spectrum are determined. The second phase is the *qualitative analysis*, in which these peaks are explained and correctly associated with the radionuclides present in the sample using a reference radionuclide library containing data about radionuclides and their gamma quanta. The latter task is also generally known as *radionuclide identification*. In this phase the activities and concentrations of nuclides in the sample are also calculated.

Expert system SHAMAN is a computer software package for carrying out nuclide identification of gamma spectra [7–12]. SHAMAN has been developed at the Helsinki University of Technology. SHAMAN attempts to mimic a human expert analyst in selecting the correct nuclides from a comprehensive radionuclide library using various heuristic criteria. The library contains data of all the 2600 known radionuclides. Recent performance evaluations have shown SHAMAN to be very reliable in finding the correct nuclides and discarding the spurious ones.

A typical feature of expert systems is that the program execution is data driven, i.e., governed by the problem-specific data rather than a pre-programmed sequential algorithm [16]. Knowledge is typically expressed using *rules* that trigger specific actions based on changes in the data. An *inference engine* controls this process by monitoring the specified data items and *firing* appropriate rules at suitable instances.

SHAMAN rules are simple if-then constructs directly accessible to the inference engine. Rules consist of an *antecedent* holding logical clauses, which depend on the data in the system, and a *consequent* holding the actions to be taken when the rule fires. Rules are grouped according to their application domain, which allows one to control inclusion of rules concerning specific issues.

Rules and data objects in the SHAMAN system are specified using a special rule language and machine-translated into a more compact C-language form by a rule compiler. The SHAMAN inference engine features a conceptually straightforward *forward chaining* inference method. In addition, numerical routines for doing the quantitative calculations associated with nuclide identification have been implemented using C-language.

SHAMAN has an interactive command-line user interface to make it easier for the user to control the identification process. All critical parameters affecting identification can be changed if necessary. A graphical user interface has also been implemented for browsing and graphical visualization of identification results.

The recent development effort in methodology of SHAMAN has concentrated on making the identification more reliable particularly in cases relevant to CTBT monitoring. The most important of these changes are true and random coincidence corrections, self-absorption correction, estimation of escape peak areas, and support for functional representation of calibrations.

### SHAMAN in routine analysis

In November 1997, the CTBT radionuclide monitoring network consisted of 20 particulate sampling stations and 2 xenon sampling stations. They were using over 20 different detectors in different combinations, ranging from a single station with two detectors to four stations using a single detector. Almost 200 spectra were processed and reviewed monthly, resulting in an inventory of almost 4000 reviewed spectra by the end of November 1997. Thus, this gamma spectrum database provided a great variety of cases for various kinds of investigation.

In the SHAMAN test runs presented here, the test cases were chosen more or less at random with the goal of having at least one spectrum from each station and detector in the network. Another goal was to have a number of groups of spectra so that the variability in performance could be assessed. This resulted in five groups of 50 randomly chosen spectra, whose analysis results were carefully verified manually.

The test results were obtained with the November 1997 version of SHAMAN using a comprehensive gamma library with 2600 nuclides and over 80 000 gamma and X ray lines. The parameters of SHAMAN were adjusted for the best performance with air filter spectra, and they were kept essentially constant for all analyzed spectra.

SHAMAN's identification results of the randomly chosen 250 spectra, divided into five groups, were carefully analyzed, and all peculiarities were recorded to a file.

The condensed statistics of these test runs are shown in Tables I–IV. In Tables I and II, the number of present nuclides is the number of nuclides that is required for a complete explanation of the spectrum peaks. It must be noted that this quantity is not always well defined. For instance, the nuclides  $^{226}\text{Ra}$  and  $^{235}\text{U}$  have their primary gammas at 186 keV, and if the other energies of the latter are not seen, it is virtually impossible to divide a peak at 186 keV between these two nuclides. In the analysis of SHAMAN's results, it was considered sufficient to identify one of these nuclides. If both were identified, they were considered as one nuclide.

The missing nuclides in Tables I and II include the nuclides that would explain one or several unidentified or misidentified peaks. Usually these nuclides have been identified in other air filter spectra measured with the same detector and/or at the same station. Naturally, there are several nuclides that could be present in the samples, but no nuclides have been accepted or required unless there is an acceptable explanation for their presence in air filter samples.

TABLE 1. NUCLIDE IDENTIFICATION IN THE 250 TEST SPECTRA BY SHAMAN

Group	Number of present nuclides/spectrum	Number of missing nuclides/spectrum	Number of spurious nuclides/spectrum	Nuclide-ID percentage
1 (50)	10.06	0.060	0.64	99.40
2 (50)	9.20	0.060	0.48	99.35
3 (50)	8.92	0.080	0.28	99.10
4 (50)	9.44	0.120	0.54	98.73
5 (50)	9.64	0.160	0.48	98.34
all (250)	9.45	0.096	0.48	98.98
mean				99.0 ± 0.5

TABLE 2. NUCLIDE IDENTIFICATION IN THE 166 SHORT-CYCLE TEST SPECTRA BY SHAMAN

Group	Number of present nuclides/spectrum	Number of missing nuclides/spectrum	Number of spurious nuclides/spectrum	Nuclide-ID percentage
1 (25)	9.80	0.040	0.48	99.59
2 (39)	9.26	0.077	0.54	99.17
3 (33)	9.18	0.030	0.24	99.67
4 (32)	9.09	0.094	0.38	98.97
5 (37)	9.89	0.054	0.35	99.45
all (166)	9.43	0.060	0.40	99.36
mean				99.4 ± 0.3

In Tables III and IV, the number of found peaks is the number of peaks found and fitted by the Canberra-based IDC analysis software.

The column of unexplained peaks includes both the significant peaks that have been left unidentified, and the peaks that have been misidentified. If the peak area has been distorted in the peak fitting phase, the correct nuclide may have a peak explanation percentage far from the ideal 100%, but the peak was considered correctly identified. Occasionally, SHAMAN's activity calculation results in negative activity values for some correct nuclides, and this leads to negative peak explanation percentages. This is usually a result of an over-determined peak-nuclide interference group in the activity calculation and is often an indication of another incorrect nuclide in the interference group distorting the overall solution. It can also indicate errors in efficiency calibration. Peaks with negative explanations were also considered identified, because the association is correct even if the explanation percentage is not.

The identification percentages in Tables I..IV were calculated for each spectrum group as follows:

$$\begin{aligned} \text{nuclide-ID percentage} &= 100\% \times (1 - \#missing / \#present), \\ \text{peak-ID percentage} &= 100\% \times (1 - \#unexpl / (\#found - \#insign)). \end{aligned}$$

When the experimental mean and standard deviation of the percentages in Tables I and III for the five groups are calculated, the following values are obtained for all 250 spectra in the test set:

$$\begin{aligned} \text{nuclide-ID percentage} &= (99.0 \pm 0.5)\%, \\ \text{peak-ID percentage} &= (98.7 \pm 0.4)\%. \end{aligned}$$

TABLE 3. PEAK IDENTIFICATION IN THE 250 TEST SPECTRA BY SHAMAN

Group	Number of found peaks/spectrum	Number of unexpl. Peaks/spectrum	Number of insign. peaks/spectrum	Peak-ID percentage
1 (50)	34.90	0.40	2.46	98.77
2 (50)	38.76	0.54	1.80	98.54
3 (50)	35.14	0.28	2.10	99.15
4 (50)	35.96	0.62	1.78	98.19
5 (50)	37.78	0.36	2.32	98.98
all (250)	36.51	0.44	2.09	98.72
Mean				98.7 ± 0.4

TABLE 4. PEAK IDENTIFICATION IN THE 166 SHORT-CYCLE TEST SPECTRA BY SHAMAN

Group	Number of found peaks/spectrum	Number of unexpl. Peaks/spectrum	Number of insign. peaks/spectrum	Peak-ID percentage
1 (25)	43.52	0.12	2.20	99.71
2 (39)	43.85	0.59	1.92	98.59
3 (33)	42.06	0.09	1.88	99.77
4 (32)	42.31	0.44	1.50	98.93
5 (37)	43.38	0.14	2.24	99.67
all (166)	43.04	0.29	1.95	99.30
Mean				99.3 ± 0.5

If the long-cycle spectra and spectra of gaseous samples are omitted, the ID-percentages can be calculated for the remaining 166 short-cycle spectra in the five groups of Tables II and IV:<sup>1</sup>

$$\text{nuclide-ID percentage} = (99.4 \pm 0.3)\%$$

$$\text{peak-ID percentage} = (99.3 \pm 0.5)\%$$

It is seen that the identification percentages of short-cycle spectra are slightly better than those for all spectra, although the difference cannot be proven statistically significant with this number of spectra.

The peak identification percentage for short-cycle spectra can be compared to the published IDC-software percentage [3–6] If we take into account the first eight monthly peak identification percentages of 1997, when the peak identification percentage showed no significant trends, the IDC value is  $(97.2 \pm 0.5)\%$  [17]. It must be noted that this value “does not account for peaks that were incorrectly associated to a nuclide” [6, p. 31] in contrast to the presented SHAMAN figure. Also, the spectrum set is much larger. In any case, a clear indication of a performance difference between SHAMAN and the IDC-software can be seen.

### SHAMAN with complicated spectra

The number of gamma peaks in the measured spectrum increases drastically in a spectrum measured from a sample containing fresh fission debris. An average short-cycle particulate spectrum has 43 gamma peaks and 9 nuclides to be identified, as shown in Tables II and IV, but in a fresh fission product spectrum, the number of peaks can be over 100 and the number of nuclides to be identified over 30. This will cause further problems for traditional identification software, especially because coincidence and random summing become more significant, leading to an increase in the number of unidentified peaks.

SHAMAN’s performance is less affected by the increase of complexity of this kind. This is shown by the results from test runs with eight test spectra, which contain a variable number of peaks of fission and activation products. These spectra were created at the Reactor Laboratory of the University of Virginia by measuring different irradiated samples simultaneously with the routine air filter samples. The following anthropogenic radionuclides can be identified from these spectra in addition to the usual air filter nuclides:

- Spectrum ID d-6269: <sup>95</sup>Zr, <sup>95</sup>Nb, <sup>103</sup>Ru, <sup>131</sup>I, <sup>135</sup>I, <sup>140</sup>Ba, <sup>140</sup>La, <sup>141</sup>Ce.
- Spectrum ID d-6343: <sup>82</sup>Br, <sup>131</sup>I.

<sup>1</sup> Short-cycle operation, which has been chosen as the operational mode, consists of 24 hour sampling, 4–24 hour decay, and 20–24 hour spectrum acquisition. Other operational modes are referred to as long-cycle. The network will also collect noble gas samples, which will be analysed by gamma spectrometry or beta-gamma coincidence. The full test set contains a few gas sample gamma spectra.

- Spectrum ID d-6501:  $^{82}\text{Br}$ ,  $^{95}\text{Zr}$ ,  $^{99\text{m}}\text{Tc}$ ,  $^{103}\text{Ru}$ ,  $^{132}\text{Te}$ ,  $^{131}\text{I}$ ,  $^{132}\text{I}$ ,  $^{140}\text{Ba}$ ,  $^{140}\text{La}$ ,  $^{141}\text{Ce}$ .
- Spectrum ID d-7021:  $^{91}\text{Sr}$ ,  $^{91\text{m}}\text{Y}$ ,  $^{93}\text{Y}$ ,  $^{95}\text{Zr}$ ,  $^{97}\text{Zr}$ ,  $^{97}\text{Nb}$ ,  $^{99}\text{Mo}$ ,  $^{99\text{m}}\text{Tc}$ ,  $^{103}\text{Ru}$ ,  $^{105}\text{Rh}$ ,  $^{131}\text{Te}$ ,  $^{131\text{m}}\text{Te}$ ,  $^{132}\text{Te}$ ,  $^{131}\text{I}$ ,  $^{132}\text{I}$ ,  $^{133}\text{I}$ ,  $^{135}\text{I}$ ,  $^{133}\text{Xe}$ ,  $^{135}\text{Xe}$ ,  $^{140}\text{Ba}$ ,  $^{140}\text{La}$ ,  $^{141}\text{Ce}$ ,  $^{143}\text{Ce}$ ,  $^{151}\text{Pm}$ ,  $^{153}\text{Sm}$ .
- Spectrum ID s-4154:  $^{95}\text{Zr}$ ,  $^{95}\text{Nb}$ ,  $^{103}\text{Ru}$ ,  $^{137}\text{Cs}$ ,  $^{141}\text{Ce}$ ,  $^{144}\text{Ce}$ .
- Spectrum ID s-4473:  $^{131\text{m}}\text{Te}$ ,  $^{131}\text{I}$ .
- Spectrum ID s-4529:  $^{95}\text{Zr}$ ,  $^{97}\text{Zr}$ ,  $^{95}\text{Nb}$ ,  $^{99}\text{Mo}$ ,  $^{99\text{m}}\text{Tc}$ ,  $^{103}\text{Ru}$ ,  $^{132}\text{Te}$ ,  $^{131}\text{I}$ ,  $^{132}\text{I}$ ,  $^{133}\text{I}$ ,  $^{140}\text{Ba}$ ,  $^{140}\text{La}$ ,  $^{141}\text{Ce}$ ,  $^{143}\text{Ce}$ ,  $^{144}\text{Ce}$ ,  $^{147}\text{Nd}$ .
- Spectrum ID s-4569:  $^{95}\text{Zr}$ ,  $^{95}\text{Nb}$ ,  $^{99\text{m}}\text{Tc}$ ,  $^{103}\text{Ru}$ ,  $^{140}\text{La}$ ,  $^{147}\text{Nd}$ .

TABLE 5. IDENTIFICATION RESULTS OF EIGHT COMPLICATED SPECTRA

Spectrum ID	Number of found peaks	Number of unexpl. peaks	Number of insign. peaks	Number of present nuclides	Number of missing nuclides	Number of spurious nuclides
d-6269	58	0	2	18	0	3
d-6343	81	2	7	13	1	9
d-6501	66	0	2	21	0	1
d-7021	116	0	1	34	1	4
s-4154	48	1	2	14	0	6
s-4473	49	0	1	13	0	0
s-4529	51	1	0	24	1	2
s-4569	39	0	1	14	0	1

These spectra were analyzed with the November 1997 version of SHAMAN *using exactly the same standard parameters and comprehensive library as in the routine testruns presented above*. The condensed statistics of these testruns are shown in Table V.

There are only three unidentified nuclides in these eight relatively complicated spectra:  $^{234\text{m}}\text{Pa}$  in spectrum d-6343,  $^{133}\text{Xe}$  in spectrum d-7021, and  $^{144}\text{Ce}$  in spectrum s-4529. These three nuclides have been discarded by SHAMAN due to problems in resolving difficult nuclide interferences. The number of spurious nuclides increases from 0.4 per spectrum in routine PIDC-spectra to 3, but this is to be expected as the number of peaks increases. The spurious nuclides are mainly associated with insignificant peaks, or they have a small share of one or several peaks making the peak explanation closer to 100%, i.e., a mathematically more correct solution. Altogether, the increase in the number of spurious nuclides is not serious, since the identification of correct nuclides does not suffer. Furthermore, an analyst would carefully review this kind of spectra in any case because of the correctly identified anthropogenic nuclides.

This set of eight spectra is too small for rigorous analysis, but we can calculate the following identification percentages without uncertainty estimates for comparison purposes:

$$\text{nuclide-ID percentage} = 98.0\%,$$

$$\text{peak-ID percentage} = 99.2\%.$$

Comparison of these figures to the results of routine short-cycle spectra shows that *the identification performance of SHAMAN is not significantly deteriorated in the analysis of complex spectra*. This is a clear demonstration of SHAMAN's robust design. However, a larger number of test cases is required for more quantitative conclusions.

## Conclusion

The evaluation results of SHAMAN presented above are very good. According to these results, SHAMAN can currently identify  $(99.4 \pm 0.3)\%$  of the present nuclides in routine short-cycle air filter spectra. Since there is an average of 9–10 nuclides in a spectrum, an incorrect discarding is made in

less than one out of fifteen spectra. This figure can still be improved by further developing SHAMAN's identification methodology and the application-specific knowledge in processing air filter spectra.

Short-cycle spectrum peaks become well explained by SHAMAN:  $(99.3 \pm 0.5)\%$  of all significant peaks have a correct explanation, while the comparable figure of the IDC-software is  $(97.2 \pm 0.5)\%$ . This is a result of, on one hand, using a larger library, which provides an explanation for virtually all peaks of the common air filter nuclides and fission and activation products, and on the other hand, a more advanced nuclide identification methodology. The present approach of the IDC is to attempt to find an explanation for all detected peaks, which ensures that the purpose of the CTBT radionuclide monitoring, i.e. detecting and identifying releases from evasive nuclear events, can be fulfilled. With SHAMAN, this goal seems to be within reach.

SHAMAN was also found reliable in the analysis of other than short-cycle spectra. Its performance with long-cycle air filter spectra as well as spectra of gas samples was found to be almost as good as with short-cycle spectra, when the same comprehensive library and the same processing parameters were in use. Moreover, SHAMAN's performance was not significantly deteriorated in the analysis of eight complicated test spectra with man-made nuclide contents. SHAMAN's capability of using the comprehensive nuclide library seemed to make *virtually all spectra routine cases*, which was shown by the fact that the identification percentages for the complicated spectra remained very close to the level of routine spectrum percentages. A direct comparison to the IDC-software was not possible in these cases, because some of the man-made nuclides are not included in its reference library, but the performance difference can be expected to be similar to or larger than with routine spectra. SHAMAN's robust performance with complicated spectra is probably the most important observation for SHAMAN's application in the CTBT radionuclide monitoring.

SHAMAN's quantitative identification results, i.e., nuclide activities, concentrations, and MDCs, were found to be more reliable and accurate than those of the IDC-software. The major advantages of SHAMAN in this respect are the robust activity calculation method SVD, which gives the nuclide activity estimates in the least-squares sense, and coincidence summing correction, which compensates for the distortions in peak areas with respect to library emission probabilities in a close measuring geometry. The additional reliability and accuracy in the calculated activities is valuable in radionuclide activity ratio calculations, which are used in sample timing and backtracking calculations. The MDCs of SHAMAN were seen to give a realistic estimate for the actual detection limits, whereas those of the IDC-software were approximately a factor of 2 too large, mainly due to an excessively wide baseline integration interval.

The ultimate goal of this project was to verify, using several criteria and sufficiently large numbers of spectra, that SHAMAN introduces a substantial improvement in the quality of radionuclide analysis in connection with monitoring compliance with the CTBT. As the discussions above show, this was successfully done, and SHAMAN can be recommended for application at the operational IDC.

## REFERENCES

- [1] Comprehensive Nuclear-Test-Ban Treaty, United Nations General Assembly resolution 50/245. September 10, 1996.
- [2] "Preliminary User's Guide for Radionuclide Data Processing Software, Version 1.2." Pacific-Sierra Research Corporation, Arlington 1996.
- [3] MASON, L.R., WILLIAMS, D.L., EVANS, W.C., BOHNER, J.D., BOHLIN, J.B., KEKSZ, K.K., SHNEKENDORF, E.A., "Radionuclide Monitoring Operations Report of the Prototype International Data Center — Third Quarter CY1996", Pacific-Sierra Research Corporation Technical Report 2682, Arlington 1996.

- [4] MASON, L.R., BOHNER, J.D., EVANS, W.C., BOHLIN, J.B., WILLIAMS, D.L., KEKSZ, K.K., “Radionuclide Monitoring Operations Report of the Prototype International Data Center — Fourth Quarter CY1996”, Pacific-Sierra Research Corporation Technical Report 2698, Arlington 1997.
- [5] MASON, L.R., BOHNER, J.D., EVANS, W.C., “Radionuclide Monitoring Operations Report of the Prototype International Data Center — First Quarter CY1997”, Pacific-Sierra Research Corporation Technical Report 2715, Arlington 1997.
- [6] BOHNER, J.D., MASON, L.R., BIEGALSKI, S.R., “Radionuclide Monitoring Operations Report of the Prototype International Data Center — Second Quarter CY1997”, Pacific-Sierra Research Corporation Technical Report 2726, Arlington 1997.
- [7] AARNIO, P.A., HAKULINEN, T.T., “Developing a Personal Computer Based Expert System for Radionuclide Identification”. Article in book *New Computing Techniques in Physics Research*. Proceedings of the first International Workshop on Software Engineering, Artificial Intelligence and Expert Systems in High Energy and Nuclear Physics. March 19–24, 1990, Lyon Villeurbanne, France. Editions du Centre National de la Recherche Scientifique, Paris 1990.
- [8] AARNIO, P.A., HAKULINEN, T.T., ROUTTI, J.T., “Expert System for Nuclide Identification and Interpretation of Gamma Spectrum Analysis”, *Journal of Radioanalytical and Nuclear Chemistry* **160** 1 (1992) 245–252. Presented at ANS Topical Conference on Methods and Applications of Radioanalytical Chemistry – II, Kona, Hawaii, April 21–27, 1991.
- [9] HAKULINEN, T.T., “Knowledge Based System for Identification of Gamma Sources”, Report TKK-F-B147, Otaniemi 1993.
- [10] AARNIO, P.A., ALA-HEIKKILÄ, J.J., HAKULINEN, T.T., ROUTTI, J.T., “Expert System for Nuclide Identification in Gamma Spectrum Analysis”. *Journal of Radioanalytical and Nuclear Chemistry* **193** 2 (1995) 219–227. Presented at ANS Topical Conference on Methods and Applications of Radioanalytical Chemistry – III, Kailua–Kona, Hawaii, April 10–16, 1994.
- [11] ALA-HEIKKILÄ, J.J., *Expert System for Nuclide Identification in Environmental Gamma Spectra*. Report TKK-F-B159, Otaniemi 1995.
- [12] AARNIO, P.A., ALA-HEIKKILÄ, J.J., HAKULINEN, T.T., NIKKINEN, M.T., “Application of the Nuclide Identification System SHAMAN in Monitoring the Comprehensive Test Ban Treaty”. *Journal of Radioanalytical and Nuclear Chemistry* **235** 1–2 (1998) 95–103. Presented at the ANS Topical Conference on Methods and Applications of Radioanalytical Chemistry – IV, Kailua–Kona, Hawaii, April 6–11, 1997.
- [13] ALA-HEIKKILÄ, J.J., HAKULINEN, T.T., AARNIO, P.A., TOIVONEN, H.I.K., MASON, L.R., EVANS, W.C., BOHLIN, J.B., “Evaluation of Expert System SHAMAN in Processing Gamma ray Spectra at the Comprehensive Test Ban Treaty Prototype International Data Center —Phase I”, CMR Technical Report CMR–97/05, Arlington 1997.
- [14] AARNIO, P.A., ALA-HEIKKILÄ, J.J., HAKULINEN, T.T., NIKKINEN, M.T., “Evaluation of Expert System SHAMAN in Processing Gamma ray Spectra at the Comprehensive Test Ban Treaty Prototype International Data Center — Phase II”, CMR Technical Report CMR–97/13, Arlington 1997.
- [15] ALA-HEIKKILÄ, J.J., HAKULINEN, T.T., AARNIO, P.A. NIKKINEN, M.T., TOIVONEN, H.I.K., “Evaluation of Expert System SHAMAN in Processing Gamma ray Spectra at the Comprehensive Test Ban Treaty Prototype International Data Center“, Helsinki University of Technology Report TKK-F-B171, Otaniemi 1997.
- [16] HARMON, P., KING, D., “Expert Systems”, John Wiley & Sons, Inc., New York 1985.
- [17] BOHNER, J. D., private communications, September 1997.

## CONTRIBUTORS TO DRAFTING AND REVIEW

Aarnio, P.A.	Helsinki University of Technology, Finland
Calderin, L.	Physics Dept., CEADEN, Cuba
Capote, R.	Physics Dept., CEADEN, Cuba
Fazinic, S.	International Atomic Energy Agency
Heydorn, K.	Riso National Laboratory, Denmark
Iskander, F.Y.	University of Texas, United States of America
Kondrashov, V.	Drew University, United States of America
Korun, M.	Jozef Stefan Institut, Slovenia
Landsberger, S.	University of Texas, United States of America
Mishev, P.L.	Institute for Nuclear Research & Nuclear Energy, Bulgaria
Muravsky, V.	International Sakharov Institute of Radioecology, Belarus
Niset, M.	University of Texas, United States of America
Petersone, I.	Scientific and Industrial Union, "ELLAT", Latvia
Reus, U.	Gesellschaft fuer Kernspektrometrie mbH, Germany
Siemon, K.	Gesellschaft fuer Kernspektrometrie mbH, Germany
Sudar, S.	Institute of Experimental Physics, Kossuth University, Hungary
Tolstov, S.A.	International Sakharov Institute of Radioecology, Belarus
Vidmar, T.	Jozef Stefan Institut, Slovenia
Westmeier, H.	Gesellschaft fuer Kernspektrometrie mbH, Germany
Westmeier, W.	Gesellschaft fuer Kernspektrometrie mbH, Germany

